319 | August 1975

SCHRIFTENREIHE SCHIFFBAU

T. Miloh

Determination of Critical Maneuvers for Collision Avoidance using the Theory of Differential Games

TUHH
Technische Universität Hamburg-Harburg

Determination of Critical Maneuvers for Collision Avoidance using the Theory of Differential Games

T. Miloh

Hamburg, Technische Universität Hamburg-Harburg, 1975

Schriftenreihe Schiffbau
Schwarzenbergstraße 95c
D-21073 Hamburg

http://www.tuhh.de/vss

Institut für Schiffbau der Universität Hamburg

DETERMINATION OF CRITICAL MANEUVERS FOR COLLISION AVOIDANCE USING THE THEORY OF DIFFERENTIAL GAMES

by

T. Miloh

Revised Edition

August 1975

November 1974

Bericht Nr. 319

ABSTRACT

A method is proposed for determining critical maneuvers of surface vessels for collision avoidance using the theory of differential games. The problem is formulated as a game of kind with a terminal payoff function assuming two distinct values corresponding to the events of collision avoidance and occurrence. The kinematic model of a maneuvering ship includes two controls corresponding to rudder deflection and engine setting. Examination of the true trajectory of a typical ship in a hard turn (as computed by an elaborate nonlinear dynamic model) shows that it can be well approximated by a straight line and a circular arc traversed at different average speeds (thus accounting for speed loss in a turn). This justifies the use of an approximate simple kinematic model. Three different versions of the differential game of a two-ship encounter in the open sea are considered, namely (a) one ship evades while the other is indifferent, (b) both ships evade in collaboration and (c) one ship evades in face of pursuit by the other. The solution for optimal critical maneuvers is presented both in closed form and in a graphical form suitable for radar display. For given approach conditions and maneuvering capability the analysis yields the type of optimal evasive maneuvers (usually hard turns) as well as when to start and terminate the maneuvers to ensure a prescribed miss distance.

CONTENTS

Page

APPENDICES

LIST OF FIGURES

LIST OF SYMBOLS

Abbreviations

A	The other ship
BUP	Boundary of useable part
CPA	Closest point of approach
DC	Dispersal curve
KE	Kinematic equations
Ⓛ	Hard left turn upto terminal surface
ME	Main equation
O	Own ship; Origin of relative coordinates
Ⓡ	Hard right turn upto terminal surface
UP	Useable part of terminal surface
UC	Universal curve

Variables

A_i	Coefficients in path equations, see Eq. (A3) (i = 1,...,5)
$\bar{A}_i$	Nondimensional coefficients, see Eq. (B2) (i = 1,2)
b	Coefficient in differential equation, see Eq. (D2)
c	Coefficient in differential equation, see Eq. (D2)
$\mathbb{D}$	Max-Min operator, see Eq. (3)
d	Distance AD, see Fig. 3
$\vec{f}$	Vector function $(f_1,...,f_n)$, see Eq. (1)
G	Integral payoff function, see Eq. (2)
H	Terminal payoff function, see Eq. (2)
$\vec{h}$	Vector function $(h_1,...,h_n)$, see Eq. (8)
k	Coefficient of resistance, see Eq. (14)
k_i	Coefficients in Eq. (15) (i = 1,2,3)

L_m Required minimum miss distance

l Nondimensional miss distance, see Eq. (69)

m Ship mass

n Number of state variables in dynamic system

P_i Points on turning circle, see Fig. 2 (i = 1,...,5)

P Payoff function, see Eq. (2)

Q Singular value of terminal course angle, see Eq. (92)

R Minimum turning radius of ship (see subscripts)

r Range of A from O

r_1 Range at which privileged ship may evade

r_2 Range at which privileged ship must evade

$\bar{r}_c$ Nondimensional critical range

r_i Arbitrary successive ranges in Eq. (28,29) (i = 1,2)

r_m Range at closest approach in Eq. (28-30)

S Singular value of terminal course angle, see Eq. (73)

s_1 Terminal bearing of A relative to O

s_2 Terminal course angle of A relative to O

s_3 Terminal speed of O in Eq. (47)

s_k Terminal parameters in general, see Eq. (8)

T Nondimensional retrograde time, see Eq. (69)

T_h Net thrust of ship propeller, see Eq. (14)

T_U Nondimensional retrograde time along universal curve

t Physical time

t_l Time lapse between rudder command and beginning of turn

u Ship speed in direction of keel

V Absolute speed of ship (see subscripts)

V_r Speed of A relative to O

v Ship speed normal to keel

W Value function

W_x Partial derivative of W with respect to x

x Forward coordinate of A relative to O, see Fig. 5

$\vec{x}$ Vector of state variables $(x_1,\ldots,x_n)$, see Eq. (1)

$\bar{x}$ Nondimensional coordinate, see Eq. (69)

x_o, y_o Stationary coordinates in Fig. 2

y Starboard coordinate of A relative to O, see Fig. 5

$\bar{y}$ Nondimensional coordinate, see Eq. (69)

α Bearing angle of A relative to O, see Fig. 3

α_c Bearing angle for perfect collision, see Eq. (22)

α_i Arbitrary successive bearings in Eq. (29)

α_j Coefficients in Eq. (10) ($j = 1,\ldots,n$)

α_m Bearing angle at closest approach, see Eq. (26)

β Drift angle of ship, see Fig. 3

β_j Coefficients in Eq. (10) ($j = 1,\ldots,n$)

γ_j Coefficients in Eq. (12) ($j = 1,\ldots,n$)

δ Rudder angle

δ_j Normal vector $(\delta_1,\ldots,\delta_n)$ on terminal surface

η Speed ratio, see Eq. (69)

θ Course angle of A relative to O, see Fig. 3

θ_c Relative course angle for perfect collision

λ Ratio of minimum turning radii, see Eq. (69)

λ_x Longitudinal added mass coefficient, see Eq. (14)

τ Retrograde time, see Eq. (4)

$\vec{\phi}$ Control vector $(\phi_1,\phi_2,\ldots)$ of first player

ϕ_1 Turning rate control variable of O, see Eq. (37-39)

ϕ_2 Thrust control variable of O, see Eq. (40)

$\bar{\phi}_i$ Optimal controls (strategy) of O

$\vec{\psi}$ Control vector $(\psi_1,\psi_2,\ldots)$ of second player

ψ_1 Turning rate control variable of A, see Eq. (37-39)

ψ_2 Thrust control variable of A

$\bar{\psi}_i$ Optimal controls (strategy) of A

ω_1 Nondimensional relative speed, see Eq. (70)

ω_2 Nondimensional relative speed, see Eq. (96)

Subscripts

a Of ship A

i Index for summation

j Index for summation

k Index for summation

o Of ship O

Superscripts

$\rightarrow$ Vector

$\cdot$ Forward time derivative

$\circ$ Retrogressive time derivative

$-$ Nondimensional coordinate

1 - INTRODUCTION

The frequency and cost of collisions have increased considerably during the last few years. For example, according to the 175th Annual Report of The Liverpool Underwriters' Association in 1972 approximately 3000 ships over 500 gross registered tons were involved in collisions including stranding and damages caused by contacts. Of those involved in collisions one out of forty resulted in total loss. To this figure one has to add the tonnage lost of ships involved in groundings as a result of collision which is about four times as much as the tonnage lost in collision. In an era of increased public concern about the environment attention should also be paid to the potential hazard due to mammoth oil tankers sailing along our shores. The cost of cleaning up the oil spill which may result from a collision of such tankers could well be higher than the total value of the ships themselves, say on the order of a hundred million dollars. The problem will become even more severe in the future with continued increase in ship size and traffic density and with the ruling of more restrictive ecological laws.

Recently, various devices have been developed for the purpose of helping the ship master make a correct decision in potential collision situations. These include the so-called Collision Avoidance Radar which features a real time display of the total danger surrounding own ship by automatically tracking all targets. This radar also provides a pictorial display of the data in a form suitable for instantaneous assessment of all threats. Ideally, such a device should not only serve as a threat detector but also

supply optimal navigational instructions for collision avoidance. Any legal ship maneuver must of course comply with the official Rules of the Nautical Road. These have been ably summarized in logic flow diagrams by Luse (1972) and Kwik (1973) from whom our Fig. 1 is adapted.

The Rules distinguish between the burdened ship required to take early, substantial action and the privileged ship required to maintain course and speed upto the "last minute". Evidently, if the burdened ship fails to take timely action, the privileged ship will have to evade by executing at short range a radical maneuver involving full rudder to starboard or port. However, even the burdened ship might often prefer to evade by a relatively radical maneuver at relatively short range in order to gain time for more accurate data acquisition and situation assessment. Clearly, the probability of arriving at a correct decision (based on the target's bearing, range, course and speed) and hence of collision avoidance depends on the time interval between first observation of the target and initiation of an evasive maneuver by own ship. On the other hand, neither the burdened nor the privileged ship can afford to wait until it is already too late to avoid collision by any maneuver of which the ship is capable. Hence it is practically very important to know the limiting conditions under which collision can just be avoided. Following Kenan (1972), in this report the term "critical range" will be used to denote the shortest range at which collision can still be avoided making optimal use of the maneuvering capability of own ship. The associated maneuver will be called a "critical maneuver". It is interesting to note that the Rules expect the master of a privileged ship to estimate the critical range of the burdened

ship, as this is essentially the definition of the "last minute" at which the privileged ship is required to take action. Since the critical range depends on maneuverability, lacking mutual communication such an estimate can only be accurate for nearly identical ships.

This work has been motivated by Project A (Safety of Ships against Collisions) of the *Sonderforschungsbereich 98* which is seeking to determine a formal relation between the maneuvering capability of ships and their rates of collision. Hence it seems pertinent to speculate how the consepts of critical range and critical maneuver could be useful in this connection. It follows from the Rules of the Nautical Road that a collision can only occur if both ships involved fail to take appropriate action and that a collision is always preceded by an unsuccessful (or missed) last minute maneuver (LMM). One could therefore construct a mathematical model for calculating collision probability by combining the probabilities of occurrence of the following three successive events:

First, we consider the probability that the burdened ship fails to take early evasive action so that eventually "it becomes apparent to the privileged ship that the vessel required to keep out of the way is not taking appropriate action in compliance with the Rules", see Rule 17a (ii). Let the range at this instant be denoted by r_1. Beyond r_1 it is the sole responsibility of the burdened ship to avoid collision. The probability that the burdened ship will take correct action before reaching r_1 depends on several factors such as time elapsed since first observation of the privileged ship (and subsequent recognition of danger), quality of nautical instrumentation for data acquisition and

training and experience of the officer in command. However, it will not depend significantly on the maneuvering capability of the ship.

Below range r_1 begins the next phase in which the privileged ship is allowed (though not required) by Rule 17a (ii) to take evasive action but restricted by Rule 17 (c) "not to alter course to port for a vessel on her own port side". This restriction presumably holds until a range r_2 at which "the vessel required to keep her course and speed finds herself so close that collision cannot be avoided by the action of the burdened vessel alone" at which time the privileged ship is allowed and required "to take such action as will best aid to avoid collision", see Rule 17 (b). We therefore consider next the probability that the burdened and/or the privileged ship fail to take appropriate action in the range $r_1 > r > r_2$. It will also depend on various factors such as the kinematics of the encounter, the time elapsed from range r_1 to r_2, correct mutual guessing of the other ship's action and also partly (but not crucially) on the maneuvering capability.

Finally we enter the last phase of ranges $r < r_2$ where the privileged ship is required to execute a last minute maneuver, the success of which depends obviously in a crucial manner on the maneuvering capability of the ship and its correct use by the ship master. Other factors such as instrument errors and time needed for situation assessment are here presumably less important for we may expect that accurate observations can be made at such close range and that sufficient time has already elapsed since first observation of other ship. The decisive question becomes whether the maneuverability is still sufficient to avoid collision and whether it is optimally used. In fact if r_2 is

smaller than the "critical range" previously defined, collision becomes inevitable. The critical ranges (and even the associated critical maneuvers) depend of course on whether only one ship maneuvers or both ships maneuver, in the latter case also on whether they maneuver in collaboration or conflict. Summing up, the probability of collision in a two-ship encounter in the open sea may be constructed by combining the probabilities that 1) the burdened ship will fail to take appropriate action before reaching range r_1, 2) the burdened or privileged ship will fail to take correct individual action before reaching range r_2, and 3) the privileged and burdened ship will fail to take correct joint action after reaching range r_2. The maneuvering capability is of importance mainly at the last stage.

Following Kenan (1972) and Webster (1974) we shall consider three types of critical maneuvers for avoiding collision at short range: 1) One ship maneuvers while the other maintains course and speed, 2) Both ships maneuver in collaboration (best joint two-ship maneuver) and 3) Both ships maneuver in conflict (best evasive maneuver of one ship in face of pursuit by the other). The main result of this report is the determination of critical ranges (and associated critical maneuvers) for these three types of encounters as a function of all relevant parameters such as ship speeds, maneuverability, bearing, relative course angle and required miss distance. The results are presented analytically, numerically and in graphical form suitable for radar display. The critical maneuvers are interpreted as navigational instructions such as the direction and amount of a turn and the exact instants at which to start and end the turn. The optimal maneuvers are often quite involved and sometimes in contradiction with

simple intuition and the Rules of the Nautical Road. The mathematical method used for determining the critical maneuvers is the recently evolved Theory of Differential Games which resembles the theory of optimal control. As many readers of this report will probably be unfamiliar with Differential Games, a summary of the general technique is given in the next Section before passing on to its application to our problem.

2 - METHOD OF DIFFERENTIAL GAMES

Differential games may be defined as games in which the position of each player develops continuously in time. The players are assumed to have complete information about the current motion and the current control functions employed by all other players at any instant of time. Based on such information the player chooses a new control function from a discrete or continuous set of available functions and the game continues. Since the players do not have any information about the future action of other players, there is a continuous or discrete sequence of decision-making by each one of the players, which follows a certain pattern with time. The name differential games also suggests that the analysis is based on the application of differential equations and game theory.

Isaacs' (1965) book on Differential Games was the first attempt to give a mathematical formulation of the theory of differential games. The novelty of Isaacs' book lies not so much in the rigor of the mathematical analysis but rather in the collection of many specific examples solved with varying detail using this theory, which demonstrate the practical complications inherent in these solutions. A more rigorous foundation of differential game theory was presented later on by Friedman (1971). The close analogy between differential game theory and control theory has been emphasized by Ho (1965), who pointed out that control problems may be considered as one-sided differential games.

Following Isaacs' notation let us consider the dynamic

system given by

$$\dot{\vec{x}} = \vec{f}(\vec{x},\vec{\phi},\vec{\psi}) \qquad (1)$$

where the vector $\vec{x}$ with components $(x_1,x_2,\ldots,x_n)$ denotes a point in n-dimensional Euclidean space and the dot denotes differentiation with respect to time. The vector function $\vec{f}$ with components $(f_1,f_2,\ldots,f_n)$ is a prescribed function of position $\vec{x}$ and control variables $\vec{\phi}$ and $\vec{\psi}$ which are mutually independent. One can think for example that equation (1) is the model kinematic equation of the motion of two points (players) in space. The motion of one point is controlled by choosing a value of ϕ whereas the motion of the other point is controlled by a selection of ψ. The control variables may be also numerous, in which case we denote them by vectors $\vec{\phi}$ and $\vec{\psi}$ with components $(\phi_1,\phi_2,\ldots)$ and $(\psi_1,\psi_2,\ldots)$ respectively. For example, the steering mechanism of a vehicle has in fact two distinct controls; one is the acceleration pedal and the other is the steering wheel. The choice of the suitable control function by the players depends on the information available about the control function of the other players. For this reason the kinematic equation of each one of the players depends on the control variables of all players participating in the "game". Usually the word "game" is used in the sense that the players have conflicting objectives. Such cases are of much interest. However, the word "game" can also be generalized to include the case of collaboration between players which is in fact the distinguishing property of the collision avoidance problem. In the case of conflicting objectives one player strives to maximize the numerical value of a

certain function, whereas the other player strives to minimize the value of the same function. In a collaboration situation both players strive to maximize (or minimize) this function. The numerical quantity which the players strive to minimize or maximize is defined as the "payoff function",

$$P = \int G(\vec{x},\vec{\phi},\vec{\psi})\,dt + H(\vec{s}) \qquad (2)$$

Here t denotes time, H denotes a smooth function which is defined on the "terminal surface" and $\vec{s}$ is the parametric representation of the terminal surface. The terminal surface is so defined that whenever a player reaches it the game is over. Two types of games may now be considered: an "integral payoff game" with $H = 0$ and a "terminal payoff game" with $G = 0$. The payoff function may be a continuous function of the state variables $\vec{x}$, in which case we usually speak of a "game of degree". The other case is when the payoff function has discrete values, usually two. This is a "game of kind". For example, in the present problem of collision avoidance one may define a game of kind where the payoff has only two distinct values: $P = +1$ for the case where the collision is avoided and $P = -1$ for the case where the collision occurs.

In order to minimize or maximize the payoff function the players choose a certain control (optimal control) from a set of continuous (or discrete) available values. This optimal control is also known as "strategy", a name borrowed from game theory. The value of the payoff function defined in (2) when the control variables ϕ and ψ are replaced by their optimal values here denoted by $\bar{\phi}$ and $\bar{\psi}$ is the "Value" of the game denoted by $W(\vec{x})$.

The solution of a particular problem by the method of dif-

ferential games includes the determination of the Value function, the optimal strategies and the optimal paths. The optimal paths are defined as the physical trajectories of the players when using their optimal strategies and may be found by the integration of (1) when the control variables are replaced by the optimal strategies.

The main governing equation (ME_1 in Isaacs' notation) of differential games theory is the following first order partial differential equation for the Value

$$\mathbb{D}\left[\sum_{j=1}^{n} W_{x_j} f_j(\vec{x},\vec{\phi},\vec{\psi}) + G(\vec{x},\vec{\phi},\vec{\psi})\right] = 0 \qquad (3)$$

where W_{x_j} denotes the partial differential of $W(\vec{x})$ with respect to x_j.

The operator $\mathbb{D}$ depends on the type of strategies involved in the game. For a game with conflicting objectives a typical form of $\mathbb{D}$ may be maxmin $[\vec{\phi},\vec{\psi}]$, that is to say, choose a value of $\vec{\phi}$ that maximizes the brackets of (3) and a value of $\vec{\psi}$ that minimizes the same term. In a game where the players collaborate, a typical form of $\mathbb{D}$ may be maxmax $[\vec{\phi},\vec{\psi}]$.

In the course of the solution it is useful to reverse the time scale, i.e. to define time to be zero on the terminal surface and to increase backwards from the terminal surface along an optimal path. The retrogressive time τ is then defined on an optimal path as

$$\tau = \text{const} - t \qquad (4)$$

where the constant in (4) stands for the physical time at which

the player hits the terminal surface. Denoting time derivatives with respect to τ by a small circle, the retrogressive path equations (RPE), are written in the following form, cf. Isaacs (1965, p. 82):

$$\dot{\vec{x}} = - \vec{f}(\vec{x}, \bar{\phi}, \bar{\psi}) \tag{5}$$

and

$$\dot{W}_{x_k} = \sum_{j=1}^{n} W_{x_j} \frac{\partial f_j}{\partial x_k} + \frac{\partial G}{\partial x_k} \tag{6}$$

where equation (6) has been obtained essentially by differentiation of (3) with respect to x_k. The above equations may be considered as the characteristic equations of the main equation (3). It should be also mentioned that equations (5) and (6) are identical with the Hamilton-Jacobi equations, see Friedman (1971, p. 141).

A solution of a particular problem in the retrogressive sense starts with some "initial" conditions, say values of $\vec{x}$ and $W(\vec{x})$ on the terminal surface where $\tau = 0$. Termination of a game will occur whenever one player can force himself across the terminal surface. Usually this can occur only along a finite part of the terminal surface defined as the "useable part" (UP). The conditions on the useable part are that the scalar product of the "velocity" vector $\dot{\vec{x}}$ and the outward normal vector to the terminal surface $\vec{\delta}$ with components $(\delta_1, \delta_2, \ldots, \delta_n)$ be negative. On the boundary of the useable part (BUP) we have therefore the following condition:

$$\sum_{j=1}^{n} \delta_j \, f_j(\vec{s},\bar{\Phi},\bar{\Psi}) = 0, \tag{7}$$

since here the optimal path is tangent to the terminal surface and does not penetrate it.

To complete the set of initial conditions required for the solution of the system of partial differential equations, we will denote the parametric representation of the useable part by

$$\vec{x} = \vec{h}(s_1,s_2,\ldots,s_{n-1}), \tag{8}$$

where the vector $\vec{h}$ with components $(h_1,h_2,\ldots,h_n)$ is a prescribed function of the parameters s_k. Differentiating the Value on the useable part yields an additional set of equations

$$\frac{\partial H}{\partial s_k} = \sum_{j=1}^{n} W_{x_j} \frac{\partial h_j}{\partial s_k}, \quad k = 1,2,\ldots,n-1, \tag{9}$$

since the Value is identical with the terminal part of the pay-off on the terminal surface. Equations (8) and (9), together with (3) evaluated on the useable part with optimal strategies, consist of a set of $2n$ equations for the $2n$ unknowns in the problem, that is $(x_1,x_2,\ldots,x_n)$ and $(W_{x_1},W_{x_2},\ldots,W_{x_n})$.

Very often the solution to a problem employing the method of differential games renders considerable difficulties due to the appearance of singular or switching surfaces. Singular surfaces are defined as boundaries which separate regions of different optimal strategies. We will not discuss here the different types of singular surfaces described by Isaacs (1965), but rather mention only two types of singular surfaces which play

an important role in our analysis.

Consider the optimal paths on the two sides of a singular surface (assuming that such "sides" exist and may be defined). The optimal paths may, on each side of the surface, enter the singular surface or leave it. In the case where the optimal paths on the two sides of the surface leave the singular surface (divergent paths), the surface is called a "dispersal surface" (DS). In the opposite case, where the optimal paths on the two sides of the surface enter it (convergent paths), the surface is called a "universal surface" (US). A dispersal surface is thus the locus of points on which two paths, one from each class (different optimal strategy), meet. Obviously, the Value at the meeting point is the same for both paths. The dispersal surface may be detected in the analysis by an integration of the retrogressive path equations and by determining the geometrical locus along which these optimal paths intersect. This is not the case for a universal surface, since universal surfaces involve no retrograde path leading to them. The optimal paths which lead to the universal surface were named "tributaries" by Isaacs. The technique for determining the equations of the tributaries is somewhat different from the technique of finding the retrograde paths as will be demonstrated later on in this report. It should be noted that the universal surface is within itself an optimal path, whereas, in general, the dispersal surface is not an optimal path. For this reason one may consider a ϕ-universal curve which results from a discontinuity in ϕ across the surface while ψ is continuous on both sides of the surface. Inversely one may deal with a ψ-universal surface, where only ψ is discontinuous across the surface. Such surfaces are one-control-

variable-universal surfaces.

For a problem involving a one-control-variable-universal surface (ϕ for example), a terminal payoff, and a kinematic equation of the type

$$\dot{x}_j = \alpha_j \overline{\phi} + \beta_j, \qquad j = 1,2,\ldots,n \tag{10}$$

where α_j and β_j are linearly independent smooth functions of $\vec{x}$, the conditions on the universal surface must be, see Theorem 7.4.1 of Isaacs (1965):

$$\sum_{j=1}^{n} \alpha_j W_{x_j} = \sum_{j=1}^{n} \beta_j W_{x_j} = \sum_{j=1}^{n} \gamma_j W_{x_j} = 0 \tag{11}$$

where

$$\gamma_j = \sum_{i=1}^{n} \left(\beta_i \frac{\partial \alpha_j}{\partial x_i} - \alpha_i \frac{\partial \beta_j}{\partial x_i} \right) \tag{12}$$

For the case of $n = 3$, which happens to suit our problem, equation (11) is reduced to the following determinant,

$$\begin{vmatrix} \alpha_1 & \alpha_2 & \alpha_3 \\ \beta_1 & \beta_2 & \beta_3 \\ \gamma_1 & \gamma_2 & \gamma_3 \end{vmatrix} = 0 \tag{13}$$

where it has been assumed that not all the partial derivatives of the Value are identically zero and, as previously stated, the α_j and the β_j are linearly independent. Equation (13) will be found to be useful in the detection and in the determination of the type of the various universal surfaces appearing in the

solution.

It is hoped that with this short summary even the reader previously unfamiliar with the theory of differential games will be able to follow the subsequent analysis and gain a better understanding of this technique in course of reading this report.

3 - SIMPLE MODEL OF SHIP MANEUVERING

The two basic controls in ship maneuvering are the rudder angle and the engine setting. In most ships the maximum rudder angle is limited to 35 degrees to port and to starboard and can be varied at a rate of at least 2 degrees per second. Four speed commands are usually available: Full Ahead, Half Ahead, Stop and Full Astern. The speed change is normally effected by changing the rate of fuel supplied to the engine. However, a change of rudder angle (for example in order to initiate a turning maneuver) also leads indirectly to a change of speed even at constant engine setting. The speed reduction associated with a given rudder angle (and hence a given radius of turn) depends on the type of propulsion machinery and control. For instance, diesel engines operate essentially at constant torque, whereas turbines operate at constant power, so that the loss of speed suffered in a turn is generally larger for diesel engine ships than for turbine driven ships, see Mandel (1967, Fig. 84).

The most common maneuver performed by ships to avoid a collision in the open sea is a turning maneuver. Accelerating is not practical for ships sailing at full speed ahead since the power reserve is rather small. Stopping and braking maneuvers may be found to be practical only at harbor speeds since at full speed collision usually may be avoided more readily by turning than by stopping. Only seldom would ship masters combine a rudder maneuver with a simultaneous engine maneuver since they could produce opposite effects and partially cancel each other. Normally, any two different maneuvers would be executed one at

a time.

A turning maneuver is typically executed by moving the rudder quickly to a new setting and holding it there. The resulting trajectory of the ship is a spiral shaped curve beginning with the initial straight course and ending in a steady turn of constant radius. The final turning radius, speed and drift angle will be, for a given ship, known functions of the rudder angle usually determined as part of the standard maneuvering trials. For example, an actual turning circle maneuver (at 15 kn approach speed and 35° rudder angle) of a Mariner class ship has been computer-simulated by Oltmann (1974) using an elaborate nonlinear mathematical model. The results are reproduced in Fig. 2a (trajectory) and Fig. 2b (speed loss). It is seen that the part of the trajectory relevant for collision avoidance can be closely approximated by a straight line segment of 200 m length from point P_0 (zero time) to point P_1 (26 sec) and a semicircle of 425 m radius from point P_1 to point P_3 (235 sec). If the speed loss is approximated by a step function (see Fig. 2) so chosen that the arrival time at P_3 is identical to that in the actual maneuver, then it is easily seen that the maximum error occurs nearly at point P_2 and amounts to a phase lag of about 54 m or one third ship length.

It will be seen later that the optimal maneuvers predicted by the theory of differential games are generally extreme maneuvers in the sense that the optimal path is a circular arc of constant minimum radius and extreme engine setting available to the ship. It is fortunate that the actual trajectory of a realistic ship maneuver also exhibits these properties, if only we decompose the trajectory into two phases and account for inertial

effects by introducing an appropriately reduced constant speed for the second phase.

In order to investigate the effect of a change in engine setting on ship speed, the following approximate relation may be used

$$m(1 + \lambda_x)\,\dot{u} = T_h - k\,u^2 \qquad (14)$$

where m is the mass of the ship, λ_x the longitudinal added mass coefficient, u and $\dot{u}$ are the longitudinal velocity and acceleration respectively, T_h is the net thrust (after accounting for the thrust deduction effect), and k is a constant depending on hull form. For a steady straight course the choice of thrust T_h determines the value of the advance speed $u = \sqrt{T_h/k}$. A change in the engine setting alters the thrust almost instantaneously which in return gives rise to a longitudinal acceleration or deceleration of the ship asymptotically leading to a new steady speed. Berlekom and Goddard (1972) have proposed the following generalization of the above equation in order to include the effect of nonzero rudder and drift angle on speed in a turn:

$$m(1 + \lambda_x)\,\dot{u} = T_h - k\,u^2 + k_1 v^2 + k_2\,\beta\,\delta + k_3\,\delta^2 \qquad (15)$$

where δ is the rudder angle, β the drift angle, v the transverse velocity and k_1, k_2, k_3 are given coefficients depending on hull form

In short, the simple model of ship maneuvering used in this report implies that only two controls are available (rudder and engine setting), that the trajectory consists of a straight line

and a circular arc, each with a constant speed. These simplifications, which lead to closed form solutions of our problem, are not really as restrictive as might seem at first sight. Nevertheless, further generalizations are feasible - presumably at the cost of closed form solutions - if considered necessary at a future stage.

4 - KINEMATICS OF ENCOUNTERS

4.1 - Two Ships in Steady Turns

Consider the situation depicted in Figure 1 where two ships with centres of gravity at *O* and *A* are executing constant radius turning maneuvers. Let V_o denote the velocity of own ship and V_a the velocity of another ship (the "threat"). Ship *O* is turning about point *D* with a turning radius R_o and an associated drift angle β_o measured clockwise from the vector V_o to the direction of the keel. Similarly, ship *A* is turning about point *E* with turning radius R_a and drift angle β_a. The instantaneous range between the two ships is denoted by r and the relative bearing angle by α. The latter is measured clockwise from the direction of keel of ship *O* as shown in Figure 3. The relative course angle θ is also measured clockwise from the velocity of ship *O* to the velocity of ship *A*. (Note that this will differ from the difference of the indicated heading angles by an amount $\beta_o - \beta_a$). The kinematics of encounters in which only one ship is turning, or none, may be obtained as a special case of the general situation treated here by taking the appropriate drift angle to be zero and the turning radius to be infinite.

Let us choose a Cartesian coordinate system attached to ship *O* and consider the changes in range, bearing and relative course angle as observed by ship *O* during the course of the maneuver. The angular velocity of ship *O* about point *D* is V_o/R_o. Denoting the distance *AD* by d, the linear velocity of ship *A* in the direction normal to *AD* becomes $-V_o\, d\, /R_o$. This velocity may be decomposed into two components, a linear velocity in the

direction of r:

$$-\frac{V_o d}{R_o} \cdot \frac{R_o \sin(\alpha + \beta_o - 3\pi/2)}{d} = -V_o \cos(\alpha + \beta_o) \quad (16)$$

and an angular velocity in the direction of α:

$$-\frac{V_o}{R_o} \cdot \frac{\left\{r + R_o \cos(\alpha + \beta_o - 3\pi/2)\right\}}{r} = -\frac{V_o}{R_o} + \frac{V_o}{r} \sin(\alpha + \beta_o) \quad (17)$$

In addition to the above velocities induced at A due to the turning of ship O, there are the corresponding components of velocity due to the true motion of ship A, a linear velocity in the direction of r:

$$V_a \cos(\alpha + \beta_o - \theta)$$

and an angular velocity in the direction of α:

$$-\frac{V_a}{r} \sin(\alpha + \beta_o - \theta)$$

We may now write the following relations for the rate of change of range and bearing as observed by ship O:

$$\dot{r} = -V_o \cos(\alpha + \beta_o) + V_a \cos(\alpha + \beta_o - \theta) \quad (18)$$

$$\dot{\alpha} = -\frac{V_o}{R_o} + \frac{V_o}{r} \sin(\alpha + \beta_o) - \frac{V_a}{r} \sin(\alpha + \beta_o - \theta) \quad (19)$$

where again the dot denotes differentiation with respect to time. The above system of equations is incomplete unless we add a similar relation for the rate of change of the relative course

angle θ. For this we note that a right turn of ship *O* tends to decrease θ, whereas a right turn of ship *A* tends to increase θ. Hence we may write

$$\dot{\theta} = \frac{V_a}{R_a} - \frac{V_o}{R_o} \tag{20}$$

It is important to note that the radii R_o and R_a in (19) and (20) are defined to be positive for a right turn and negative for a left turn.

4.2 - Perfect Collision Course

Two ships moving with constant speeds on straight lines (that is $\beta_{o,a} = 0$, $R_{o,a} = \infty$) are said to be on a perfect collision course if the bearing angle remains constant ($\dot{\alpha} = 0$) while the range r is decreasing. For this situation equation (19) yields the relation

$$\frac{\sin(\alpha - \theta)}{\sin\alpha} = \frac{V_o}{V_a}, \qquad \alpha \neq 0 \text{ or } \pi \tag{21}$$

Incidentally, this shows that contrary to the current practice of taking repeated observations of the bearing angle α and/or range r, a single observation would suffice to detect instantaneously a perfect collision course if the two ships involved had a way of mutually communicating their speeds and courses. In any case, for every θ there exists a unique value of relative bearing angle α_c corresponding to a perfect collision course. It is given by one of the two solutions of

$$\alpha_c = \text{arc cot}\left\{\cot\theta - \frac{V_o}{V_a}\,\text{cosec}\,\theta\right\}, \quad \alpha \neq 0 \text{ or } \pi \tag{22}$$

This equation is not unique since both α_c and $\alpha_c + \pi$ are admissible solutions. In order to determine the desired solution we recall that for a perfect collision course in addition to $\dot{\alpha} = 0$ it is also necessary to have $\dot{r} < 0$, that is from (18)

$$V_o \cos\alpha_c - V_a \cos(\alpha_c - \theta) > 0 \tag{23}$$

Combining (21) and (23) yields

$$\sin(\alpha_c - \theta) \cot\alpha_c - \cos(\alpha_c - \theta) > 0 \tag{24}$$

which can be simplified to

$$\sin\alpha_c \sin\theta < 0 \tag{25}$$

Hence equations (22) and (25) determine uniquely the bearing angle α_c for a perfect collision course, except when $\alpha_c = 0$ or π. For these particular values the original equation (23) should be used for testing whether a true collision risk exists.

In passing it may be noted that if $V_a < V_o$, then there are two values of θ corresponding to each value of α_c. The latter are all contained in the sector

$$|\alpha_c| \leq \text{arc sin}\left(\frac{V_a}{V_o}\right)$$

4.3 - Closest Approach

Returning now to the general case of α varying with time, it would be useful to know in advance the value of range r_m and

bearing angle α_m at the point of closest approach (CPA) under the assumption that both ships maintain speed and course, that is $\beta_{o,a} = 0$, $R_{o,a} = \infty$. The bearing angle is readily found from equation (18) since at the closest approach clearly $\dot{r} = 0$ and

$$\alpha_m = \arctan \left\{ \frac{V_o}{V_a} \operatorname{cosec}\theta - \cot\theta \right\} \tag{26}$$

The singular cases $\theta = 0$ or π can be treated separately: If $\alpha = 0$ or π then α_m is also 0 or π, otherwise α_m is $\pi/2$ or $3\pi/2$.

In order to find the minimum range we note that a solution to the system of equations (18) and (19) can be given in parametric form as

$$r(\alpha) = r_1 \frac{V_o \sin\alpha_1 - V_a \sin(\alpha_1 - \theta)}{V_o \sin\alpha - V_a \sin(\alpha - \theta)} \tag{27}$$

where r_1, α_1 denote the range and bearing from any single observation. Substituting (26) into (27), the minimum range r_m, also called the predicted passing distance, becomes

$$r_m = r_1 \cdot \frac{V_o \sin\alpha_1 - V_a \sin(\alpha_1 - \theta)}{\sqrt{V_o^2 + V_a^2 - 2 V_a V_o \cos\theta}} \tag{28}$$

where the denominator is just the speed of ship *A* relative to *O*. The predicted passing distance is, of course, a very useful criterion for evaluating any collision threat. An alternative but equivalent formula based on a pair of observations of range and bearing (r_1, α_1) and (r_2, α_2) was derived by Kwik (1973):

$$r_m = \frac{r_1 r_2 \sin(\alpha_1 - \alpha_2)}{\sqrt{r_1^2 + r_2^2 - 2 r_1 r_2 \cos(\alpha_1 - \alpha_2)}} \tag{29}$$

Various alternative expressions can be derived using rates of change of range and/or bearing, for instance

$$r_m = \frac{r^2 \dot{\alpha}}{\sqrt{(r\dot{\alpha})^2 + \dot{r}^2}} = r \sqrt{\frac{2r\ddot{r}}{(\ddot{r}^2)}} \tag{30}$$

The present analysis shows that a single observation of range and bearing would suffice to establish the predicted passing distance if there were exchange of information between the ships concerning speed and course. In the absence of such communication, however, the relative course angle θ and the speed of the other ship V_a can still be determined from continued observations of range r and bearing α by own ship O, for example using the relations:

$$\theta = \alpha - \arctan\left[\frac{V_o \sin\alpha - r\dot{\alpha}}{V_o \cos\alpha + \dot{r}}\right]$$

$$\operatorname{sgn}(\alpha - \theta) = \operatorname{sgn}(V_o \sin\alpha - r\dot{\alpha}) \tag{31}$$

$$V_a = \left[(V_o \sin\alpha - r\dot{\alpha})^2 + (V_o \cos\alpha + \dot{r})^2\right]^{1/2} \tag{32}$$

The most efficient way of calculating these quantities in practice would depend on the system of information acquisition and processing available on board.

5 - ANALYSIS AND RESULTS

5.1 - General Considerations

The polar form of the kinematic equations, given in the previous section, was found to be useful in deriving some practical relations between the bearing, the relative course angle and the speeds of the ships for determining the perfect collision course or the predicted passing distance. However, for the analysis in this section it was found to be more convenient to use Cartesian representation rather than polar. Let a two-dimensional Cartesian coordinate system be defined such that the x-axis is in the direction of V_o and the y-axis is normal to V_o toward starboard in conformity with nautical practice. The origin of the coordinate system is chosen to coincide with the center of gravity of ship *O*. We may then make the following transformation

$$x = r \cos(\alpha + \beta_o), \quad y = r \sin(\alpha + \beta_o) \tag{33}$$

Substituting the above into equations (18) and (19) yields

$$\dot{x} = \frac{V_o}{R_o} y - V_o + V_a \cos\theta \tag{34}$$

$$\dot{y} = -\frac{V_o}{R_o} x + V_a \sin\theta \tag{35}$$

$$\dot{\theta} = \frac{V_a}{R_a} - \frac{V_o}{R_o} \tag{36}$$

which are identical with the reduced-space kinematic equations

in the two-car game of Isaacs (1965, p. 238).

The kinematic equations in the above form do not contain variable control functions. For this purpose let us assume that R_o and R_a denote the minimum turning radii of the ship *O* and *A* respectively. Each ship maneuvers by choosing a turning radius which is larger or utmost equal to its minimum turning radius. Let the chosen radii be denoted by R_o/ϕ_1 and R_a/ψ_1, where both ϕ_1 and ψ_1 in absolute value are smaller or equal to unity. Thus ϕ_1 and ψ_1 represent the control variables by which the ships maneuver. According to our notations, positive values of ϕ_1 or ψ_1 mean right turns, while negative values mean left turns.

In order to indicate the dependence of the kinematic equations on the control variables for turning, equations (34) to (36) are rewritten as

$$\dot{x} = \frac{V_o}{R_o} y \phi_1 - V_o + V_a \cos\theta \tag{37}$$

$$\dot{y} = -\frac{V_o}{R_o} x \phi_1 + V_a \sin\theta \tag{38}$$

$$\dot{\theta} = \frac{V_a}{R_a} \psi_1 - \frac{V_o}{R_o} \phi_1 \tag{39}$$

Note that a zero value for ϕ_1 or ψ_1 means that the ship is on a straight course ($R \to \infty$).

A second control available to the ship is the engine setting or thrust. Let T_{ho} now be the maximum thrust the engine can produce and let $-1 \leq \phi_2 \leq 1$ be the thrust control variable for ship *O*. Then equation (14) can be rewritten as

$$m_o(1 + \lambda_{xo}) \dot{u}_o = \phi_2 T_{ho} - k_o u_o^2 \tag{40}$$

Similarly, for ship A

$$m_a(1 + \lambda_{xa})\,\dot{u}_a = \psi_2\, T_{ha} - k_a\, u_a^2 \tag{41}$$

where $-1 \leq \psi_2 \leq 1$ is the thrust control variable of ship A. For the sake of simplicity, it is assumed that equations (40) and (41) hold also for turning maneuvers with

$$u_o = V_o \cos\beta_o\,, \quad u_a = V_a \cos\beta_a \tag{42}$$

In fact u and V may be interchanged without much error, since the drift angle in the maximum turn is rather small for most ships, for instance $\beta \leq 10^{\circ}$ for the standard ship Mariner in the turn shown in Fig. 2 and 3. It is clear that it is also possible to use equation (15) instead of (14), but it will be shown later that our critical maneuvers are not sensitive to the choice of a model equation for longitudinal acceleration.

Our problem is formulated in such a way that each ship has two control variables at its disposal: the amount of rudder deflection (turning radius) and the engine setting (thrust level). Following Kenan (1972) and Webster (1974), we may now consider three distinct types of critical maneuvers as already indicated in the Introduction: 1) Best maneuver of one ship while the other ship is indifferent 2) Best collaborative maneuver of both ships 3) Best maneuver of one ship combined with the worst (i.e. most conflicting) maneuver of the other ship. Each of these possibilities will be treated in detail with the intention of obtaining optimal maneuvering rules for overcoming the risk of collision.

5.2 - One-Ship Maneuvers

In the case where only one ship maneuvers, say ship 0, we set $\psi_1 = 0$ and ψ_2 = a constant such that $\dot{u}_a = 0$ in equations (39) and (41). The problem then degenerates to a one-player-game with two controls ϕ_1 and ϕ_2. The governing equations are (37) to (40) with ψ_1 set equal to zero in (39). We are dealing here with what Isaacs (1965) calls a "game of kind" in which the pay-off function has only two distinct values corresponding to the alternative events of collision avoidance and occurrence. We assign to pay-off the value +1 in case of collsion avoidance and -1 in case of collision occurrence. The maneuvering ship strives to maximize the pay-off. We now have to ask for a precise definition of collision occurrence. For the present prupose it would suffice to define "collsions" as the occurrence of a range (measured between the centers of gravity of the two ships) less than some given distance L_m. Since in the following analysis L_m is an arbitrary parameter, we can simulate different problems just by the choice of L_m. When applying the analysis to a burdened ship in the far-field situation, we would choose L_m equal to some critical range (say one or two miles) below which the encounter would have to be regarded as potentially dangerous in view of all relevant factors such as traffic density, ship maneuverability, nautical instrumentation, crew training, sea state, visibility, maneuvering space etc. On the other hand, when applying the analysis to the last-minute-maneuver of a privileged ship in the near-field situation, we would choose L_m equal to about one ship length, roughly corresponding to an actual physical collision of the two ships. Of course, safety margins may be applied to L_m in either case to compensate for instru-

ment and human errors. In any case, the question we are trying to answer is the following: At what minimum range must a ship (burdened or privileged) initiate a critical maneuver and at what stage (bearing change) must the maneuver be terminated so as to just achieve the desired miss distance L_m?

In the present situation we have four "state variables", i.e. x, y, θ and u_o (or V_o) and two control variables ϕ_1 and ϕ_2. The main equation (ME_1) of differential games (3) then reads

$$\max(\phi_1,\phi_2)\left[W_x\left(\frac{V_o}{R_o}y\phi_1 - V_o + V_a\cos\theta\right) + W_y\left(\frac{-V_o}{R_o}x\phi_1 + V_a\sin\theta\right)\right.$$
$$\left. - W_\theta\frac{V_o}{R_o}\phi_1 + W_{V_o}\frac{(\phi_2 T_{ho} - k_o V_o^2)}{m_o(1+\lambda_{xo})}\right] = 0 \qquad (43)$$

The solution of this equation implies

$$\bar{\phi}_1 = \operatorname{sgn}\left\{V_o\,(-x\,W_y + y\,W_x - W_\theta)\right\} \qquad (44)$$

$$\bar{\phi}_2 = \operatorname{sgn}\,(W_{V_o}) \qquad (45)$$

where $\bar{\phi}_1$ and $\bar{\phi}_2$ denote the optimal controls. The above equations demonstrate that the optimal strategy requires choosing extreme values of the control variables in accordance with the bang-bang principle in control theory. In other words, the optimal maneuver requires the commands: Full Rudder to port or starboard and Full Ahead or Full Astern as engine setting.

Following our notation, we shall define the "terminal surface" as a circle of radius L_m about the center of gravity of ship *O*. In order to determine the "useable part" of this surface, we write, in accordance with equations (7), (37) and (38),

$$x\dot{x} + y\dot{y} = x(V_a\cos\theta - V_o) + y\,V_a\sin\theta \leq 0 \tag{46}$$

where the equality condition in (46) holds at the "boundary of the useable part" (BUP). Further, let the parametric form of the terminal surface be given by

$$x = L_m\cos s_1,\quad y = L_m\sin s_1,\quad \theta = s_2,\quad V_o = s_3 \tag{47}$$

where s_1, s_2 and s_3 are parameters defined on the terminal surface. Substituting (47) into (46) yields a relation between s_1 and s_2 valid on the boundary of the useable part, see Isaacs (1965, p. 240):

$$\sin s_1 = \pm\,\frac{V_o - V_a\cos s_2}{V_r}$$

$$\cos s_1 = \pm\,\frac{V_a\sin s_2}{V_r} \tag{48}$$

where V_r is the relative velocity given by

$$V_r^2 = V_o^2 + V_a^2 - 2\,V_o\,V_a\cos s_2 \tag{49}$$

Equation (48) shows that the boundary of the useable part consists of two diametrically opposite points on the circle of radius L_m. The initial conditions given in (8), (9) and (47) together with the kinematic equations imply the following condition on the useable part:

$$W_x = \cos s_1,\quad W_y = \sin s_1,\quad W_\theta = W_{V_o} = 0 \tag{50}$$

since in our solution the terminal pay-off does not depend on the parameters s.

Substituting (50) into (44) and (45) shows, to our disgrace, that the values of $\bar{\phi}_1$ and $\bar{\phi}_2$ cannot be determined since both arguments of the signum functions are identically zero. A way to overcome this difficulty is to investigate the behavior of the arguments in the immediate neighborhood of the useable part. This may be done by taking the retrogressive time derivatives of the arguments in (44) and (45):

$$\bar{\phi}_1 = \operatorname{sgn}\left\{ V_o(-\mathring{x}W_y - x\mathring{W}_y + \mathring{y}W_x + y\mathring{W}_x - \mathring{W}_\theta) \right\} \tag{51}$$

$$\bar{\phi}_2 = \operatorname{sgn}\left(\mathring{W}_{V_o}\right) \tag{52}$$

From (37) to (40) we obtain the retrograde path equations

$$\mathring{x} = -\frac{V_o}{R_o} y\,\bar{\phi}_1 + V_o - V_a\cos\theta \tag{53}$$

$$\mathring{y} = \frac{V_o}{R_o} x\,\bar{\phi}_1 - V_a\sin\theta \tag{54}$$

$$\mathring{\theta} = \frac{V_o}{R_o}\,\bar{\phi}_1 \tag{55}$$

$$\mathring{V}_o = \frac{-\phi_2 T_{ho} + k_o V_o^2}{m_o(1+\lambda_{xo})} \tag{56}$$

To complete the set of retrograde path equations we use (6) to yield

$$\mathring{W}_x = -\frac{V_o}{R_o}\bar{\phi}_1 W_y \tag{57}$$

$$\dot{W}_y = \frac{V_o}{R_o}\bar{\phi}_1 W_x \tag{58}$$

$$\dot{W}_\theta = V_a (W_y \cos\theta - W_x \sin\theta) \tag{59}$$

$$\dot{W}_{V_o} = \frac{\bar{\phi}_1}{R_o}(-xW_y + yW_x - W_\theta) - W_x - W_{V_o}\frac{2k_o V_o}{m_o(1+\lambda_{xo})} \tag{60}$$

Substituting (53) to (60) into (51) and (52), and recalling that these functions are evaluated on the useable part where (47), (48) and (50) hold, we get

$$\bar{\phi}_1 = \operatorname{sgn}(-W_y), \quad \bar{\phi}_2 = \operatorname{sgn}(-W_x) \tag{61}$$

Combining (48) and (50) and substituting the resulting values of W_x and W_y into (61) finally yields

$$\begin{aligned} \bar{\phi}_1 &= \operatorname{sgn}(-\sin s_1) \\ &= \operatorname{sgn}\left\{\mp (V_o - V_a \cos s_2)\right\} \\ \bar{\phi}_2 &= \operatorname{sgn}(-\cos s_1) \\ &= \operatorname{sgn}(\mp \sin s_2) \end{aligned} \tag{62}$$

which are the desired expressions for the optimal control variables.

The upper and lower signs in equation (62) have the following meaning. Equation (47) defines a cylindrical surface of radius L_m and an axis of symmetry in the direction of s_2 normal to the x and y-axes. This cylinder is in fact the terminal surface. The parameter s_1 denotes a terminal bearing angle measured clockwise from the positive x-axis in the plane s_2 = const. Equation (48) defines the boundary of the useable part as two

curves which are wrapped around the cylinder. If $V_o > V_a$ one part of the BUP will lie in the half space $y > 0$ (righthand side of x) and may be called the righthand BUP. The other part lies in $y < 0$ and may be called the lefthand BUP. On the other hand, if $V_o < V_a$ then the two parts of the BUP do not stay on their respective sides of the x-axis, but spiral around the cylinder. To avoid confusion between left and right in case $V_o < V_a$ we shall then speak of upper (lower) BUP when referring to solutions corresponding to the upper (lower) signs in equation (48). This is further illustrated in Fig. 4 which can be also interpreted as showing the relation between relative bearing s_1 and relative course angle s_2 at the closest point of approach with speed ratio $\eta = V_a/V_o$ as parameter. The upper and lower signs in equation (62) as well as in all following equations may now be explained as always corresponding to the upper BUP and lower BUP respectively.

In order to proceed further, it will be convenient to distinguish the cases $V_o > V_a$ and $V_o < V_a$ and deal with them individually.

5.2.1 - Case I $(V_o > V_a)$

We consider first the case that own ship, i.e. the one aiming to avoid the collision, is faster than the other ship involved in the encounter. Assuming $V_o > V_a$, equation (62) yields

$$\begin{aligned} \bar{\phi}_1 &= \mp 1 \\ \bar{\phi}_2 &= \mp 1 \quad \text{if} \quad 0 < s_2 < \pi \\ &\quad \pm 1 \quad \text{if} \quad \pi < s_2 < 2\pi \end{aligned} \tag{63}$$

where the upper and lower signs apply to the righthand and lefthand BUP respectively.

Equation (63) in conjunction with (62) implies that if at CPA the target *A* is toward port (starboard) the optimal strategy of *O* is to turn right (left), and if at CPA the target *A* is forward (aft) of abeam the optimal strategy of *O* is to apply backward (forward) thrust. It is satisfying to note that the rather formal theory of Differential Games has provided us with a maneuvering rule in conformity with the simple intuitive argument that we should always turn away from the target, and decrease speed when trying to pass behind, but increase speed when trying to pass in front of the target. This rule will be useful specially for vehicles capable of achieving a considerable acceleration or deceleration by changing the thrust or power. Such a vehicle, for instance, is the automobile with its accelerator and brake pedals.

Ships (and aircraft) however can, in general, generate only

small accelerations by changing the thrust level. With a ship sailing at service speed, the power reserve is very limited so that an increase of speed is almost totally impractical. It is therefore assumed in the following that the critical maneuver is executed only by a rudder command and that the speed of the ship remains constant from the moment it enters the turn. In principle it is possible to take into account a thrust change using (56) and (63) as the model equations for ship speed, but it is believed that the results will not differ significantly from those obtained for constant speed turns. Moreover, the variable speed generalization may cost us the delight of obtaining a closed form solution to the problem.

Under the assumption of constant turning speed the retrograde path equations (53) to (55) together with the initial conditions (47) can be integrated to give (see Appendix A):

$$x = L_m \cos\left(\frac{V_o}{R_o}\bar{\phi}_1\tau + s_1\right) + R_o\bar{\phi}_1 \sin\left(\frac{V_o}{R_o}\bar{\phi}_1\tau\right) - V_a\tau\cos\left(\frac{V_o}{R_o}\bar{\phi}_1\tau + s_2\right) \tag{64}$$

$$y = L_m \sin\left(\frac{V_o}{R_o}\bar{\phi}_1\tau + s_1\right) + R_o\bar{\phi}_1\left\{1-\cos\left(\frac{V_o}{R_o}\bar{\phi}_1\tau\right)\right\} - V_a\tau\sin\left(\frac{V_o}{R_o}\bar{\phi}_1\tau + s_2\right) \tag{65}$$

$$\theta = \frac{V_o}{R_o}\bar{\phi}_1\tau + s_2 \tag{66}$$

Substitution of (48), which holds on the BUP, into (64) and (65) finally yields after elimination of s_2 using (66):

$$\bar{x} = \pm\frac{l}{\omega_1}\left\{-\sin(\bar{\phi}_1 T)+\eta\sin\theta\right\} + \bar{\phi}_1\sin(\bar{\phi}_1 T) - \eta T\cos\theta \tag{67}$$

$$\bar{y} = \pm \frac{l}{\omega_1}\left\{\cos(\bar{\phi}_1 T)-\eta\cos\theta\right\} + \bar{\phi}_1\left\{1-\cos(\bar{\phi}_1 T)\right\} - \eta T\sin\theta \tag{68}$$

where we have introduced the following nondimensional quantities

$$\eta = \frac{V_a}{V_o}\ ,\ T = \frac{V_o}{R_o}\tau,\ l = \frac{L_m}{R_o}\ ,\ \bar{x} = \frac{x}{R_o}\ ,\ \bar{y} = \frac{y}{R_o} \tag{69}$$

and

$$\omega_r = \frac{V_r}{V_o} = \left\{1 + \eta^2 - 2\eta\cos(\theta-\bar{\phi}_1 T)\right\}^{1/2} \tag{70}$$

Equations (64) to (66) are in fact the equations of the optimal paths which meet the terminal surface at the BUP. The optimal paths leading to the righthand BUP form the right barrier, while the optimal paths leading to the lefthand BUP form the left barrier. Equations (67) and (68) are the desired equations for intersections of the two barriers with planes θ = const. The upper and lower signs correspond to the intersections of the right and left barrier respectively. Equation (63) implies a left turn ($\bar{\phi}_1 = -1$) on the right barrier and a right turn ($\bar{\phi}_1 = +1$) on the left barrier.

To understand this maneuvering rule let us consider the situation depicted in Fig. 5. We are seeking the critical maneuver of own ship *O* so as to avoid collision with another ship *A* moving at a relative course angle θ. As defined above, collision avoidance means that the minimum passing distance be larger than L_m. The righthand and lefthand BUP are indicated by points *E* and *D* respectively, found by setting $T = 0$ in (67) and (68). The right barrier is the curve emerging from *E*, while the left barrier is the curve emerging from *D*. The two barriers meet at the point *F*. The region enclosed by the two barriers along with

arc DE (the useable part of the terminal surface) may be called the "danger zone". The strategy of ship O is to avoid, by timely action, the penetration of ship A into the danger zone. The semi-infinite band bounded by the two tangents drawn from E and D along with the arc DE may be called the "alert zone". A risk of collision exists only if ship A is observed inside the alert zone. It should be noted that the two tangents drawn at the BUP are parallel to the relative velocity vector V_r.

As noted in Section 3, there is a certain time lag t_l between the moment a rudder command is given on the bridge and the moment the ship begins to turn. During this time the ship A will appear to move a distance

$$AA_1 = V_r t_l \tag{71}$$

toward ship O in the direction of the relative velocity vector V_r as shown in Fig. 5. This may be anticipated by displaying ship A on the radar screen of ship O as the vector AA_1 rather than as a discrete point A.

The anti-collision maneuvering rules are now as follows. Observe the motion of point A_1, if in the alert zone, until it meets one of the barriers. If A_1 hits the right barrier, then turn left and vice-versa, as indicated by the marks (L) and (R) on the barriers. For instance, if A_1 hits the barrier at point G, the command should be "full rudder to starboard". By giving the rudder command at the moment A_1 hits the barrier, it is ensured that the actual turning maneuver will start when point A, which represents the center of gravity of ship A, first hits the barrier. (The speed reduction in the turn can also be

approximately taken into account if the barriers are calculated using for the own ship instead of the approach speed V_o a reduced speed appropriate to the rudder angle to be applied).

Now the question arises when such a maneuver should be terminated. The answer is simple; the turn should be executed until point A touches the circle of radius L_m drawn about O. This denotes the point of closest approach (CPA). At this instant the turn may be terminated. After waiting until a safe distance has been reached the original course may be resumed.

The equations of the barrier are given in a parametric form in terms of the nondimensional time T, which means that to each point on the barrier there corresponds a certain value of T. The physical interpretation is that T is the time taken to reach the UP of the terminal surface along an optimal path. Hence T is the time of execution of the critical maneuver until the CPA is reached. Ship O, originally at a relative course angle θ with respect to ship A, should execute the turn until the relative course angle is as given by equation (66)

$$s_2 = \theta - \bar{\phi}_1 T$$

which amounts to increasing θ by $-\bar{\phi}_1 T$. Thus the barriers uniquely define the type of critical maneuver needed to avoid collision as well as the instants at which the maneuver must be started and terminated.

In a restricted or crowded sea a ship is, in general, not in a position to turn to port or starboard at will. This may also be the case when the mariner is following the popular Right Turn Rule preferred also by international regulations. Our ma-

neuvering rules can easily be modified to allow for such restrictions. Let the left barrier in Fig. 5 be continued beyond F until it intersects the tangent drawn from E at the point H_R. Similarly, the right barrier is continued up to its intersection at H_L with the tangent drawn from D. The danger zone for the case where only right turns are allowed is the region enclosed by the barrier DH_R, the tangent EH_R and the arc DE. Ship O should execute a right turn at the instant A_1 is first observed on the barrier DH_R. Similarly, the danger zone for the case where only left turns are allowed is the region enclosed by the barrier EH_L, the tangent DH_L and the arc DE. Ship O then executes a left turn when A_1 is first observed on the barrier EH_L.

A particular solution of (67) and (68) yields the barrier when the threat ship A is stationary. It simply consists of two circular arcs of radii $\ell + 1$ centered at $\bar{y} = \pm 1$ for arbitrary angles θ.

The danger and alert zones as well as the maneuvering rules are presented graphically in Fig. 6 to 10 for $\eta = 1/\sqrt{2} \simeq 0.707$, $\ell = 2$ and selected values of θ.

5.2.2 - Case II ($V_o < V_a$)

We now consider the case that own ship O, i.e. the one aiming to avoid the collision, is slower than the other ship A involved in the encounter. Here equation (62) yields

$$\begin{aligned} \bar{\phi}_1 = \pm 1 \quad &\text{if} \quad 0 < s_2 < S \\ \mp 1 \quad &\text{if} \quad S < s_2 < (2\pi - S) \\ \pm 1 \quad &\text{if} \quad (2\pi - S) < s_2 < 2\pi \end{aligned} \tag{72}$$

where

$$\cos S = \frac{V_o}{V_a} = \eta^{-1} \tag{73}$$

Also, as in the previous case

$$\begin{aligned} \bar{\phi}_2 = \mp 1 \quad &\text{if} \quad 0 < s_2 < \pi \\ \pm 1 \quad &\text{if} \quad \pi < s_2 < 2\pi \end{aligned} \tag{74}$$

This last equation implies that the optimal maneuver involves increasing speed if the terminal bearing is abaft of abeam and decreasing speed if the terminal bearing is afore of abeam, see also Fig. 4. At $s_2 = S$ and $s_2 = (2\pi - S)$ one may expect to encounter singular surfaces. Let us consider first the upper barrier, i.e. the upper sign in (72), which implies by virtue of (55) that there is an abrupt decrease in the value of θ at $s_2 = S$ and an abrupt increase at $s_2 = (2\pi - S)$. This means that at $s_2 = S$ the optimal paths are divergent and we have a dispersal curve, whereas at $s_2 = (2\pi - S)$ the optimal paths are convergent and we have a universal curve. On the lower barrier (lower sign) the opposite is true, i.e. a universal curve at $s_2 = S$ and a dispersal

curve at $s_2 = (2\pi - S)$.

The calculation, or more correctly the detection, of the dispersal curve is straightforward. The intersection of the dispersal curve with the plane θ = const yields a point on the barrier at which there is an abrupt change in the value of $\bar{\phi}_1$. In order to determine this point we must plot the optimal paths given by (67) and (68) twice for each barrier, i.e. for $\bar{\phi}_1 = \pm 1$. The intersection of these two curves determines the point on the barrier which divides it into two sub-barriers with different strategies.

The calculation of the universal curve is more complicated. We must first identify the kind of universal curve we have to deal with. For this we return to the conditions prevailing on a universal curve as given by (13). Using equations (10), (12) and (53) to (55) we derive the following table

x_i	α_i	β_i	γ_i
y	$-\frac{V_o}{R_o} x$	$V_a \sin\theta$	$\frac{V_o^2}{R_o}$
x	$\frac{V_o}{R_o} y$	$V_a \cos\theta - V_o$	0
θ	$-\frac{V_o}{R_o}$	0	0

Table 1

Inserting the above coefficients into (13) yields $\theta = \mp S$. Equation (66) then implies that on this universal curve $\bar{\phi}_{1U} = 0$. The physical meaning is that the ship sails along on a straight

course without turning. Putting $\bar{\phi}_{1U} = 0$ in the path equations (53) to (55) yields

$$\begin{aligned} \dot{\bar{y}} &= -V_a \sin\theta \\ \dot{\bar{x}} &= V_o - V_a \cos\theta \\ \dot{\theta} &= 0 \end{aligned} \tag{75}$$

Integration of the above differential equations with the proper initial conditions, $\bar{x} = -l$, $\bar{y} = 0$, $\theta = \mp S$, yields in nondimensional form

$$\begin{aligned} \bar{x} &= -l \\ \bar{y} &= \pm T_U \sqrt{\eta^2 - 1} \\ \theta &= \mp \arccos\left(\frac{1}{\eta}\right) \end{aligned} \tag{76}$$

where

$$T_U = \frac{V_o}{R_o} t_U \tag{77}$$

Here t_U denotes the physical travelling time along the universal curve from any particular point up to the intersection with the terminal surface.

Our next step will be to determine the equations of the tributaries of this universal curve ($\bar{\phi}_{1U} = 0$). The governing equations of the tributaries are again the kinematic equations (53) to (55). However, the initial conditions for the tributaries differ from (47) to (49) since the tributaries do not intersect the terminal surface. What they do intersect is the universal curve. Hence the proper initial conditions are given by (75) and (76). One can now proceed with the integration of the kinematic equations and show (see Appendix B) that intersections of the

tributaries with planes θ = const form the straight lines given by

$$\bar{x}\cos(\theta\pm S)+\bar{y}\sin(\theta\pm S)+\bar{\ell}+\bar{\phi}_1\left\{(\theta\pm S)-\sin(\theta\pm S)\right\} = 0 \qquad (78)$$

The danger and alert zones along with the appropriate maneuvering rules are shown in Fig. 11 to 17 for $\eta = \sqrt{2}$, $\ell = 2$ and selected values of θ. In order to understand these rules, which at first glance seem to be more complicated than those for $\eta < 1$, consider the situation depicted in Fig. 15 for $\theta = 90^{\circ}$. The coordinate origin is attached to own ship at O, which is moving with velocity V_o in the direction of the x-axis. A threat ship A moving with velocity V_a at relative course angle $\theta = 90^{\circ}$ is observed within the alert zone bounded by the arc CD and the tangents at C and D. For a preselected minimum passing distance L_m the barrier is shown in Fig. 15. It consists of five distinct parts. Appearance of A on the part CE of the barrier calls for a left turn, whereas appearance of A on parts EF or HD calls for a right turn. The switching-strategy-point E is in fact the point where the dispersal curve meets the plane θ = const. The three segments of the barrier marked (L) or (R), for left and right turns respectively, are intersections of this plane with optimal paths which terminate on the BUP tangent to the terminal surface. These paths are given in a parametric form in terms of the retrograde nondimensional time T which uniquely determines a point on the optimal path. The maneuvering rules for these three segments of the barrier are identical to those discussed in the previous section. When the point A_1 hits the barrier, start a turn as marked and continue until point A reaches the basic circle of radius L_m. At this instant ship O may terminate the

turn. The change in relative course angle resulting from a critical maneuver starting at a point corresponding to T on the barrier is exactly $\pm T$.

It now remains to explain the symbol (R) marked on the segment FGH of the barrier in Fig. 15. The straight lines FG and GH are intersections of the tributaries of the ϕ-universal curves with plane θ = const. The equation of these lines is given by (78). The tributaries terminate on the universal curve, which in the present problem is simply given by $\theta = \mp S$. When the threat ship A hits a segment of the barrier like FG, which is a tributary and optimal path, a two-step maneuver is required to avoid collision. This is indicated by the mark (L) or (R) in the diagrams. It means that ship O should execute a turn in the direction shown until the relative course angle θ equals $\mp S$, then terminate the turn and proceed along a straight course (which is not necessarily the original course) until the point A reaches the lowest point of the basic circle about O, i.e. the point $x = -L_m$, $y = 0$. After awaiting a safe separation ship O may resume original course. This two-step strategy is better understood if we recall that the universal curve is given by $\bar{\phi}_{1U} = 0$ (straight course) and that it emerges from the lowest point of the terminal surface.

A special case is the situation for $\theta = S$ as depicted in Fig 13. Here the barrier consists only of an (R) type segment.

5.2.3 - Case III ($V_o = V_a$)

We now briefly consider the special case where ships O and A have equal velocities. The limiting solutions for $\eta = 1$ as obtained from Case I ($\eta < 1$) and Case II ($\eta > 1$) are identical.

However, they are found to be indeterminate for $\theta = \bar{\phi}_1 T$, that is to say $s_2 = 0$. The reason is that the boundary of the useable part cannot be defined when the two ships are moving with equal speeds on the same course angle. The indeterminacy can, however, be removed by rewriting (67) and (68) as

$$\bar{x} = \pm l\cos\left(\frac{\theta+\bar{\phi}_1 T}{2}\right) + \bar{\phi}_1 \sin(\bar{\phi}_1 T) - T\cos\theta \qquad (79)$$

$$\bar{y} = \pm l\sin\left(\frac{\theta+\bar{\phi}_1 T}{2}\right) + \bar{\phi}_1 \left\{1-\cos(\bar{\phi}_1 T)\right\} - T\sin\theta \qquad (80)$$

These equations are valid for all $\theta \neq 0$. It is clear that for $\theta = 0$ a barrier does not exist since the range remains constant as long as the two ships maintain their common speed and course angle. In other words, the barrier degenerates into the terminal circle $\bar{x}^2 + \bar{y}^2 = l^2$ itself and any starting condition is itself the optimal final condition.

Note, however that with $\eta = 1$ and $s_2 = 0$ any value of s_1 satisfies equation (48). Therefore, in addition to the optimal paths given by (79) and (80) we must calculate a third family of paths obtained simply from (64) to (66) by putting $s_2 = 0$ and using $0 \leq s_1 \leq 2\pi$ as the parameter instead of T for calculating intersections with planes θ = const.

5.3 - Collaborative Two-Ship Maneuvers

We now proceed to analyse the situation where both ships involved in the encounter maneuver in collaboration with the aim of avoiding a collision. Mathematically this means that in general besides ϕ_1 also ψ_1 will be nonzero. However, for the sake of simplicity we shall allow only rudder angle control, assuming ϕ_2 and ψ_2 are constants such that $\dot{u}_o = \dot{u}_a = 0$.

The operator $\mathbb{D}$ defined in (3) now takes the form "maxmax". Under assumption of constant turning speed we have three state variables x, y, θ and two control variables ϕ_1 and ψ_1. The main equation (3) then yields the following relation for the Value:

$$\begin{aligned}\max\max(\phi_1,\psi_1)\Big[W_x\Big(\frac{V_o}{R_o}y\phi_1 - V_o + V_a\cos\theta\Big) + W_y\Big(-\frac{V_o}{R_o}x\phi_1 + V_a\sin\theta\Big)\\ + W_\theta\Big(\frac{V_a}{R_a}\psi_1 - \frac{V_o}{R_o}\phi_1\Big)\Big] = 0 \end{aligned} \tag{81}$$

The solution of (81) implies

$$\bar{\phi}_1 = \operatorname{sgn}(y\,W_x - x\,W_y - W_\theta) \tag{82}$$

$$\bar{\psi}_1 = \operatorname{sgn}(W_\theta) \tag{83}$$

The initial conditions at the BUP do not depend on the maneuvers of ship A and are therefore identical with those given in (47) to (50). It follows that the arguments of the signum functions in (82) and (83) are identically zero on the BUP. Hence, in order to evaluate these functions we resort to differentiation with respect to the retrograde time and obtain

$$\bar{\phi}_1 = \operatorname{sgn}(\dot{y} W_x + y \dot{W}_x - \dot{x} W_y - x \dot{W}_y - \dot{W}_\theta) \tag{84}$$

$$\bar{\psi}_1 = \operatorname{sgn}(\dot{W}_\theta) \tag{85}$$

The retrograde path equations for x and y are given by (53) and (54). However, the path equation for θ has to be modified to read

$$\dot{\theta} = \frac{V_o}{R_o} \bar{\phi}_1 - \frac{V_a}{R_a} \bar{\psi}_1 \tag{86}$$

The expressions for the retrogressive time derivatives of the Value function (6) are identical with (57) to (59). By repeating the analysis of Section 5.2 we find that the optimal control variable $\bar{\phi}_1$ is given by (61). In order to evaluate the optimal control variable $\bar{\psi}_1$, we substitute (59) into (85) and get

$$\bar{\psi}_1 = \operatorname{sgn}(W_y \cos s_2 - W_x \sin s_2) \tag{87}$$

which holds on the BUP. Substituting (50) and (48) into (87) yields the final expression

$$\bar{\psi}_1 = \operatorname{sgn}\left\{ \mp(V_a - V_o \cos s_2) \right\} \tag{88}$$

As before, $\bar{\phi}_1$ is given by (62) which we repeat for ready comparison

$$\bar{\phi}_1 = \operatorname{sgn}\left\{ \mp(V_o - V_a \cos s_2) \right\} \tag{89}$$

In order to proceed further with the solution it is again con-

venient to treat separately the cases $V_o > V_a$ and $V_o < V_a$.

5.3.1 - Case I ($V_o > V_a$)

In this case equations (88) and (89) yield

$$\bar{\phi}_1 = \mp 1 \tag{90}$$

$$\begin{aligned} \bar{\psi}_1 = \pm 1 \quad &\text{if} \quad 0 < s_2 < Q \\ \mp 1 \quad &\text{if} \quad Q < s_2 < (2\pi - Q) \\ \pm 1 \quad &\text{if} \quad (2\pi - Q) < s_2 < 2\pi \end{aligned} \tag{91}$$

where Q is given by

$$\cos Q = V_a/V_o = \eta \tag{92}$$

According to our notation the upper sign in equations (90) and (91) applies to points on the right barrier (ending at the right-hand BUP) and the lower sign to points on the left barrier (ending at the lefthand BUP). Thus we see that the value of $\bar{\phi}_1$ is constant on each barrier whereas $\bar{\psi}_1$ changes sign twice within the cycle $0 < s_2 < 2\pi$. For reasons of symmetry we may limit our discussion to the half-interval $0 < s_2 < \pi$ while the other half $\pi < s_2 < 2\pi$ is obtained by taking the mirror image with respect to the x-axis. In all we find two singular points at $s_2 = \pm Q$ (on each barrier) where we may expect to encounter singular surfaces. The question is: what kind of singular surface?

On substituting (90) and (91) into (86) it is found that as s_2 passes through Q in the positive sense, the value of $\mathring{\theta}$ suffers an abrupt increase on the right barrier and an abrupt decrease on

the left barrier. This means that the righthand BUP at $s_2 = Q$ lies on a ψ-universal curve whereas the lefthand BUP at $s_2 = Q$ lies on a dispersal curve, and vice versa at $s_2 = -Q$.

Our next step should be to find the type of the ψ-universal curve and the conditions prevailing along it. Since we have here three state variables, these conditions are given by the solution of (13). Before evaluating the determinant in (13) we summarise the values of the coefficients α,β and γ as obtained from the substitution of (37) to (39) into (10), where ϕ is replaced by ψ, and in (12):

x_i	α	β	γ
y	0	$-\frac{V_o}{R_o}\bar{\phi}_1 x + V_a \sin\theta$	$-\frac{V_a^2}{R_a}\cos\theta$
x	0	$\frac{V_o}{R_o}\bar{\phi}_1 y - V_o + V_a \cos\theta$	$\frac{V_a^2}{R_a}\sin\theta$
θ	$\frac{V_a}{R_a}$	$-\frac{V_o}{R_o}\bar{\phi}_1$	0

Table 2

Solving (13) with the above coefficients yields $\bar{\psi}_{1U} = 0$ on the universal curve (see Appendix C). It should be noted that in general the optimal control variable is nonzero on the universal curve and its value has to determined from the proper equations.

In order to determine the optimal path we integrate the retrograde path equations (53), (54) and (86) to obtain the following nondimensional equations (see Appendix D):

$$\bar{x} = \pm \frac{l}{\omega_2} \left\{ -\sin(\bar{\phi}_1 T) + \eta \sin(\theta + \frac{\eta}{\lambda} \bar{\psi}_1 T) \right\} + \bar{\phi}_1 \sin(\bar{\phi}_1 T)$$

$$- \lambda \bar{\psi}_1 \left\{ \sin(\theta + \frac{\eta}{\lambda} \bar{\psi}_1 T) - \sin\theta \right\} \qquad (93)$$

$$\bar{y} = \pm \frac{l}{\omega_2} \left\{ \cos(\bar{\phi}_1 T) - \eta \cos(\theta + \frac{\eta}{\lambda} \bar{\psi}_1 T) \right\} + \bar{\phi}_1 \left\{ 1 - \cos(\bar{\phi}_1 T) \right\}$$

$$+ \lambda \bar{\psi}_1 \left\{ \cos(\theta + \frac{\eta}{\lambda} \bar{\psi}_1 T) - \cos\theta \right\} \qquad (94)$$

$$\theta = s_2 + (\bar{\phi}_1 - \frac{\eta}{\lambda} \bar{\psi}_1) T \qquad (95)$$

where in addition to (69) and (70) we have introduced the abbreviations

$$\lambda = \frac{R_a}{R_o} , \quad \omega_2 = \frac{V_r}{V_o} = \left\{ 1 + \eta^2 - 2\eta \cos\left[\theta - (\bar{\phi}_1 - \frac{\eta}{\lambda} \bar{\psi}_1) T \right] \right\}^{1/2} \qquad (96)$$

The upper and lower signs in (93) and (94) denote the right and left barrier respectively. Moreover, on each barrier $\bar{\phi}_1$ and $\bar{\psi}_1$ have different values as given by (90) and (91).

For detecting the point of switching strategy on the left barrier we have to find intersection of the dispersal curve with the plane θ = const. This can be done as follows: Since the dispersal curve intersects the left barrier, we set $\bar{\phi}_1 = +1$ in (93) and (94) in accordance with (90). Furthermore we take for the left barrier only the lower sign in (93) and (94), namely the minus sign. In the resulting equations we put first $\bar{\psi}_1 = +1$ and then $\bar{\psi}_1 = -1$. For θ = const we plot the two curves ($\bar{\psi}_1 = \pm 1$). Their point of intersection is intersection of the dispersal curve with plane θ = const or the point of switching strategy.

For $\theta < Q$ the left barrier emerging from the lefthand BUP has $\bar{\psi}_1 = -1$ which changes to $\bar{\psi}_1 = +1$ at the point of switching strategy. For $\theta > Q$ the opposite is true, i.e. the left barrier emerges from the lefthand BUP with $\bar{\psi}_1 = +1$ which changes to $\bar{\psi}_1 = -1$ at the switching point.

To complete the construction of the barriers it is necessary to calculate intersections of the tributaries with planes θ = const. These expressions have been derived in Appendix E and are given by:

$$\bar{x} = \left\{ l - \eta\bar{\phi}_1 \left[\theta \mp Q - (\bar{\phi}_1 - \tfrac{\eta}{\lambda}\bar{\psi}_1) T \right] \right\} \cos(\theta + \tfrac{\eta}{\lambda}\bar{\psi}_1 T) - \lambda\bar{\psi}_1 \left[\sin(\theta + \tfrac{\eta}{\lambda}\bar{\psi}_1 T) - \sin\theta \right] + \bar{\phi}_1 \sin(\theta \mp Q + \tfrac{\eta}{\lambda}\bar{\psi}_1 T) \quad (97)$$

$$\bar{y} = \left\{ l - \eta\bar{\phi}_1 \left[\theta \mp Q - (\bar{\phi}_1 - \tfrac{\eta}{\lambda}\bar{\psi}_1) T \right] \right\} \sin(\theta + \tfrac{\eta}{\lambda}\bar{\psi}_1 T) + \lambda\bar{\psi}_1 \left[\cos(\theta + \tfrac{\eta}{\lambda}\bar{\psi}_1 T) - \cos\theta \right] - \bar{\phi}_1 \left[\cos(\theta \mp Q + \tfrac{\eta}{\lambda}\bar{\psi}_1 T) - 1 \right] \quad (98)$$

where T is the nondimensional retrogressive time required to reach the ψ-universal curve from a point on its tributaries.

A few numerical examples of the barriers, the danger zones and the appropriate maneuvering rules for the case of collaborative two-ship maneuvers are plotted in Fig. 18 to 25 for $\eta = 1/\sqrt{2}$, $l = 2$, $\lambda = 1/2$ and selected values of θ. A second set of examples is shown in Fig. 26 to 33 with λ changed to 1, which however does not seem to alter the danger zone very much. In these figures the left barrier often consists of two segments

of different ψ-strategies marked by $(L)_a$ and $(R)_a$ in addition to the uniform ϕ-strategy $(R)_o$. The symbols (L) and (R) have their usual meaning while the indices a and o refer to ship *A* and *O* respectively. The right barrier also sometimes consists of two segments of different ψ-strategies marked by $(R)_a$ and $(R)_a$ or $(L)_a$ and $(L)_a$ in addition to the uniform ϕ-strategy $(L)_o$. The symbols (L) and (R) occur on intersections of the tributaries with planes θ = const. These curves are given by (97) and (98) in terms of the parameter T. Hence to each point on these curves there corresponds a unique value of T. If ship *A* hits such a segment of the barrier the appropriate maneuvering rules are as follows: Ship *O* executes a left turn until the desired minimum passing distance ℓ has been reached. Ship *A* executes a left turn, if barrier is marked $(L)_a$, or a right turn, if barrier is marked $(R)_a$, until the relative course angle θ has changed by the amount $(\bar{\psi}_1 \frac{\eta}{\lambda} - \bar{\phi}_1)\, T$ which may be positive or negative. A this point ship *A* switches to $\bar{\psi}_1 = 0$ which means that it terminates the turn and moves along a straight course until the desired minimum passing distance ℓ is reached. This is the end of the collaborative critical maneuver.

5.3.2 - Case II ($V_o < V_a$)

In this case equations (88) and (89) yield

$$\bar{\psi}_1 = \mp 1 \tag{99}$$

$$\begin{aligned} \bar{\phi}_1 &= \pm 1 \quad \text{if} \quad 0 < s_2 < S \\ &\mp 1 \quad \text{if} \quad S < s_2 < (2\pi - S) \\ &\pm 1 \quad \text{if} \quad (2\pi - S) < s_2 < 2\pi \end{aligned} \tag{100}$$

with S as defined in (73). Again, for reasons of symmetry we need consider only the half-interval $0 < s_2 < \pi$. Here we have a singular point on the BUP at $s_2 = S$. From the retrograde path equation (86) we find that the singular point on the upper barrier lies on a dispersal curve, whereas the singular point on the lower barrier lies on a ϕ-universal curve. The opposite holds for $s_2 = -S$. In order to determine the type of the ϕ-universal curve we use equations (10), (12), (37) to (39) to solve for the determinant (13). The following table contains the values of the coefficients used:

x_i	α	β	γ
y	$-\frac{V_o}{R_o}x$	$V_a \sin\theta$	$\frac{V_o^2}{R_o}$
x	$\frac{V_o}{R_o}y$	$V_a\cos\theta - V_o$	0
θ	$-\frac{V_o}{R_o}$	$\frac{V_a}{R_a}\bar{\psi}_1$	0

Table 3

The solution of (13) with the above coefficients renders $\bar{\phi}_{1U} = 0$ on the ϕ-universal curve (see Appendix F).

The optimal paths for the case $\eta > 1$ are also given by (93) to (96), the difference from the case $\eta < 1$ lying in the values of $\bar{\phi}_1$ and $\bar{\psi}_1$ to be used. However, the equations of the tributaries for the case $\eta > 1$ cannot be determined from (97) and (98) since the universal curve is of a different type. For $\eta < 1$ we had a ψ-universal curve, whereas for $\eta > 1$ we have a ϕ-universal

curve. The proper equations for the tributaries are derived in Appendix G; their intersections with planes θ = const are given by

$$\bar{x} = \left\{ -l-T+\frac{\lambda}{\eta}\bar{\psi}_1(\bar{\phi}_1 T \mp S-\theta) \right\} \cos(\bar{\phi}_1 T)+\bar{\phi}_1 \sin(\bar{\phi}_1 T)$$

$$+\lambda\bar{\psi}_1 \left\{ \sin\theta - \sin(\bar{\phi}_1 T \mp S) \right\} \qquad (101)$$

$$\bar{y} = \left\{ -l-T+\frac{\lambda}{\eta}\bar{\psi}_1(\bar{\phi}_1 T \mp S-\theta) \right\} \sin(\bar{\phi}_1 T)+\bar{\phi}_1 \left\{ 1-\cos(\bar{\phi}_1 T) \right\}$$

$$+\lambda\bar{\psi}_1 \left\{ \cos(\bar{\phi}_1 T \mp S)-\cos\theta \right\} \qquad (102)$$

The critical maneuvers in the present case $\eta > 1$ are similar to those given previously for the case $\eta < 1$, except that the roles of ship *O* and ship *A* are reversed. Ship *A* now excutes a right turn on the lower barrier and a left turn on the upper barrier. The strategy of ship *O* on either barrier may be discontinuous due to the presence of a dispersal curve. On either barrier the optimal strategy of ship *O* may comprise two steps: a partial turn until the relative course angle θ has increased by the amount $(\bar{\psi}_{\pm}\frac{\eta}{\lambda} - \bar{\phi}_1)T$ and then continuing tangentially along a straight course until ship *A* is observed at the lowest point of the basic circle, that is $\bar{x} = -l$, $\bar{y} = 0$. Such maneuvers, marked as $(R)_o$ or $(L)_o$, are required whenever ship *A* hits a segment of the barrier which is composed from the tributaries. It should be noted that it is always the slower ship which has to change its strategy at singular points according to the appearance of the singular surfaces.

Some numerical examples of critical collaborative two-ship maneuvers from the point of view of the slower ship ($\eta > 1$) are presented for selected values of θ in Fig. 34 to 40 for $\eta = \sqrt{2}$, $\ell = 2$, $\lambda = 1/2$ and in Fig. 41 to 48 for $\eta = \sqrt{2}$, $\ell = 2$, $\lambda = 1$.

5.3.3 - Case III ($V_o = V_a$)

Finally, we note that in the special case $\eta = 1$ the solutions obtained from the above Case I ($\eta < 1$) and Case II ($\eta > 1$) coincide except at

$$\theta = (\bar{\phi}_1 - \frac{\eta}{\lambda}\,\bar{\psi}_1)\,T \tag{103}$$

where the optimal path equations (93) and (94) become indeterminate. This indeterminacy can be removed by taking the limit of (93) and (94) which yields for $\eta = 1$,

$$\bar{x} = \pm\ell\cos\left\{\frac{\theta+\bar{\phi}_1 T+\bar{\psi}_1 T/\lambda}{2}\right\}+\bar{\phi}_1\sin(\bar{\phi}_1 T)$$
$$-\lambda\bar{\psi}_1\left\{\sin(\theta+\frac{\bar{\psi}_1 T}{\lambda})-\sin\theta\right\} \tag{104}$$

$$\bar{y} = \pm\ell\sin\left\{\frac{\theta+\bar{\phi}_1 T+\bar{\psi}_1 T/\lambda}{2}\right\}+\bar{\phi}_1\left\{1-\cos(\bar{\phi}_1 T)\right\}$$
$$+\lambda\bar{\psi}_1\left\{\cos(\theta+\frac{\bar{\psi}_1 T}{\lambda})-\cos\theta\right\} \tag{105}$$

These equations are valid for all $\theta \neq 0$, with the optimal controls $\bar{\phi}_1 = \mp 1$, $\bar{\psi}_1 = \mp 1$. For $\theta = 0$ a danger zone does not exist, for the barrier degenerates into the terminal circle $\bar{x}^2 + \bar{y}^2 = \ell$. An additional barrier is obtained from the terminal condition $s_2 = 0$ as mentioned at the end of Section 5.2.3.

5.4 - Conflicting Two-Ship Maneuvers

We shall now consider the case of conflicting two-ship maneuvers assuming that ship *O* follows the strategy best suited to avoid collision whereas ship *A* follows the strategy best suited to cause collision. This is what Kenan (1972) and Webster (1974) have investigated as the "best" maneuver of ship *O* combined with the "worst" maneuver of ship *A*. Such an extreme situation can sometimes arise in practice due to lack of communication between ships, due to a blunder on the part of one of the ships, or as a side effect of a collision avoidance maneuver with respect to a third ship. It is, of course, more likely to occur in warfare, whenever one ship is trying to attack another. Isaacs' (1965) book deals mainly with such pursuit problems. In his terminology we might call ship *O* the evader and ship *A* the pursuer.

The solution for the pursuit problem is similar to that of the collaboration problem of Section 5.3 in the sense that the governing equations (the retrograde path equations and the initial conditions) are identical. What is different is the operator D in equation (3). Recalling the definition of the pay-off function, we obtain the main equation

$$\max\min(\phi_1,\psi_1)\left[W_x\left(\frac{V_o}{R_o}y\phi_1 - V_o + V_a\cos\theta\right) + W_y\left(-\frac{V_o}{R_o}x\phi_1 + V_a\sin\theta\right) + W_\theta\left(\frac{V_a}{R_a}\psi_1 - \frac{V_o}{R_o}\phi_1\right)\right] = 0 \qquad (106)$$

The analysis then follows closely the analysis of Section 5.3 from (82) to (89) except for the appearance of a minus sign on the right-hand side of equations (83), (85), (87) and (88). The final expressions for optimal strategies are now

$$\bar{\phi}_1 = \text{sgn}\left\{\mp(V_o - V_a \cos s_2)\right\} \tag{107}$$

$$\bar{\psi}_1 = \text{sgn}\left\{\pm(V_a - V_o \cos s_2)\right\} \tag{108}$$

As before, we now distinguish two cases depending upon the relative speeds of the evader and the pursuer.

5.4.1 - Case I ($V_o > V_a$)

In case the evader is faster than the pursuer equations (107) and (108) imply

$$\bar{\phi}_1 = \mp 1 \tag{109}$$

$$\begin{aligned} \bar{\psi}_1 = {} & \mp 1 \quad \text{if} \quad 0 < s_2 < Q \\ & \pm 1 \quad \text{if} \quad Q < s_2 < (2\pi - Q) \\ & \mp 1 \quad \text{if} \quad (2\pi - Q) < s_2 < 2\pi \end{aligned} \tag{110}$$

where Q is defined by (92).

Again we consider only the half-interval $0 < s_2 < \pi$ and investigate the singular points $s_2 = Q$ on the left and right barriers. As s_2 increases through Q, the value of $\dot{\theta}$ as given by (86) increases abruptly on the left barrier and decreases abruptly on the right barrier. Hence, we have a ψ-universal curve on the left barrier and a dispersal curve on the right barrier. The opposite is true at the points $s_2 = -Q$. The value of $\bar{\phi}_1$ remains constant on each barrier; it is -1 on the right and +1 on the left barrier. Following the analysis of Appendix C, which is also valid for the pursuit problem, we find that on the ψ-universal curve $\bar{\psi}_{1U} = 0$. The general tributaries of the universal curve and their intersections with planes $\theta = \text{const}$ are derived in Appendix E and

summarized in (97) and (98). The integration of the retrograde path equations with the proper initial conditions has been carried out in Appendix D resulting in (93) to (95). In all these expressions the values of $\bar{\phi}_1$ and $\bar{\psi}_1$ dictated by (109) and (110) must be substituted, and the signs of ℓ, Q reversed in (97-98).

The critical maneuvers of the pursuit problem are similar to those of the collaboration problem in so far as separate instructions are indicated for each ship on every segment of the barrier. We recall that the maneuver marked for ship *A* is the optimal maneuver for causing a collision with ship *O*. From a practical point of view, we are interested mainly in the extent of the danger zone and in the optimal strategy of the evader (ship *O*), but not so much in the strategy of the pursuer (ship *A*).

Typical barriers for the case of conflicting two-ship maneuvers are shown in Fig. 49 to 56 for $\eta = 1/\sqrt{2}$, $\ell = 2$, $\lambda = 1$ and selected values of θ. The maneuvering rules for the evader (ship *O*) are simple: turn right on the left barrier and turn left on the right barrier. The strategy for the pursuer (ship *A*), however, is beset with the discontinuities introduced by the dispersal and the universal curves as shown in Fig. 54 for example.

In the pursuit problem there is no guarantee that the two barriers will intersect. In other words, the evader may not always be able to avoid collision irrespective of the action of the pursuer. It depends on the relative speeds and turning radii of the two ships. However, for $\eta < 1$ and $\lambda = 1$ the two barriers do intersect as depicted in Fig. 49 to 56, so that a correct timely maneuver of the faster ship *O* can avoid collision.

5.4.2 - Case II ($V_o < V_a$)

Finally, we investigate the critical evasive maneuvers of a slower ship required to avoid collision with a faster pursuer. Equations (107) and (108) now imply

$$\bar{\psi}_1 = \pm 1 \tag{111}$$

$$\begin{aligned} \bar{\phi}_1 &= \pm 1 \quad \text{if} \quad 0 < s_2 < S \\ &\mp 1 \quad \text{if} \quad S < s_2 < (2\pi - S) \\ &\pm 1 \quad \text{if} \quad (2\pi - S) < s_2 < 2\pi \end{aligned} \tag{112}$$

where S is defined by (73). It can be shown that at $s_2 = S$ we have a dispersal curve on the upper barrier and a ϕ-universal curve on the lower barrier. The analysis of Appendix F may be repeated to show that here on the ϕ-universal curve we have $\bar{\phi}_{1U} = 0$. The equations of intersections of the tributaries of the ϕ-universal curve with planes θ = const are given by (101) and (102) after substituting from (111) and (112) for $\bar{\phi}_1$ and $\bar{\psi}_1$. Similarly, the optimal paths are given by (93) and (94).

Having derived the equations of the optimal paths and of the tributaries, the two barriers emerging from the BUP may be constructed. When the pursuer is faster than the evader, in most cases the two barriers in a coordinate system attached to the evader will not intersect. In other words, the pursuer can capture the evader. This may be of some interest in warfare, but need not be pursued any further in the present context.

Cockayne (1967) has shown for the special case of a point pursuer A and a point evader O that the pursuer can capture the evader from any initial state if and only if

$$\eta > 1 \quad \text{and} \quad \eta^2 \geq \lambda \tag{113}$$

The generalization for finite pursuers and evaders, i.e. for a nonzero miss distance ℓ, is formulated but not completely solved in the two-car game of Isaacs (1965). It is intended to take up this question in a subsequent report.

6 - DISCUSSION AND CONCLUSIONS

Collsion between surface vessels occurs ultimately due to a failure of the so-called last minute maneuver at short range. In an attempt to propose a method for collision avoidance it is therefore necessary to study the critical evasive maneuvers for various geometries and kinematics of ship encounters. The method used here for the determination of optimal maneuvers is based on the application of differential game theory. The problem is formulated as a game of kind with a terminal pay-off function assuming one of two distinct values corresponding to the cases where collision does or does not occur. There is no time limitation on the duration of the game and the game is said to terminate whenever the passing distance is smaller than a prescribed value.

The mathematical model used in this report describes the relative motion of two ships. The simple model of ship maneuvering takes into account non-linear effects including speed loss in a turn by approximating the true trajectory of the ship in a hard turn by a straight line and a circular arc each with different constant speed. Three different possibilities for a two-ship encounter were considered, namely (a) one-ship maneuvers while other ship is indifferent (b) collaborative two-ship maneuver and (c) conflicting two-ship maneuver which resembles the pursuit and evasion problem. The type of the optimal maneuver is also determined by the speed-ratio of the ships and for this reason the cases where the speed of own ship is larger, equal or smaller than the speed of the threatening ship were considered separately.

The navigational instructions of a critical maneuver are given in terms of two intersecting barriers which enclose the danger zone. The strategy of own ship is to prevent the threatening one from entering the danger zone. The type of the optimal maneuver is determined by the point at which the threatening ship is first observed at the barriers. The advantage of this graphical representation is that it could be easily plotted on the radar display knowing the heading of the other ship. The plotting of the barriers will show if there is a danger of collision, i.e. if the other ship is observed within the alert zone. In case the other ship is threatening, it may be allowed to approach own ship until reaching a point on the barrier. At this instant the evasive maneuver should start and be terminated when the range between the ships equals the miss distance. For use in a crowded sea it is also possible to plot different barriers for each ship which may threaten own ship and determine against which ship avoidance action should be taken first. It should be noted that the closer vessel is not always the most threatening as far as collision risk is concerned. It may happen that an evasive maneuver against one ship may lead to a collision situation with another ship. For this reason it is recommended to use continuous plotting or displaying of barriers to determine the several-step optimal maneuver which avoids collision in crowded sea. It should also be noted that the minimum passing distance is a choice of the ship's master. Since the barriers are presented in a dimensionless form it is also possible to determine the long-range maneuver which yields a desired passing distance.

One of the more important conclusions of this work is that it is impossible to give a simple recipe for critical maneuvers

(frequently attempted in the literature) and each encounter situation has to be treated separately. Another result of the analysis is that the optimal maneuver is not always a one-step or a hard maneuver. This happens for example in the case of the appearance of universal surface which calls for a two-step maneuver part of which consists of a straight course. In addition it should be mentioned that the optimal maneuvers are not always uniquely defined, and two equivalent optimal maneuvers may exist as in the case of the appearance of a dispersal surface.

An attempt to relate optimal evasive maneuvers to ship maneuverability is also given in Kenan's (1972) work. The method used is a computer-simulation technique and the results are restricted in the sense that they are valid only for MARINER class ship. The critical range is defined by Kenan as the minimum distance for a given bearing angle, at which an optimal maneuver may still avoid collision. Kenan claims that the critical range is uniquely determined by the bearing angle α and by the speed ratio η. For identical values of α and η the largest critical range is supposed to occur when both ships are on a perfect collision course. Kenan also presents plots displaying the critical ranges versus the bearing angle for some selected geometries of two-ship encounters.

The relative course angle for two ships on a perfect collision course θ_c is related to the bearing angle α by Equation (21) which may be rewritten as

$$\eta \sin(\alpha - \theta_c) = \sin\alpha \qquad (114)$$

A plot of the critical range $\bar{r}_c$ (normalized by R_o) versus the

relative course angle θ, is given in Figure 57 for two bearing angles, namely $\alpha = 270^{\circ}$ and $\alpha = 315^{\circ}$ corresponding to speed ratios $\eta = \sqrt{2}$ and $\eta = 1/\sqrt{2}$ respectively. The magnitude of the various critical ranges were measured from the corresponding plots of the barriers as given in Figures 6 to 17. For the two encounters depicted in Figure 57, the value of the perfect-collision-course angle, as computed from Equation (114), is $\theta_c = 45^{\circ}$. It is clearly seen from this Figure that, generally, the critical range for a given bearing angle does not attain its maximum value where both ships are on a perfect collision course. This important conclusion may raise some questions as to the validity and the usefulness of Kenan's graphical presentation of his results. It is therefore believed that instead of a single critical-range versus bearing-angle plot, it is preferable to present the results for different relative course angles as depicted in Figures 6 to 56.

A further generalization of Kenan's analysis is given in Webster (1974) who studied critical maneuvers of large super-tankers, again using a computer simulation technique. The numerical values of the non-linear hydrodynamic coefficients used in Webster's analysis were those given by Berlekom and Goddard (1972). The numerical results of the critical maneuvers are also presented in a way similar to Kenan's, i.e. as a display of the critical range versus the bearing angle. Based on these curves Webster concluded that "the optimum command is not always the maximum command". That is to say that critical maneuvers are not always obtained by a maximum rudder deflection. This conclusion seems to violate the well known bang-bang principle of mechnical control systems and also contradicts the result presented in this

report, namely that critical maneuvers are hard maneuvers. It is believed that the reason for this disagreement is inherent in Webster's basic assumption that the critical maneuver consists of only one rudder command which is overlooking the possibility of a multi-step optimal maneuver. In fact the theory of differential games implies that in certain cases a critical maneuver may be a two-step maneuver part of which is a hard turn and the rest is "straight ahead". It is important to note that it is always the slower ship which is obliged to execute the two-step maneuver.

The effect of combining a rudder command with an engine setting command has been considered only in the case of one-ship maneuver. As discussed in the text such a combined maneuver is not usually executed at service speed. It is satisfying to note however, that a rather formal theory of differential games has provided us with a maneuvering rule in conformity with the simple intuitive argument that speed should be decreased when trying to pass behind other ship and should be increased when trying to pass in front of other ship, see Jones (1971). Critical maneuvers which combine rudder and engine commands may be also analysed in the same manner for the two-ship maneuver cases.

A study of optimal evasive maneuvers based on the application of optimal control theory is given in Merz (1973). The problem is formulated as a game of degree with the miss distance separating the two ships at closest approach taken as the payoff function to be minimized. Merz's mathematical model for the relative motion of the two-ships, represents both ships as distinct points hence ignoring the ship dimensions. Numerical results are given only for encounters of two identical ships (same speed and turning radius). It is demonstrated in Merz's analysis

that the optimal maneuver is not always unique, a result which has been also found here on dispersal surfaces.

The present analysis could be refined by considering a more elaborate non-linear model for single-ship maneuverability. However, it is expected that the present simplified model which partially accounts for non-linear effects does exhibit the main features of the solution and the gain in accuracy acquired when using a more complicated model would be negligible in comparison with the additional amount of computational work required.

7 - ACKNOWLEDGEMENTS

This report was prepared during a six-weeks summer leave from the University of Tel-Aviv in 1974 spent at the *Institut für Schiffbau der Universität Hamburg* at the invitation of the *Sonderforschungsbereich 98*, Project A "Safety of Ships against Collisions".

I wish to express my special thanks to Dr. Sharma for suggesting the problem and the approach to its solution. His stimulating discussions and critical review of the manuscript were most helpful. Thanks are also due to Professors Brull and Wygnanski of Tel-Aviv University for granting me the summer leave and to Frau Jurschek for typing the difficult manuscript and drawing the numerous figures.

My stay in Hamburg was all the more enjoyable thanks to the warm hospitality of the Institute Director Professor Krappinger, Dr. Sharma and other staff members of the *Institut für Schiffbau*.

8 - REFERENCES

Anon.: International Regulations for Preventing Collision at Sea, 1972. Carl Heymanns Verlag KG, Köln, (1972).

Berlekom, W.B. van; Goddard, T.A.: Maneuvering of large tankers. Trans. SNAME 80 (1972) 264-298.

Cockayne, E.: Plane Pursuit with Curvature Constraints. SIAM Journal of Appl. Math. 15 (1967) 1511-1516.

Friedman, A.: Differential Games. John Wiley and Sons, New York (1971).

Ho, Y.C.: Book review of "Differential Games" by R. Isaacs. IEEE Trans. on Automatic Control 10 (1965) 501-503.

Isaacs, R.: Differential Games. John Wiley and Sons, New York (1965).

Jones, K.D.: Practical Manoeuvres to Avoid Collision at Sea. Journ. Inst. Navig. 24 (1971) 60-66.

Kenan, G.: Collision Avoidance between Surface Ships at Short Range. Soc. Nav. Arch. Mar. Eng. Northern California Section (1972).

Krappinger, O.: Die Kollisionsrate als Element des Systemansatzes im Schiffbau. Institut für Schiffbau, Hamburg, Bericht Nr. 289 (1972).

Kwik, K.H.: Kinematik der Begegnung von Schiffen und Kollisionsverhütung mit einer Betrachtung der Fahrregeln. Institut für Schiffbau, Hamburg, Bericht Nr. 294 (1973).

Luse, J.D.: Collision Avoidance Systems and the Rules of the Nautical Road. Navigation 19 (1972) 80-87.

Mandel, P.: Ship Maneuvering and Control - Chapter VIII in Principles of Naval Architecture by J.P. Comstock (Editor). SNAME, New York (1967).

Merz, A.W.: Optimal Evasive Maneuvers in Maritime Collision Avoidance. Navigation 20 (1973) 144-152.

Oltmann, P.: Auswertung von Bahnkurven freifahrender Schiffsmodelle. Institut für Schiffbau, Hamburg, Bericht Nr. 298 (1973).

Webster, W.E.: When is Collision Unavoidable? Trans. 10th Naval Hydrodynamics Symposium, Boston, Mass. (1974).

APPENDIX A

Barrier for the Case of One-Ship Maneuvers

Differentiate the retrograde path equations for the present case as given by (53) to (55) and obtain

$$\begin{aligned} \ddot{x} + c^2 x &= 2c\, V_a \sin\theta \\ \ddot{y} + c^2 y &= cV_o - 2c\, V_a \cos\theta \\ \dot{\theta} &= c \end{aligned} \tag{A1}$$

where

$$c = \frac{V_o}{R_o}\,\bar{\Phi}_1 \tag{A2}$$

The solution of the above differential equations is given by

$$\begin{aligned} x &= A_1 \sin c\tau + A_2 \cos c\tau - V_a \tau \cos\theta \\ y &= A_3 \sin c\tau + A_4 \cos c\tau + \frac{V_o}{c} - V_a \tau \sin\theta \\ \theta &= c\tau + A_5 \end{aligned} \tag{A3}$$

As we have the constraints $A_3 = A_2$, $A_4 = -A_1$ from (53) or (54), this leaves three unknown coefficients A_1, A_2, A_5 to be determined from initial conditions (47) at $\tau = 0$, leading to

$$\begin{aligned} x &= L_m \cos(c\tau + s_1) + \frac{V_o}{c} \sin c\tau - V_a \tau \cos\theta \\ y &= L_m \sin(c\tau + s_1) + \frac{V_o}{c}\,(1 - \cos c\tau) - V_a \tau \sin\theta \\ \theta &= c\tau + s_2 \end{aligned} \tag{A4}$$

Inserting the value of c from (A2) into (A4) finally yields the equations (64) to (66).

APPENDIX B

Tributaries for the Case of One-Ship Maneuvers

The tributaries for the case of one-ship maneuvers with $\eta > 1$ may be considered to be a two-parametric family of curves. The two parameters are chosen to be the nondimensional retrogressive times T (from the point of intersection with the universal curve up to a point on the tributary) and T_U (measured along the universal curve from the terminal surface up to the intersection with a particular member of the family of tributaries). Hence we may seek parametric equations of the type $\bar{x}(T,T_U)$, $\bar{y}(T,T_U)$ and $\theta(T)$, where following (75) and (76)

$$\begin{aligned} \bar{x}(0,T_U) &= -\ell, \\ \bar{y}(0,T_U) &= \pm T_U\sqrt{\eta^2 - 1}, \\ \theta(0) &= \mp S, \end{aligned} \tag{B1}$$

The kinematic equations of the tributaries are identical to those given in (53) to (55). Their solution has been found in (A3) which we repeat here in nondimensional form

$$\begin{aligned} \bar{x}(T,T_U) &= \bar{A}_1\sin(\bar{\phi}_1 T) + \bar{A}_2\cos(\bar{\phi}_1 T) - \eta T\cos\theta \\ \bar{y}(T,T_U) &= \bar{A}_2\sin(\bar{\phi}_1 T) - \bar{A}_1\cos(\bar{\phi}_1 T) + 1/\bar{\phi}_1 - \eta T\sin\theta \\ \theta(T) &= \bar{\phi}_1 T + A_5 \end{aligned} \tag{B2}$$

Determination of the unknown coefficients $\bar{A}_1$, $\bar{A}_2$ and A_5 to satisfy the initial conditions (B1) yields

$$\bar{x}(T,T_U) = -l\cos(\bar{\phi}_1 T) + (1/\bar{\phi}_1 \mp T_U\sqrt{\eta^2-1})\sin(\bar{\phi}_1 T) - \eta T\cos\theta$$
$$\bar{y}(T,T_U) = -l\sin(\bar{\phi}_1 T) - (1/\bar{\phi}_1 \mp T_U\sqrt{\eta^2-1})\cos(\bar{\phi}_1 T) + 1/\bar{\phi}_1 - \eta T\sin\theta$$
$$\theta(T) = \bar{\phi}_1 T \mp S \qquad \text{(B3)}$$

These are the parametric equations of the surface formed by the tributaries. We can find the curves of intersection of this surface with individual planes θ = const by substituting for T from the θ-equation into the $\bar{x}$- and $\bar{y}$-equations:

$$\bar{x}(\theta,T_U) = -l\cos(\theta\pm S)+(\bar{\phi}_1 \mp T_U\sqrt{\eta^2-1})\sin(\theta\pm S)-\eta\bar{\phi}_1(\theta\pm S)\cos\theta$$
$$\bar{y}(\theta,T_U) = -l\sin(\theta\pm S)-(\bar{\phi}_1 \mp T_U\sqrt{\eta^2-1})\cos(\theta\pm S)$$
$$+\bar{\phi}_1-\eta\bar{\phi}_1(\theta\pm S)\sin\theta \qquad \text{(B4)}$$

Here we have made use of $\bar{\phi}_1 = \pm 1$ in order to simplify the expressions. Now multiply the first equation in (B4) by $\cos(\theta\pm S)$, the second by $\sin(\theta\pm S)$, and add to obtain

$$\bar{x}\cos(\theta\pm S)+\bar{y}\sin(\theta\pm S)+l-\bar{\phi}_1\sin(\theta\pm S)+\eta\bar{\phi}_1(\theta\pm S)\cos S = 0 \qquad \text{(B5)}$$

Upon substitution of (73) the above equation is seen to be identical with (78).

APPENDIX C

ψ-Universal Curve for Collaborative Two-Ship Maneuvers ($V_o > V_a$)

The solution of (13) with the coefficients from Table 2 is

$$\frac{V_o}{R_o}\bar{\phi}_1(y\cos\theta - x\sin\theta) - V_o\cos\theta + V_a = 0 \qquad (C1)$$

This equation in itself provides little information about the type of the universal curve. Hence, we follow Isaacs (1965,p.24) and differentiate (C1) with respect to the retrogressive time to get

$$\frac{V_o}{R_o}\bar{\phi}_1(\mathring{y}\cos\theta - \mathring{x}\sin\theta) + \mathring{\theta}\left\{V_o\sin\theta - \frac{V_o}{R_o}\bar{\phi}_1(y\sin\theta + x\cos\theta)\right\} = 0 \qquad (C2)$$

Substituting the values of $\mathring{x}$, $\mathring{y}$ and $\mathring{\theta}$ from (53), (54) and (86) into (C2) we get

$$\frac{V_a}{R_a}\bar{\psi}_{1U}\left\{V_o\sin\theta - \frac{V_o}{R_o}\bar{\phi}_1(x\cos\theta + y\sin\theta)\right\} = 0 \qquad (C3)$$

The only admissible solution of (C3) is $\bar{\psi}_{1U} = 0$ since letting the braces in (C3) be equal to zero yields together with (53), (54) and (C1)

$$\mathring{x} = \mathring{y} = 0 \qquad (C4)$$

which cannot hold along the universal curve.

APPENDIX D

Barrier for Collaborative Two-Ship Maneuvers

The retrograde path equations (53), (54) and (86) may be rewritten in a way similar to (A1) as

$$\begin{aligned} \ddot{x} + c^2 x &= V_a(2c - b)\sin\theta \\ \ddot{y} + c^2 y &= c\,V_o - V_a(2c - b)\cos\theta \\ \dot{\theta} &= c - b \end{aligned} \tag{D1}$$

with

$$b = \frac{V_a}{R_a}\bar{\psi}_1, \qquad c = \frac{V_o}{R_o}\bar{\phi}_1 \tag{D2}$$

The solution of (D1) is given by

$$\begin{aligned} x &= A_1\sin c\tau + A_2\cos c\tau + \frac{V_a}{b}\sin\theta \\ y &= A_3\sin c\tau + A_4\cos c\tau + \frac{V_o}{c} - \frac{V_a}{b}\cos\theta \\ \theta &= (c - b)\tau + A_5 \end{aligned} \tag{D3}$$

with the constraints $A_3 = A_2$, $A_4 = -A_1$ from (53) or (54). This leaves three unknown coefficients to be determined from initial conditions (47) leading to

$$\begin{aligned} x &= L_m\cos(s_1+c\tau)+R_o\sin(c\tau)/\bar{\phi}_1 - R_a\left\{\sin(s_2+c\tau)-\sin\theta\right\}/\bar{\psi}_1 \\ y &= L_m\sin(s_1+c\tau)+R_o\left\{1-\cos(c\tau)\right\}/\bar{\phi}_1+R_a\left\{\cos(s_2+c\tau)-\cos\theta\right\}/\bar{\psi}_1 \\ \theta &= s_2 + (c - \frac{V_a}{R_a}\bar{\psi}_1)\,\tau \end{aligned} \tag{D4}$$

The θ-equation can now be solved for s_2 and the value substituted in the x- and y-equations. Finally, substitution of s_1 from (48) yields the equations (93) to (95).

APPENDIX E

Tributaries for Collaborative Two-Ship Maneuvers ($V_o > V_a$)

Following the treatment of Appendix B, we may consider the tributaries as a two-parametric family of curves $\bar{x}(T,T_U)$, $\bar{y}(T,T_U)$ and $\theta(T,T_U)$ where the parameters T and T_U denote the nondimensional retrogressive time measured along the tributaries and the universal curve respectively.

On the universal curve we have $\bar{\psi}_{1U} = 0$. Therefore the retrograde path equations of the ψ-universal curve are

$$\begin{aligned} \mathring{\bar{x}}(0,T_U) &= -cy + V_o - V_a\cos\theta \\ \mathring{\bar{y}}(0,T_U) &= cx - V_a\sin\theta \\ \mathring{\theta}(0,T_U) &= c \end{aligned} \tag{E1}$$

with c defined in (A2). Here the first two equations are identical with (53) and (54), while the third is derived from (86) by substituting $\bar{\psi}_{1U} = 0$. The initial conditions on the BUP are found from (47) and (48) to be

$$\begin{aligned} \bar{x}(0,0) &= l\cos s_1 = \frac{\eta l\sin Q}{\omega_2} = \eta l \\ \bar{y}(0,0) &= l\sin s_1 = \pm\frac{l}{\omega_2}(1-\eta\cos Q) = \pm l\sqrt{1-\eta^2} \\ \theta(0,0) &= \pm Q = \pm \arccos\eta \end{aligned} \tag{E2}$$

with Q defined in (92). The general solution of (E1) is given by (A3). If the unknown coefficients are determined to satisfy the conditions (E2) the result is

$$\bar{x}(0,T_U) = (1-\eta T_U)\cos(\bar{\phi}_1 T_U \pm Q)+\sin(\bar{\phi}_1 T_U)/\bar{\phi}_1$$
$$\bar{y}(0,T_U) = (1-\eta T_U)\sin(\bar{\phi}_1 T_U \pm Q)+\left\{1-\cos(\bar{\phi}_1 T_U)\right\}/\bar{\phi}_1$$
$$\theta(0,T_U) = \bar{\phi}_1 T_U \pm Q \qquad \text{(E3)}$$

The above set of equations form the parametric representation of the ψ-universal curve. They also serve as initial conditions (at $T = 0$) for the determination of the tributaries. The retrograde path equations of the tributaries are identical to those of the optimal paths given in (D1). The general solution of (D1) is repeated here in nondimensional form

$$\bar{x}(T,T_U) = \bar{A}_1\sin(\bar{\phi}_1 T)+\bar{A}_2\cos(\bar{\phi}_1 T)+(\lambda\sin\theta)/\bar{\psi}_1$$
$$\bar{y}(T,T_U) = \bar{A}_2\sin(\bar{\phi}_1 T)-\bar{A}_1\cos(\bar{\phi}_1 T)+1/\bar{\phi}_1-(\lambda\cos\theta)/\bar{\psi}_1$$
$$\theta(T,T_U) = A_5 + \left(\bar{\phi}_1 - \frac{\eta}{\lambda}\bar{\psi}_1\right)T \qquad \text{(E4)}$$

where the unknown coefficients $\bar{A}_1$, $\bar{A}_2$, A_5 are to be determined so as to satisfy the initial conditions (E3). The result is

$$\bar{A}_1 = (\eta T_U-1)\sin(\bar{\phi}_1 T_U \pm Q)+\cos(\bar{\phi}_1 T_U)/\bar{\phi}_1-(\lambda/\bar{\psi}_1)\cos(\bar{\phi}_1 T_U \pm Q)$$
$$\bar{A}_2 = (1-\eta T_U)\cos(\bar{\phi}_1 T_U \pm Q)+\sin(\bar{\phi}_1 T_U)/\bar{\phi}_1-(\lambda/\bar{\psi}_1)\sin(\bar{\phi}_1 T_U \pm Q)$$
$$A_5 = \bar{\phi}_1 T_U \pm Q \qquad \text{(E5)}$$

Substitution of (E5) into (E4) yields (making use of $\bar{\psi}_1 = \pm 1$)

$$\bar{x}(T,T_U) = (1-\eta T_U)\cos(\bar{\phi}_1 T+\bar{\phi}_1 T_U \pm Q)-\lambda\bar{\psi}_1\left\{\sin(\bar{\phi}_1 T+\bar{\phi}_1 T_U \pm Q)-\sin\theta\right\}$$
$$+\bar{\phi}_1\sin(\bar{\phi}_1 T+\bar{\phi}_1 T_U)$$
$$\bar{y}(T,T_U) = (1-\eta T_U)\sin(\bar{\phi}_1 T+\bar{\phi}_1 T_U \pm Q)+\lambda\bar{\psi}_1\left\{\cos(\bar{\phi}_1 T+\bar{\phi}_1 T_U \pm Q)-\cos\theta\right\}$$
$$+\bar{\phi}_1\left\{1-\cos(\bar{\phi}_1 T+\bar{\phi}_1 T_U)\right\} \qquad \text{(E6)}$$

and

$$\theta(T,T_U) = \pm Q + \bar{\phi}_1 T_U + (\bar{\phi}_1 - \frac{n}{\lambda}\bar{\psi}_1)\,T \qquad (E7)$$

In order to obtain the desired equations for intersections of the tributaries with planes θ = const, we solve (E7) for T_U and substitute into (E6). The result is the one-parametric family of curves given by (97) and (98), the single parameter being T, since θ is here considered to be a constant.

APPENDIX F

ϕ-Universal Curve for Collaborative Two-Ship Maneuvers ($V_o < V_a$)

The solution of (13) with the coefficients from Table 3 is

$$\frac{V_a}{R_a} y\bar{\psi}_1 - V_o + V_a\cos\theta = 0 \tag{F1}$$

Differentiation with respect to the retrogressive time yields

$$\frac{V_a}{R_a} \dot{y}\bar{\psi}_1 - V_a\dot{\theta}\sin\theta = 0 \tag{F2}$$

Substitution of (54) and (86) into (F2) leads to

$$\frac{V_o}{R_o} \bar{\phi}_1 \left\{ \frac{V_a}{R_a} x\bar{\psi}_1 - V_a\sin\theta \right\} = 0 \tag{F3}$$

The factor in braces cannot be zero, since

$$x\bar{\psi}_1 = R_a\sin\theta \tag{F4}$$

does not satisfy the initial conditions on the BUP. Hence, the only acceptable solution of (F3) is $\bar{\phi}_{1U} = 0$.

APPENDIX G

Tributaries for Collaborative Two-Ship Maneuvers ($V_o < V_a$)

The equations of the tributaries are again assumed to be of the two-parametric form $\bar{x}(T,T_U)$, $\bar{y}(T,T_U)$ and $\theta(T,T_U)$, where the parameters T and T_U are as defined in Appendix E.

On the ϕ-universal curve we have $\bar{\phi}_{1U} = 0$. The retrograde path equations of such a curve are found from (53), (54) and (86) to be

$$\begin{aligned} \mathring{\bar{x}}(0,T_U) &= V_o - V_a\cos\theta \\ \mathring{\bar{y}}(0,T_U) &= -V_a\sin\theta \\ \mathring{\theta}(0,T_U) &= -\frac{V_a}{R_a}\bar{\psi}_1 \end{aligned} \tag{G1}$$

On the BUP we have $s_2 = \mp S$. Hence, (48) implies that $s_1 = \pi$. The initial conditions (47) on the BUP yield

$$\bar{x}(0,0) = -\ell, \quad \bar{y}(0,0) = 0, \quad \theta(0,0) = \mp S \tag{G2}$$

The solution of the differential equations (G1) with due consideration of the initial conditions (G2) becomes

$$\begin{aligned} \bar{x}(0,T_U) &= -\ell + T_U + \lambda\left\{ \pm\sin S - \sin\left(\frac{\eta}{\lambda}\bar{\psi}_1 T_U \pm S\right)\right\}/\bar{\psi}_1 \\ \bar{y}(0,T_U) &= \lambda\left\{ \cos S - \cos\left(\frac{\eta}{\lambda}\bar{\psi}_1 T_U \pm S\right)\right\}/\bar{\psi}_1 \\ \theta(0,T_U) &= \mp S - \frac{\eta}{\lambda}\bar{\psi}_1 T_U \end{aligned} \tag{G3}$$

The general solution for the optimal path equations in case of

two-ship maneuvers is given in (E4). The three unknown coefficients occurring there are now to be determined so as to satisfy the initial conditions (G3) for the tributaries.
The result is found to be

$$\bar{A}_1 = 1/\bar{\phi}_1 - (\lambda/\bar{\psi}_1)\cos S$$

$$\bar{A}_2 = -l + T_U \pm (\lambda/\bar{\psi}_1)\sin S$$

$$A_5 = \mp S - \frac{\eta}{\lambda}\bar{\psi}_1 T_U \qquad \text{(G4)}$$

Substitution of (G4) into (E4) yields

$$\bar{x}(T,T_U) = (T_U-l)\cos(\bar{\phi}_1 T)+\sin(\bar{\phi}_1 T)/\bar{\phi}_1+(\lambda/\bar{\psi}_1)\left\{\sin\theta-\sin(\bar{\phi}_1 T\mp S)\right\} \qquad \text{(G5)}$$

$$\bar{y}(T,T_U) = (T_U-l)\sin(\bar{\phi}_1 T)+\left\{1-\cos(\bar{\phi}_1 T)\right\}/\bar{\phi}_1+(\lambda/\bar{\psi}_1)\left\{\cos(\bar{\phi}_1 T\mp S)-\cos\theta\right\} \qquad \text{(G6)}$$

$$\theta(T,T_U) = \mp S - \frac{\eta}{\lambda}\bar{\psi}_1 T_U + (\bar{\phi}_1 - \frac{\eta}{\lambda}\bar{\psi}_1)\,T \qquad \text{(G7)}$$

In order to derive the desired equations for the intersections of the tributaries with planes θ = const, we solve (G7) for T_U and substitute into (G5) and (G6). The resulting expressions after making use of $\bar{\phi}_1 = \pm 1$, $\bar{\psi}_1 = \pm 1$ are given in (101) and (102).

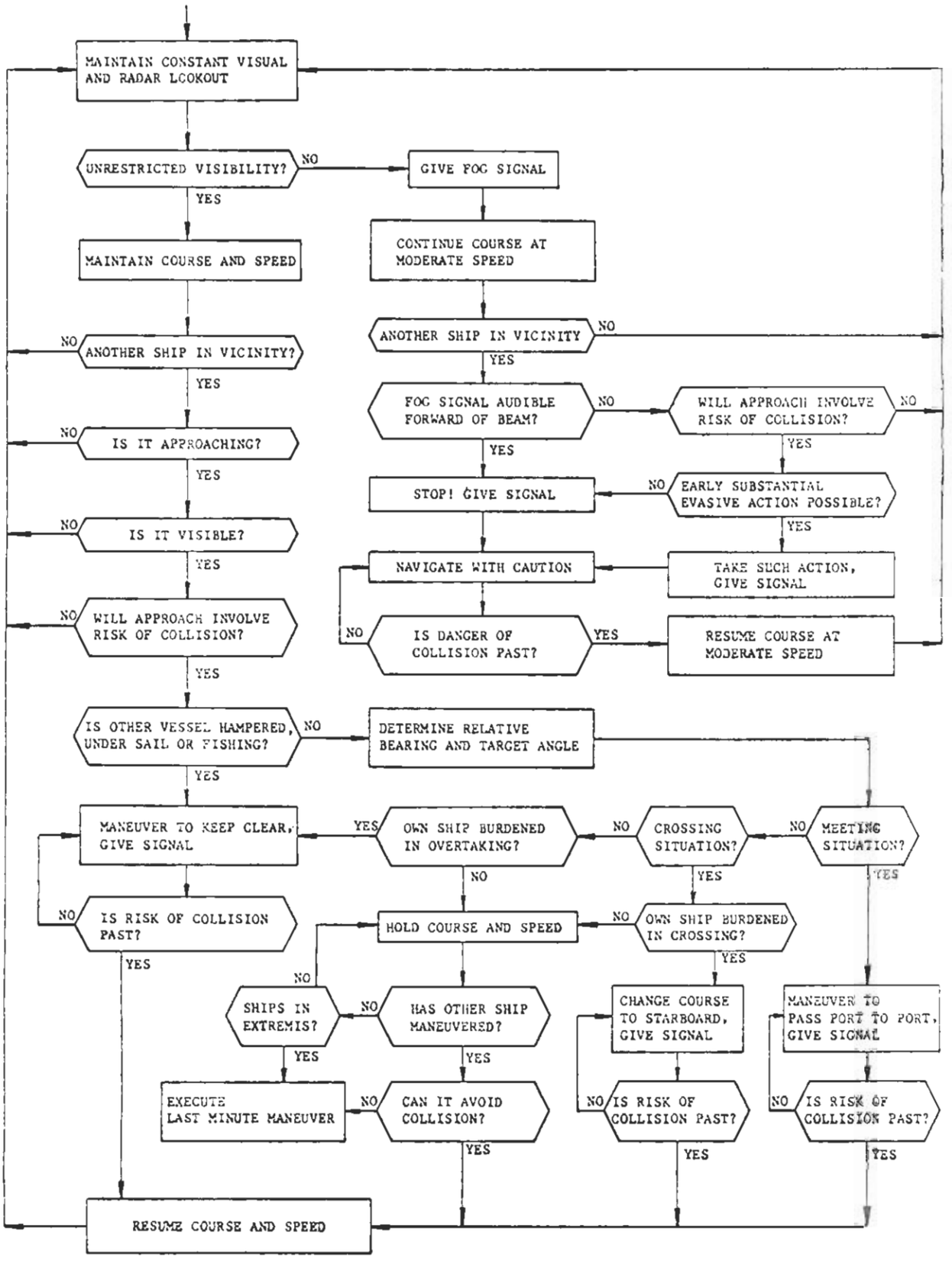

Fig. 1 Logic flow diagram of the International Rules of the Nautical Road for two-ship encounter in open sea

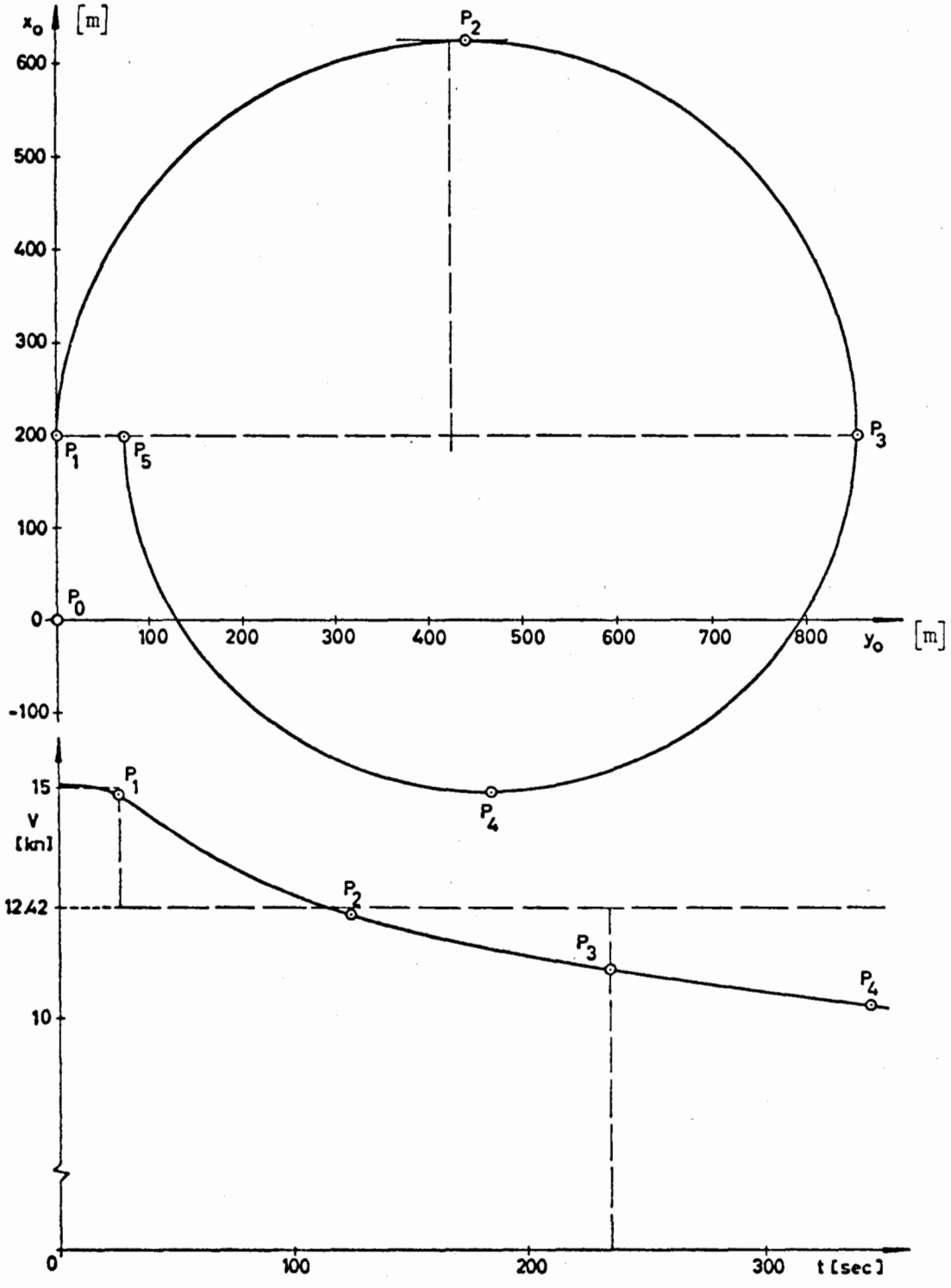

Fig. 2 Minimum-radius turn of a MARINER type ship - Trajectory (top) and speed reduction (bottom)

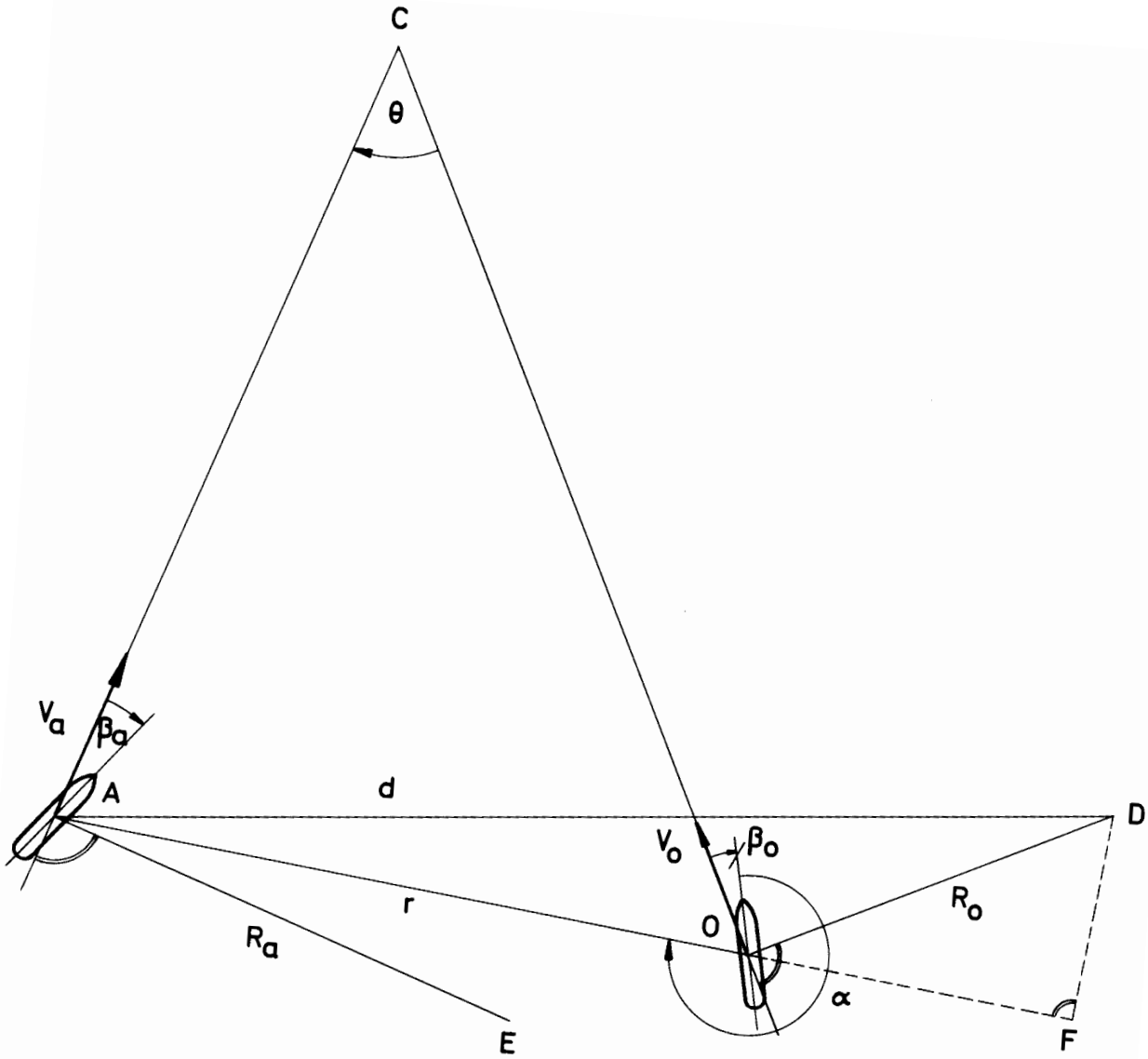

Fig. 3 Geometry of two-ship encounter

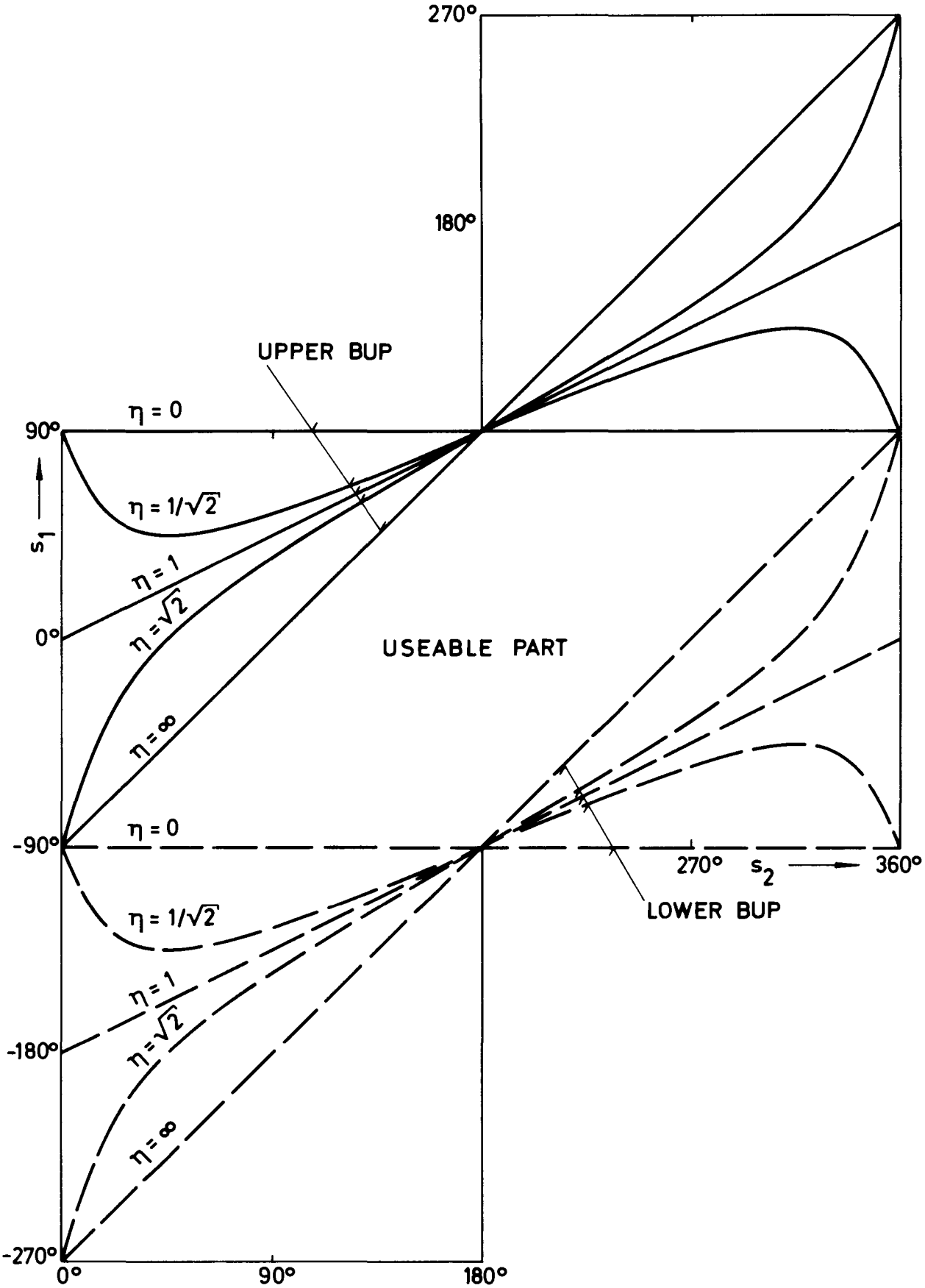

Fig. 4 Terminal bearing angle s_1 versus terminal course angle s_2

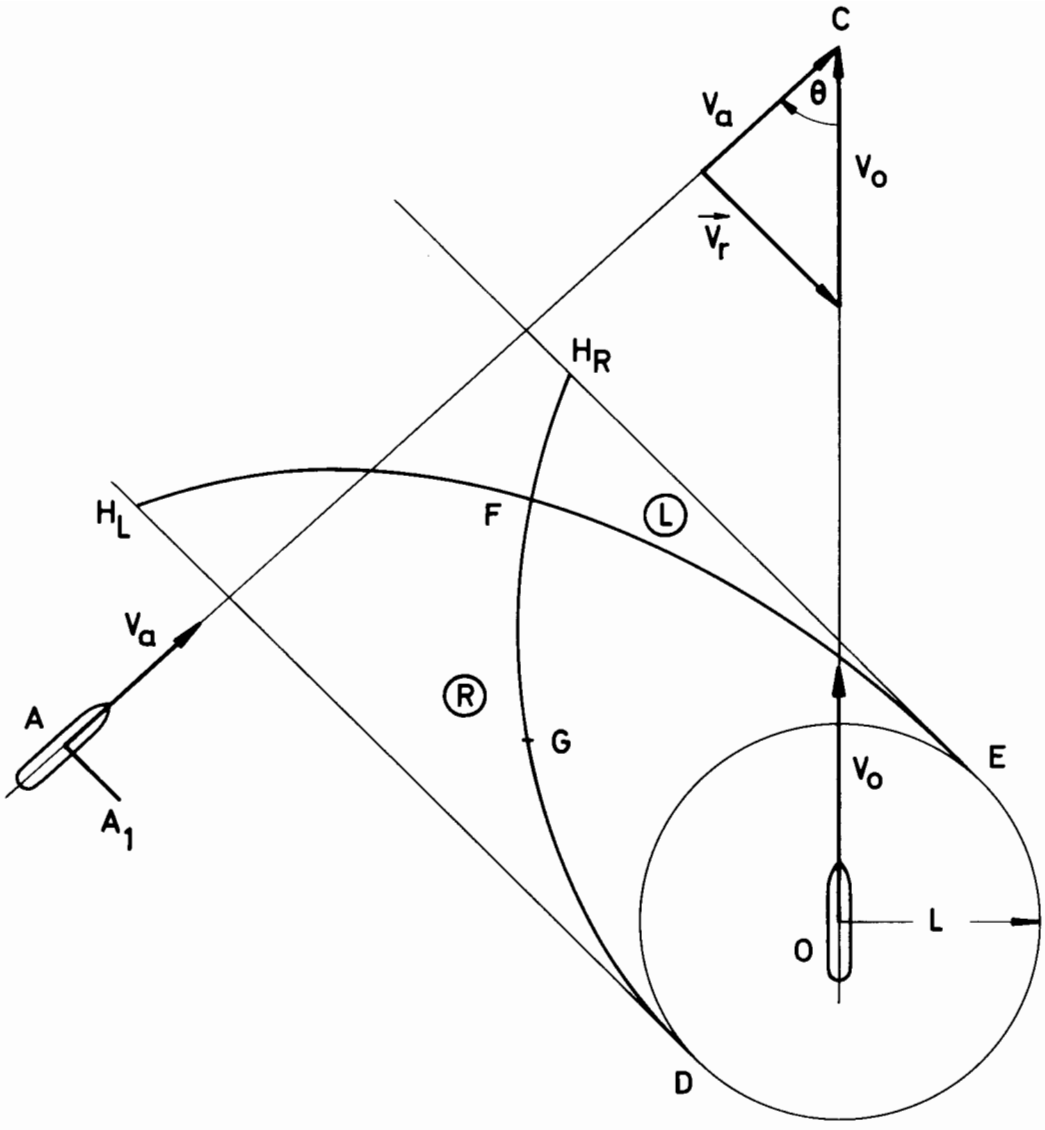

Fig. 5 Sample illustration of critical maneuvers for collisional avoidance

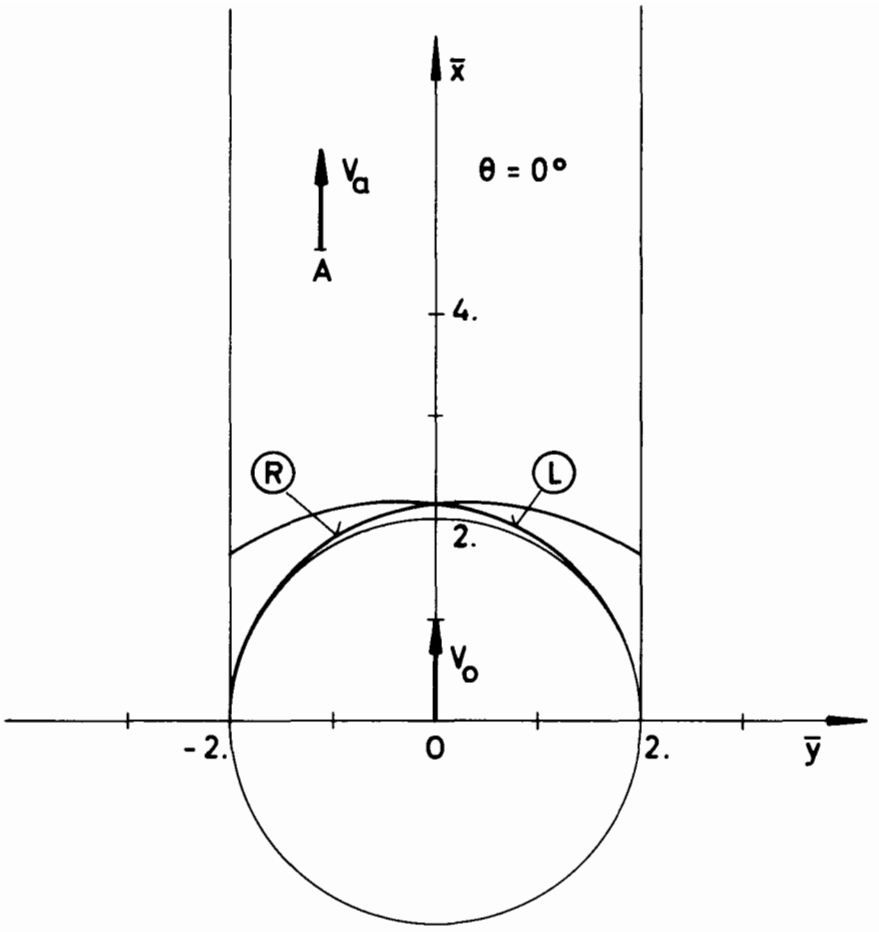

Fig. 6 Calculated barriers for one-ship maneuvers ($V_o > V_a$): Case $\eta = 1/\sqrt{2}$, $l = 2$, $\theta = 0^\circ$

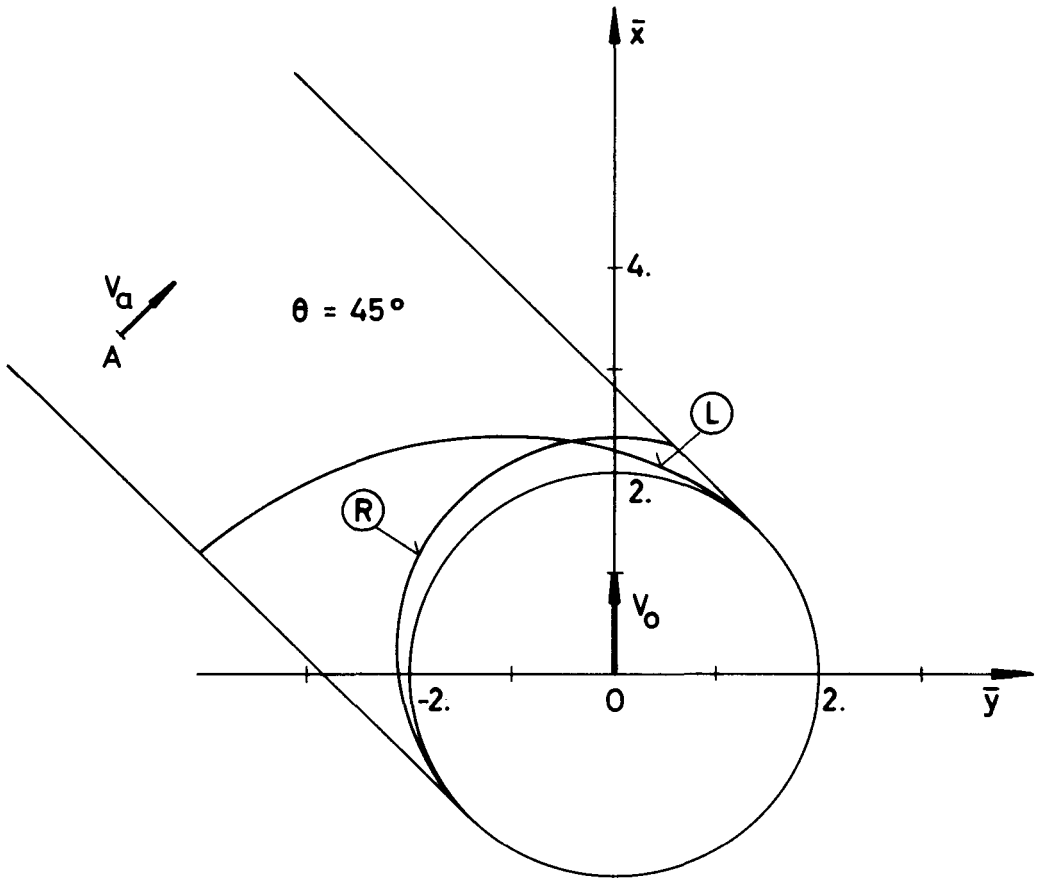

Fig. 7 Calculated barriers for one-ship maneuvers ($V_o > V_a$): Case $\eta = 1/\sqrt{2}$, $\ell = 2$, $\theta = 45^\circ$

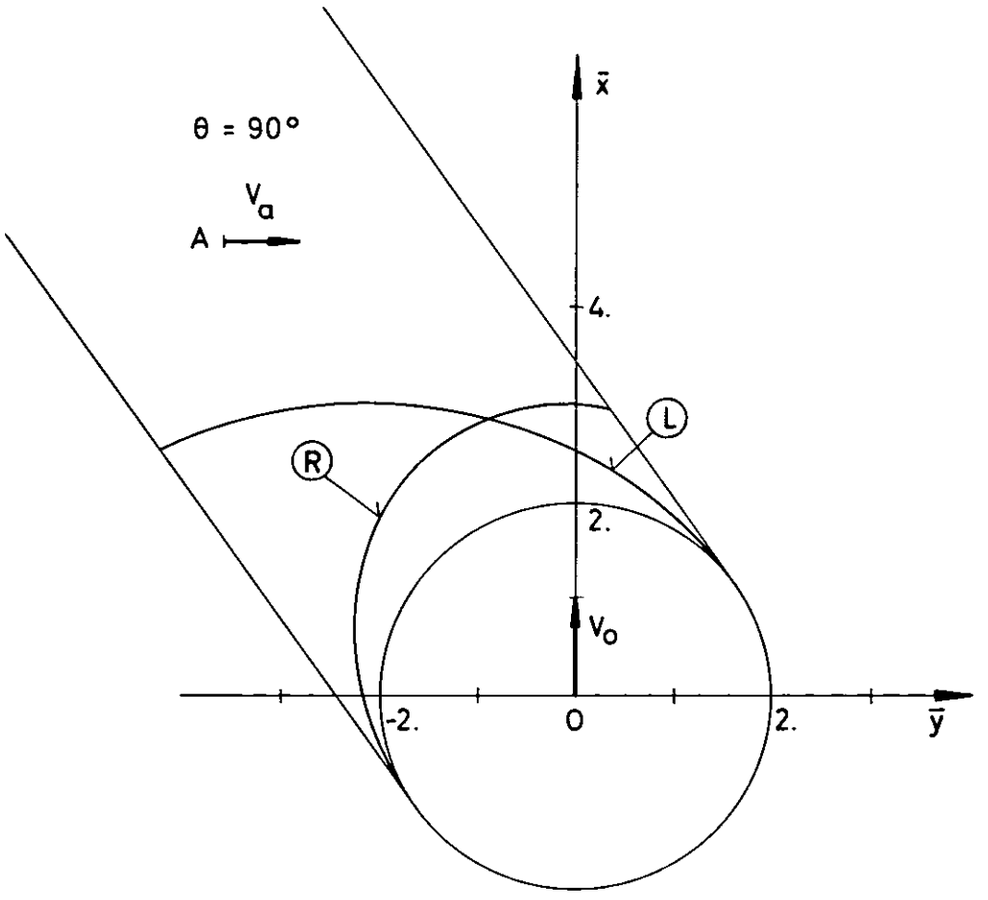

Fig. 8 Calculated barriers for one-ship maneuvers ($V_o > V_a$): Case $\eta = 1/\sqrt{2}$, $l = 2$, $\theta = 90^\circ$

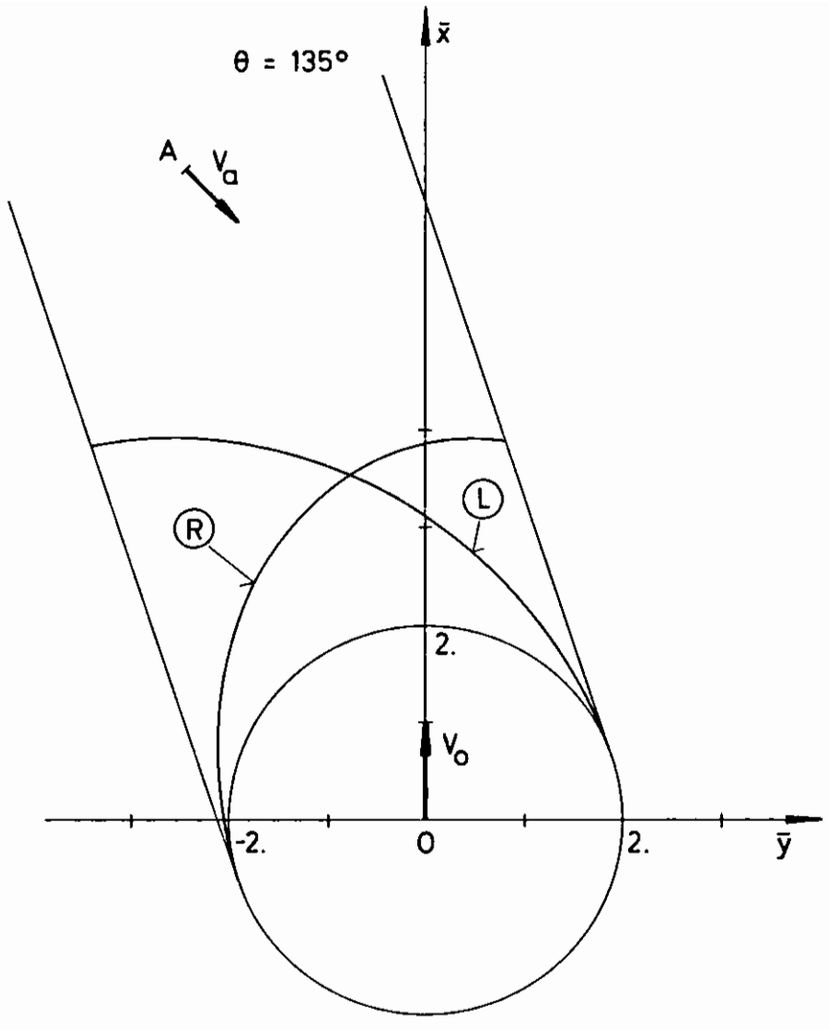

Fig. 9 Calculated barriers for one-ship maneuvers ($V_o > V_a$):
Case $\eta = 1/\sqrt{2}$, $l = 2$, $\theta = 135^\circ$

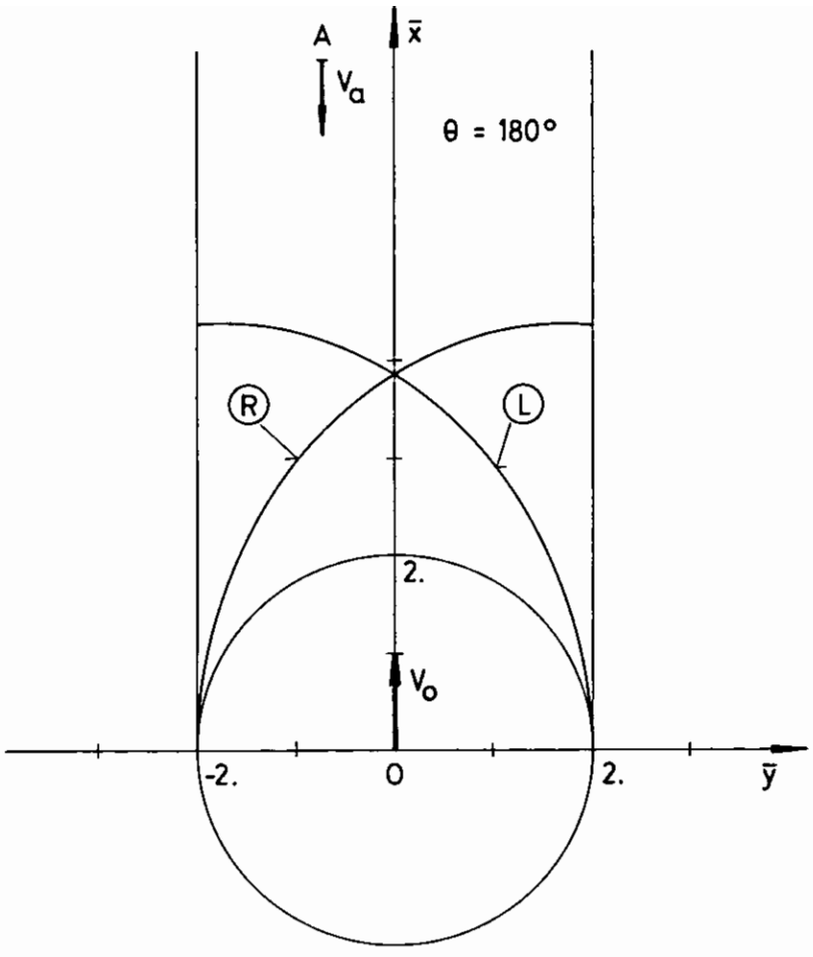

Fig. 10 Calculated barriers for one-ship maneuvers ($V_o > V_a$): Case $\eta = 1/\sqrt{2}$, $\ell = 2$, $\theta = 180^\circ$

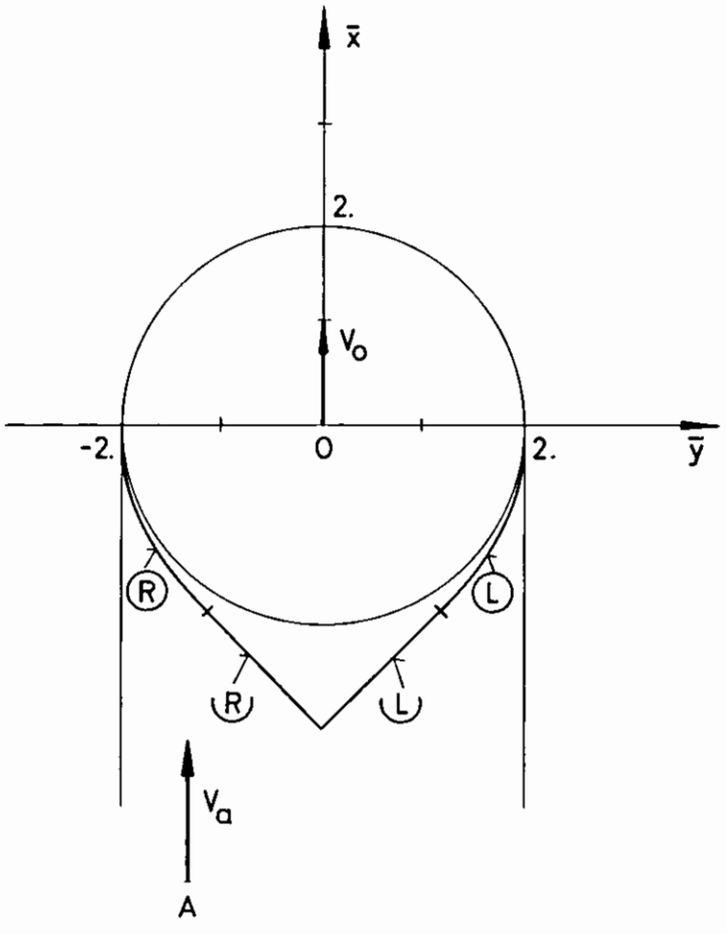

Fig. 11 Calculated barriers for one-ship maneuvers ($V_o < V_a$): Case $\eta = \sqrt{2}$, $l = 2$, $\theta = 0^o$

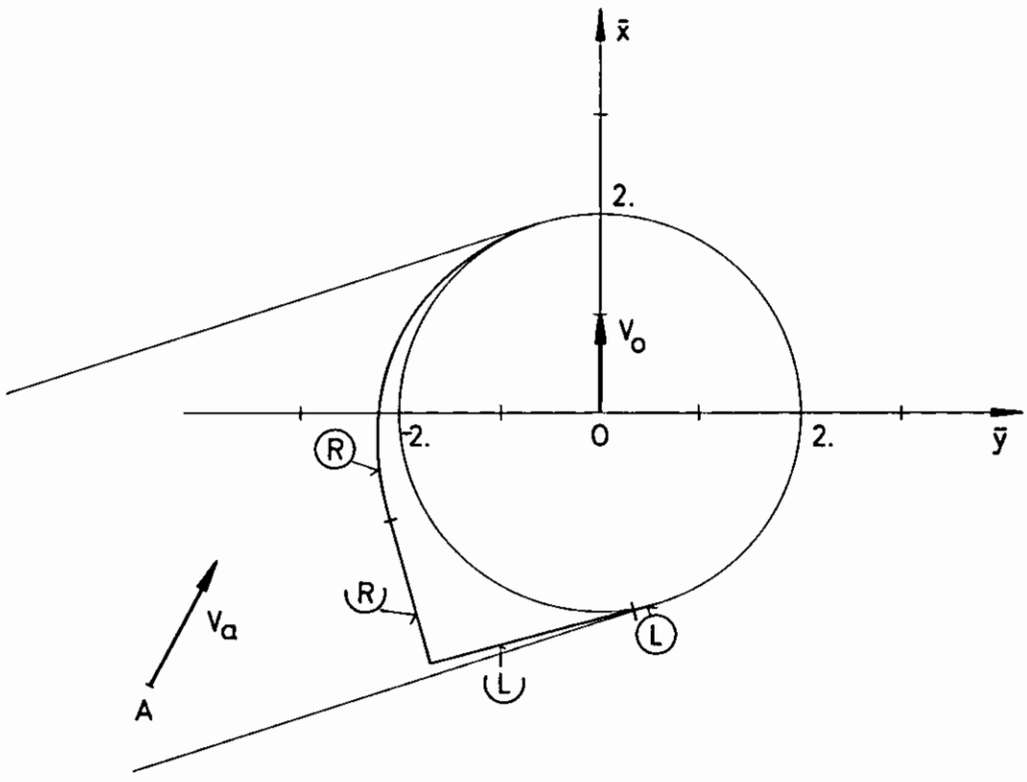

Fig. 12 Calculated barriers for one-ship maneuvers ($V_o < V_a$): Case $\eta = \sqrt{2}$, $l = 2$, $\theta = 30^o$

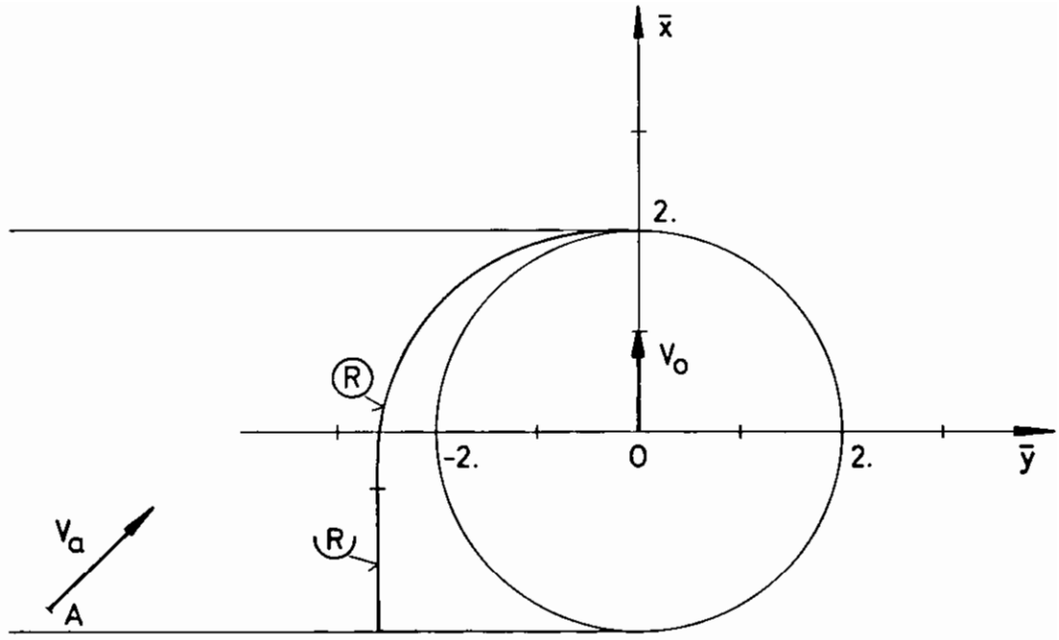

Fig. 13 Calculated barriers for one-ship maneuvers ($V_o < V_a$): Case $\eta = \sqrt{2}$, $l = 2$, $\theta = 45^o$

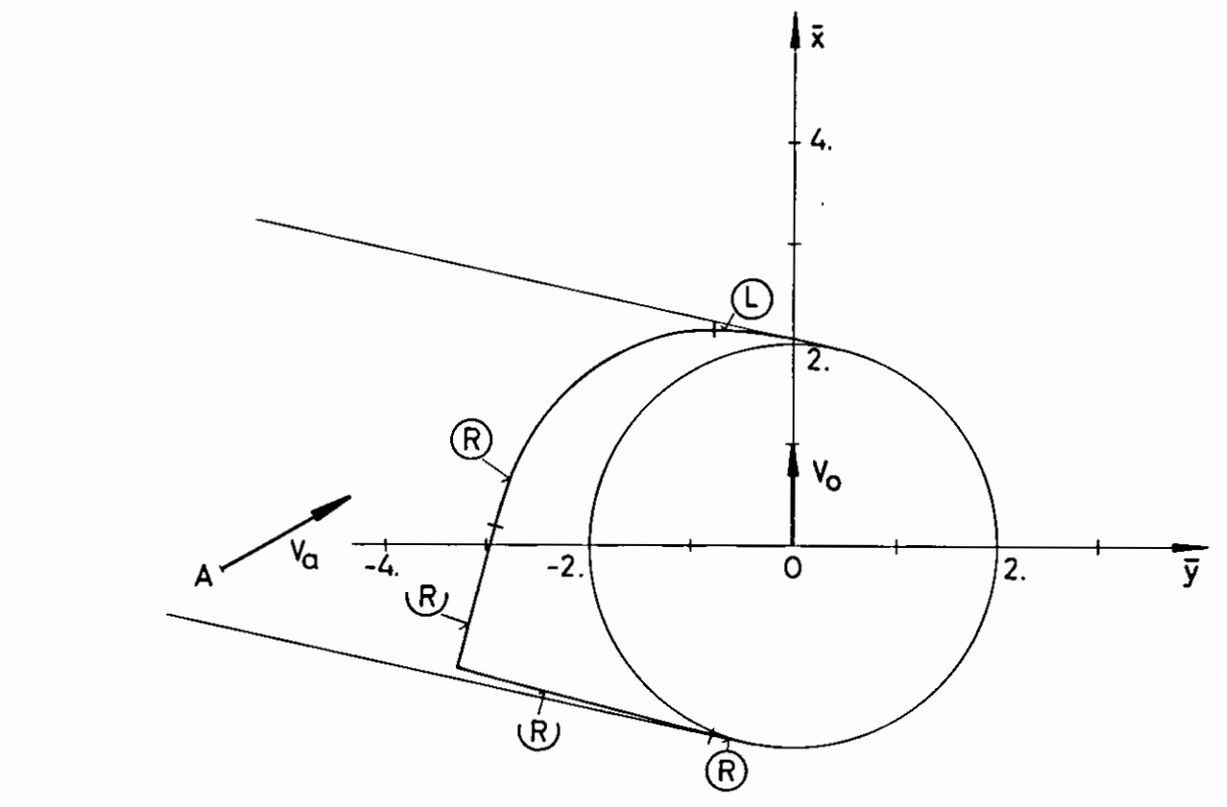

Fig. 14 Calculated barriers for one-ship maneuvers ($V_o < V_a$): Case $\eta = \sqrt{2}$, $l = 2$, $\theta = 60^\circ$

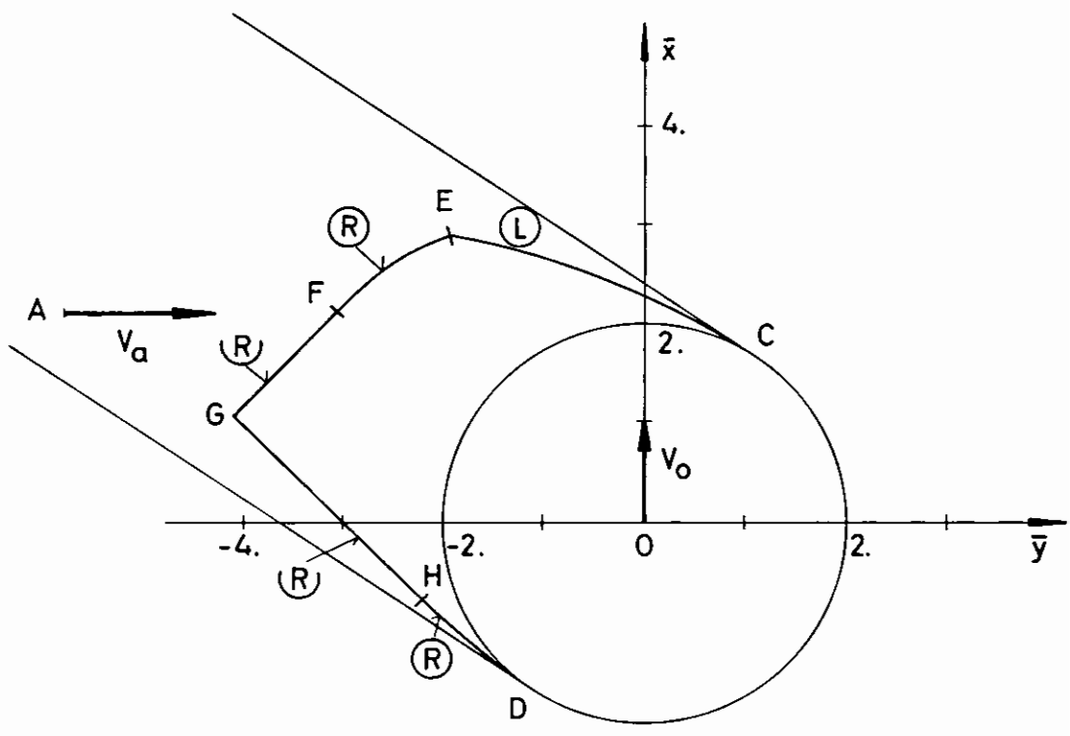

Fig. 15 Calculated barriers for one-ship maneuvers ($V_o < V_a$): Case $\eta = \sqrt{2}$, $l = 2$, $\theta = 90^o$

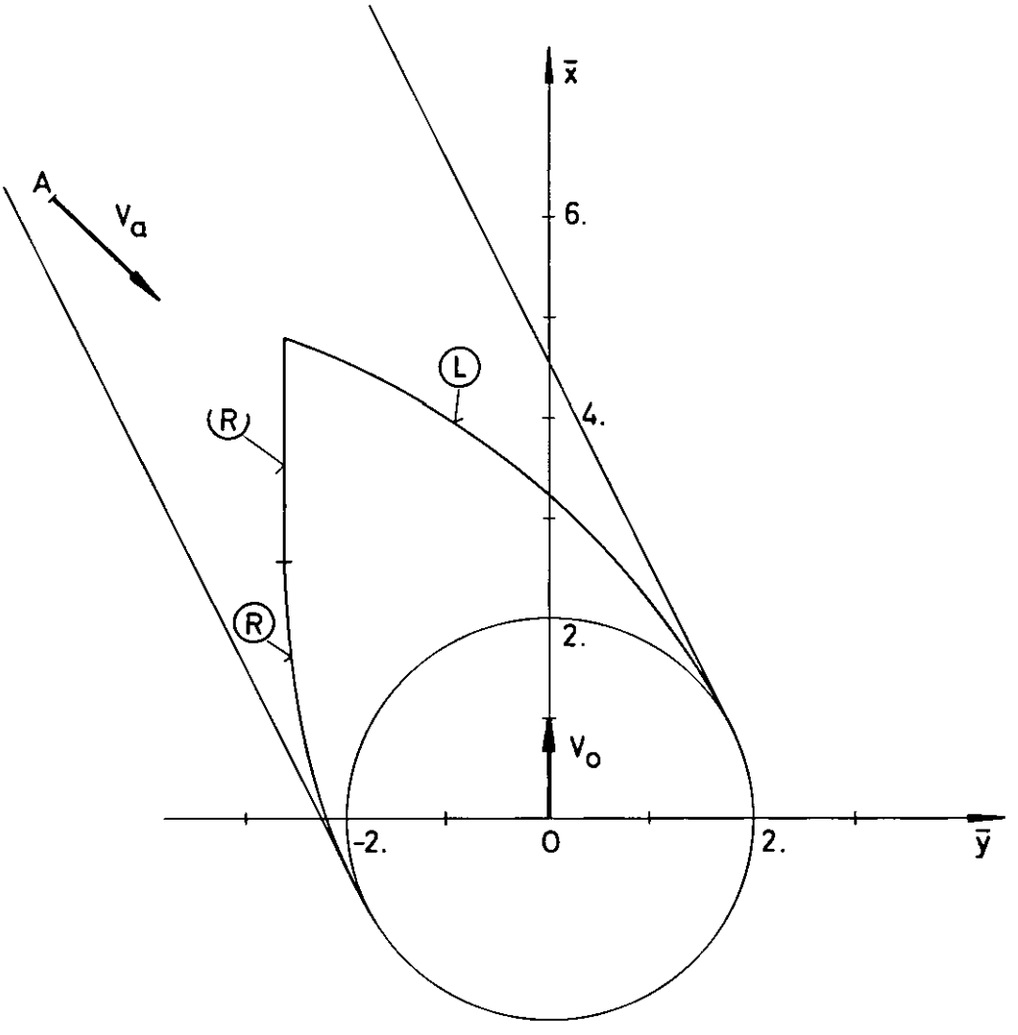

Fig. 16 Calculated barriers for one-ship maneuvers ($V_o < V_a$): Case $\eta = \sqrt{2}$, $l = 2$, $\theta = 135^\circ$

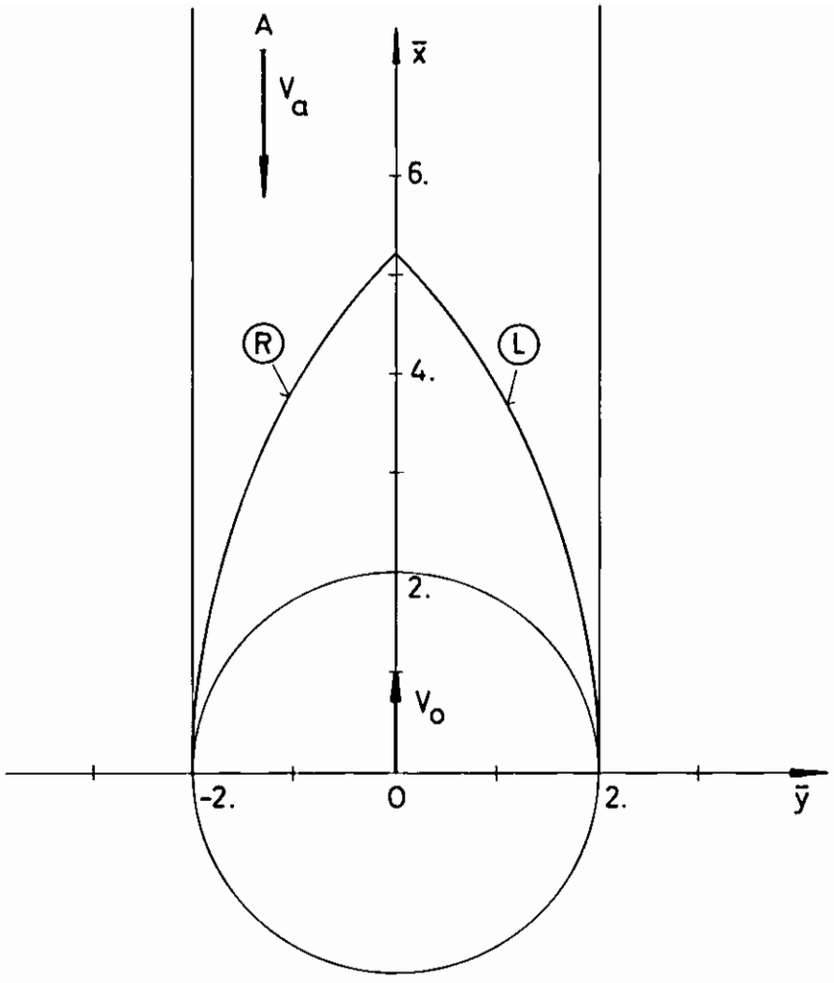

Fig. 17 Calculated barriers for one-ship maneuvers ($V_o < V_a$): Case $\eta = \sqrt{2}$, $l = 2$, $\theta = 180^\circ$

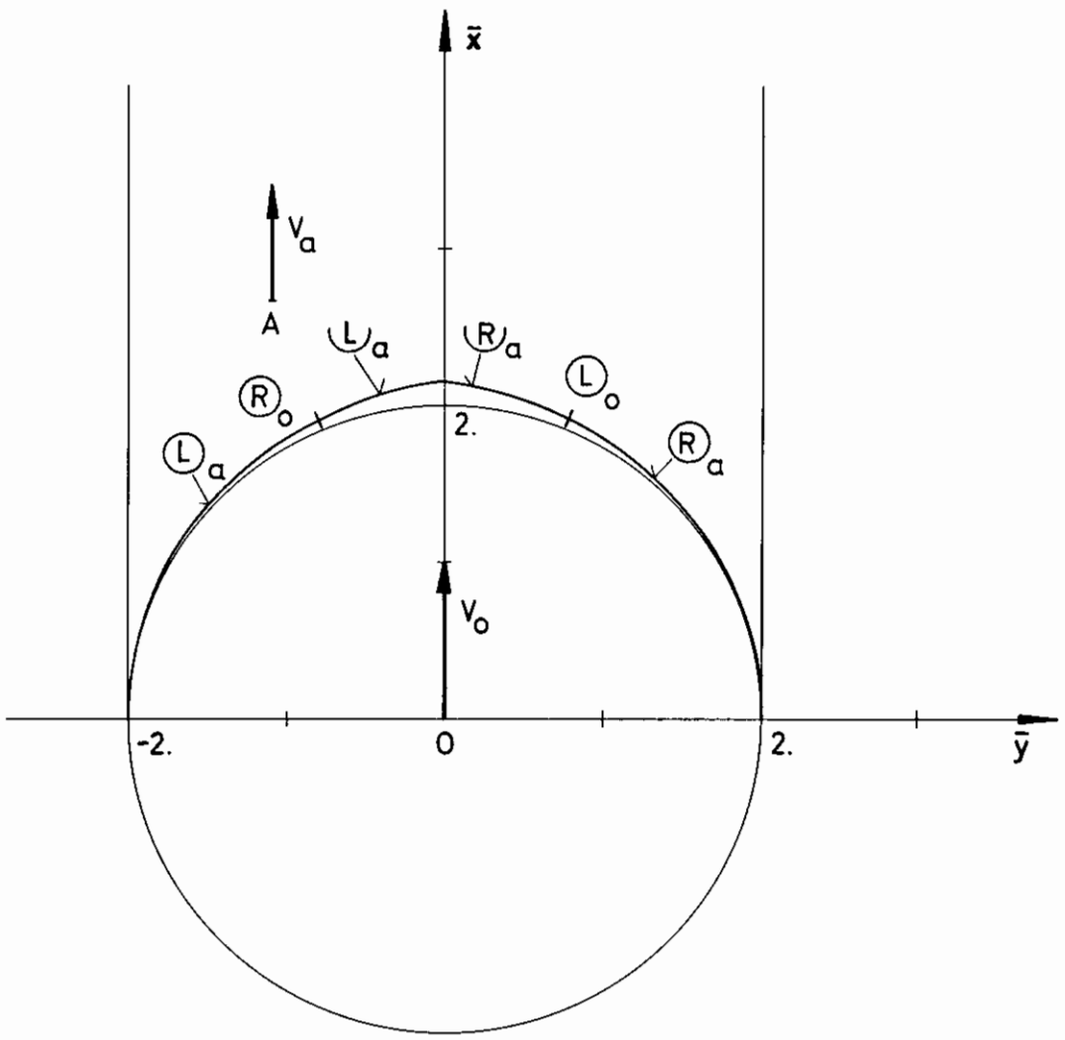

Fig. 18 Calculated barriers for collaborative two-ship maneuvers ($V_o > V_a$, $R_o > R_a$):
Case $\eta = 1/\sqrt{2}$, $l = 2$, $\lambda = 1/2$, $\theta = 0^\circ$

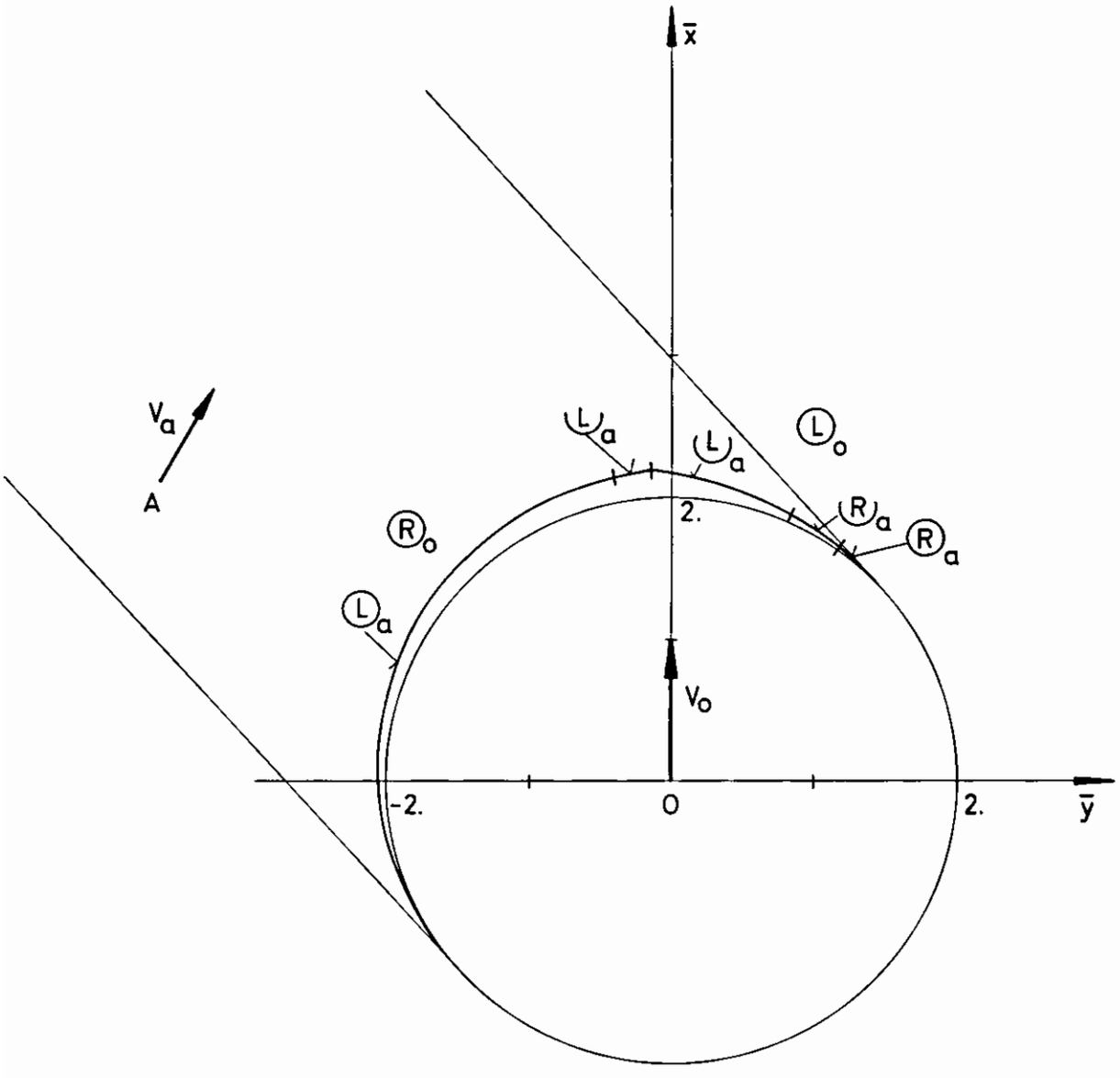

Fig. 19 Calculated barriers for collaborative two-ship maneuvers ($V_o > V_a$, $R_o > R_a$):
Case $\eta = 1/\sqrt{2}$, $l = 2$, $\lambda = 1/2$, $\theta = 30^o$

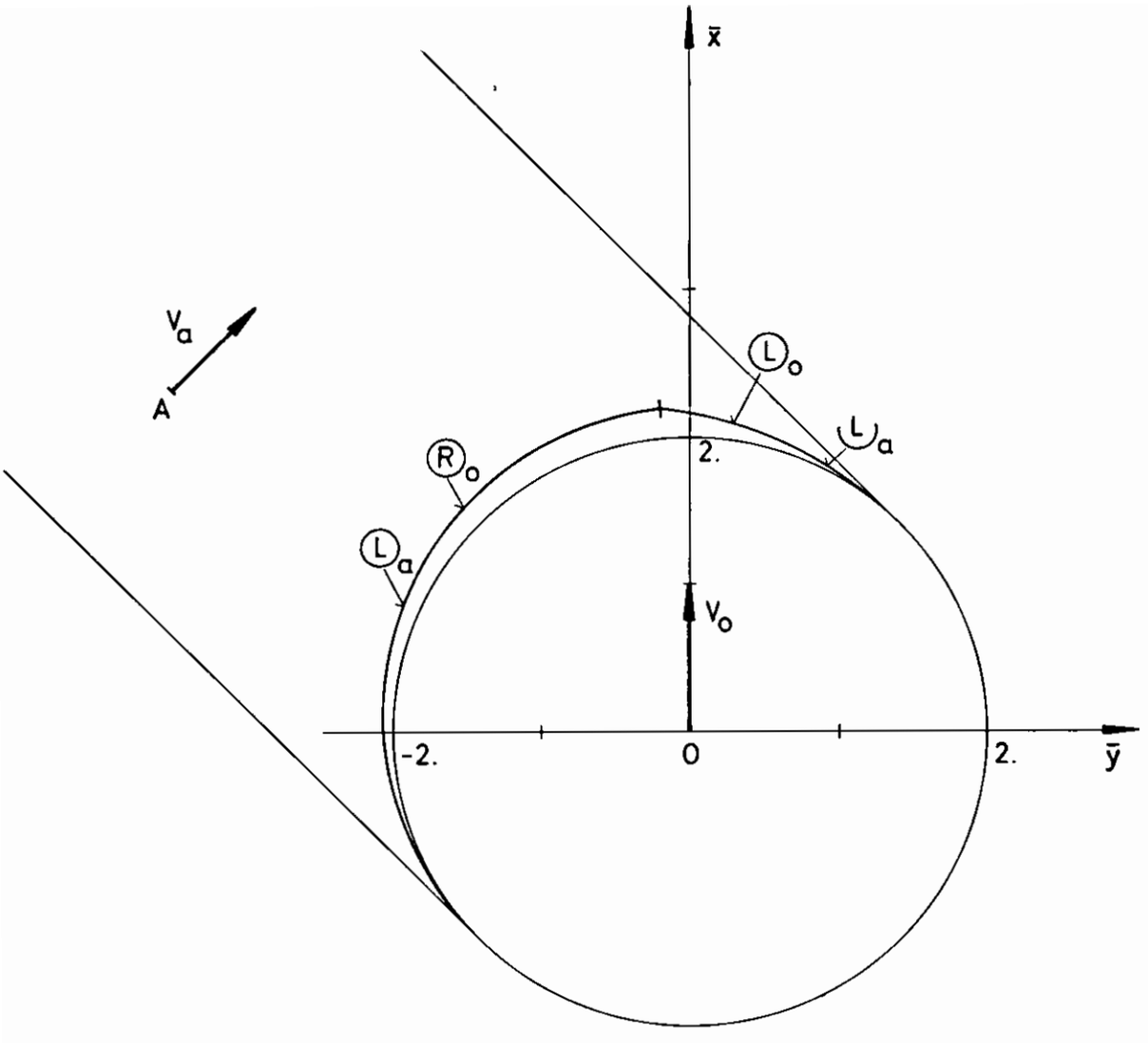

Fig. 20 Calculated barriers for collaborative two-ship maneuvers ($V_o > V_a$, $R_o > R_a$):
Case $\eta = 1/\sqrt{2}$, $l = 2$, $\lambda = 1/2$ $\theta = 45^o$

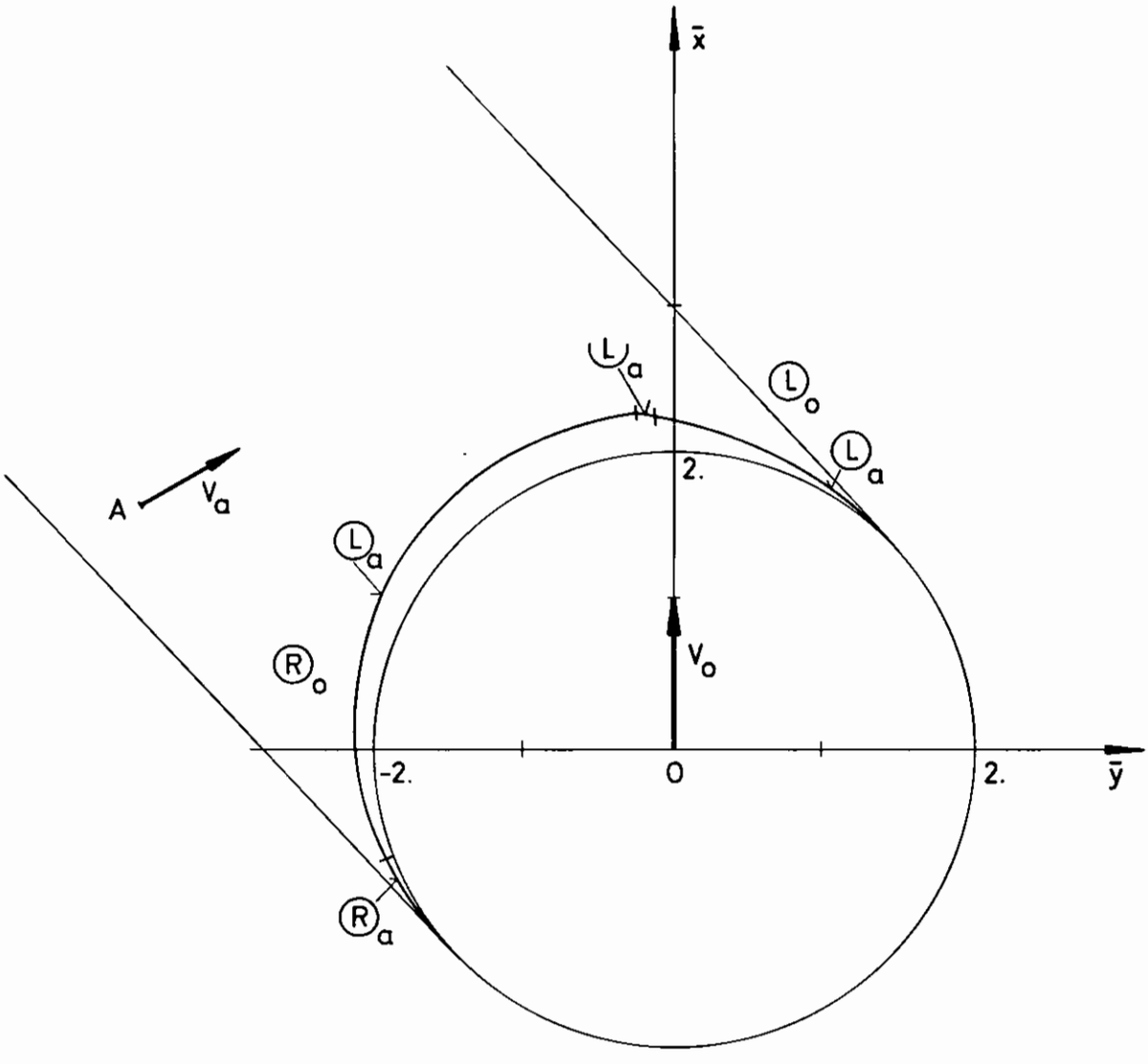

Fig. 21 Calculated barriers for collaborative two-ship maneuvers ($V_o > V_a$, $R_o > R_a$):
Case $\eta = 1/\sqrt{2}$, $l = 2$, $\lambda = 1/2$, $\theta = 60^\circ$

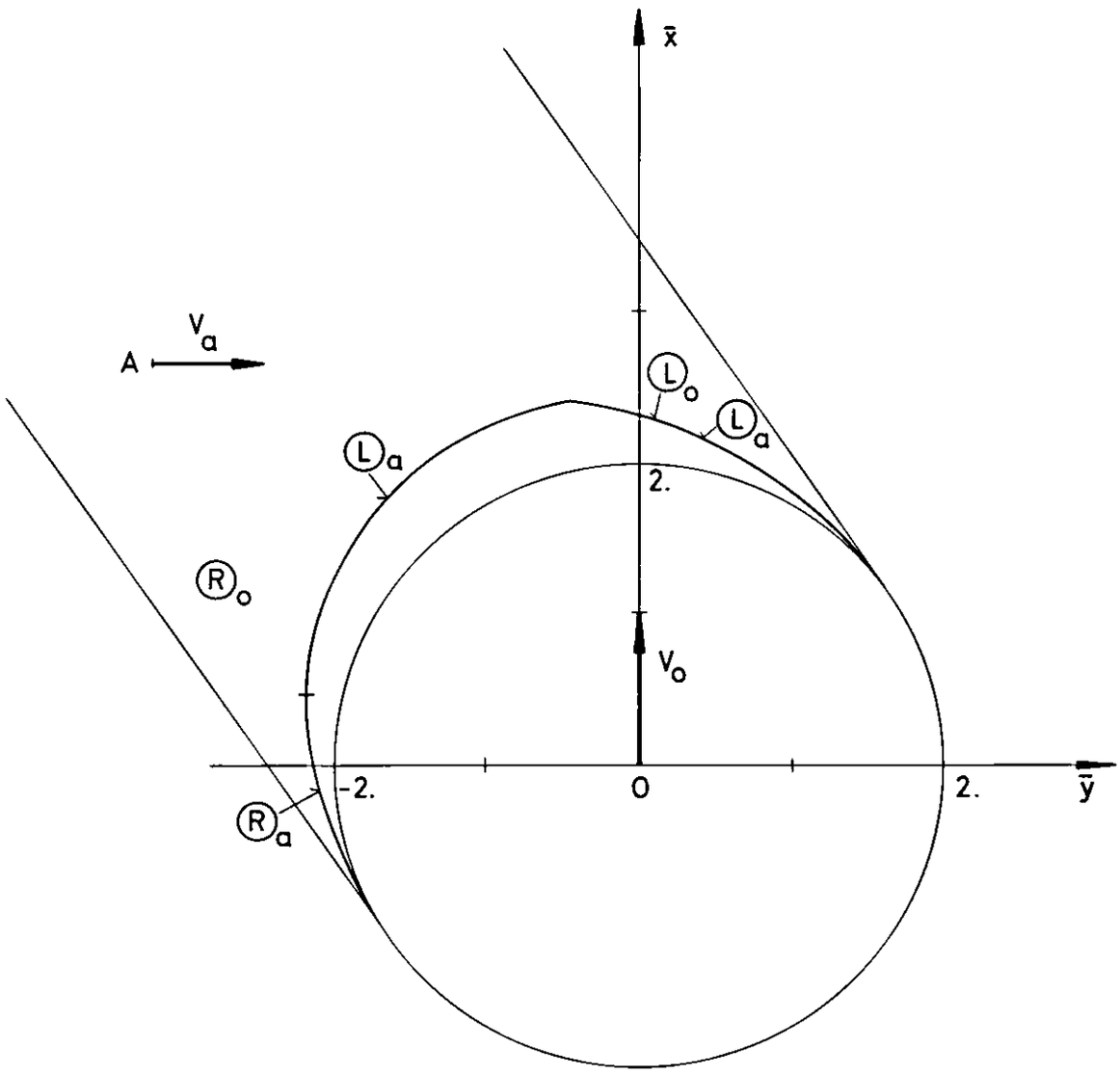

Fig. 22 Calculated barriers for collaborative two-ship maneuvers ($V_o > V_a$, $R_o > R_a$):
Case $\eta = 1/\sqrt{2}$, $l = 2$, $\lambda = 1/2$, $\theta = 90^\circ$

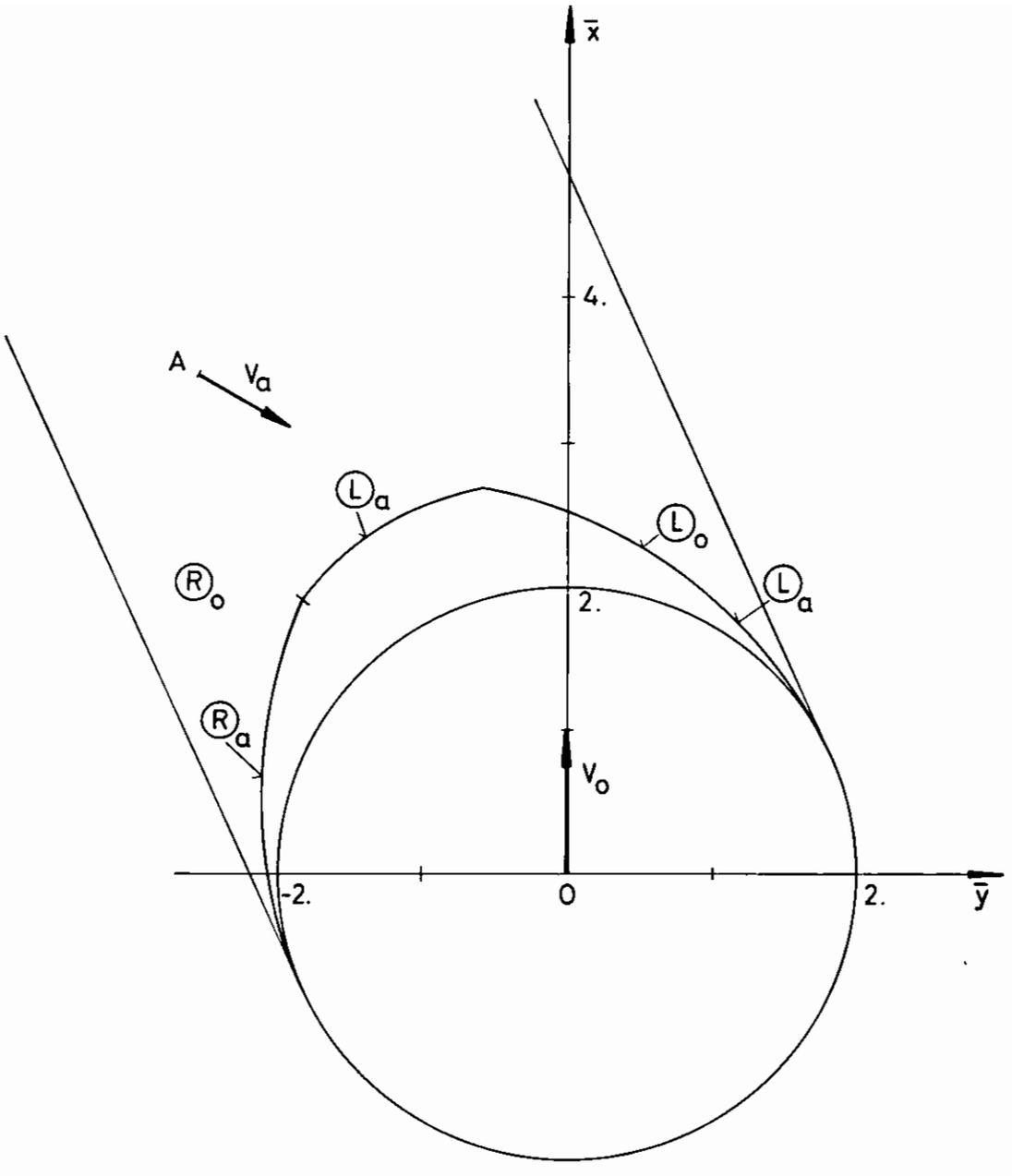

Fig. 23 Calculated barriers for collaborative two-ship maneuvers ($V_o > V_a$, $R_o > R_a$):
Case $\eta = 1/\sqrt{2}$, $l = 2$, $\lambda = 1/2$, $\theta = 120^o$

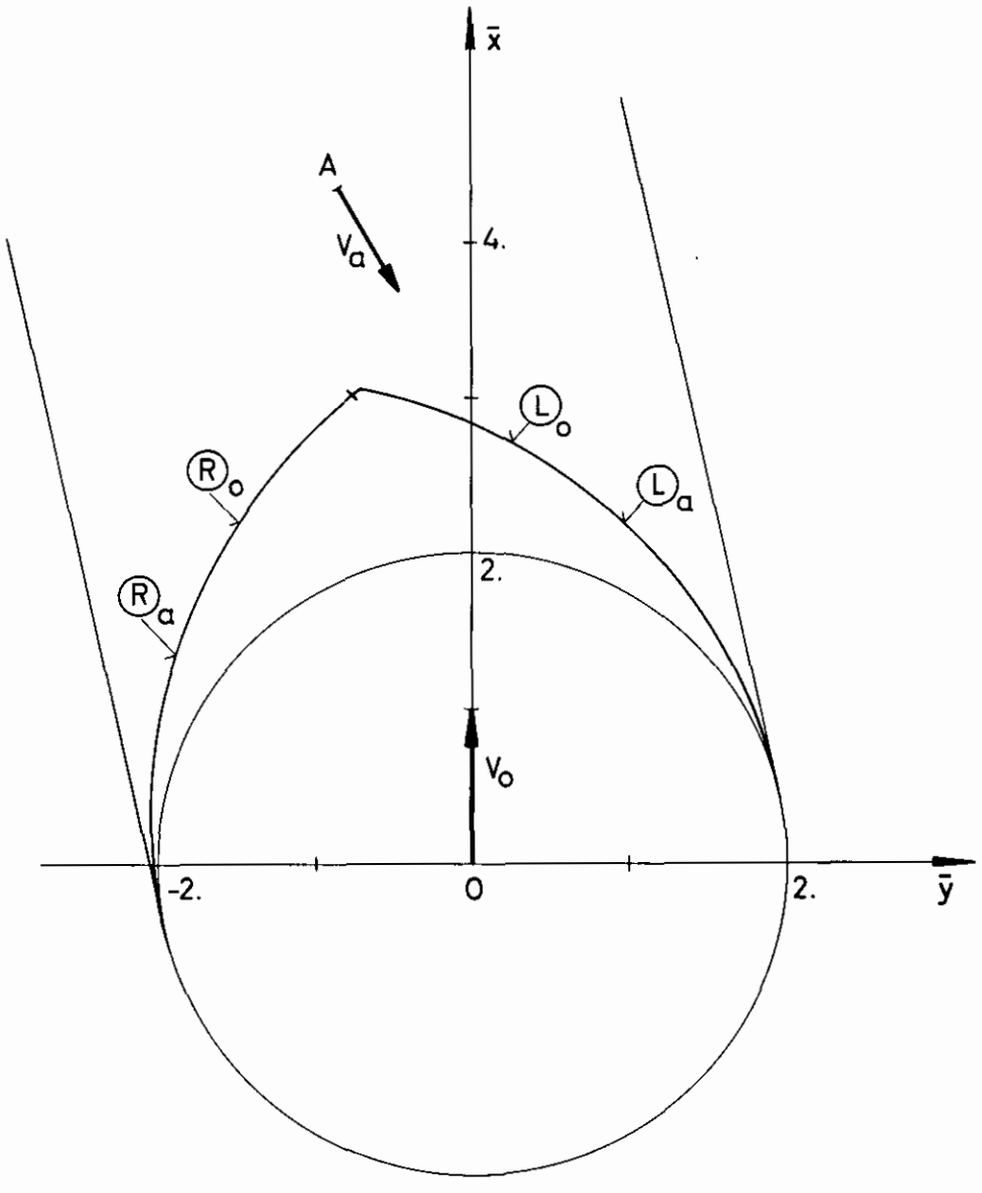

Fig. 24 Calculated barriers for collaborative two-ship maneuvers ($V_o > V_a$, $R_o > R_a$):
Case $\eta = 1/\sqrt{2}$, $\ell = 2$, $\lambda = 1/2$, $\theta = 150^o$

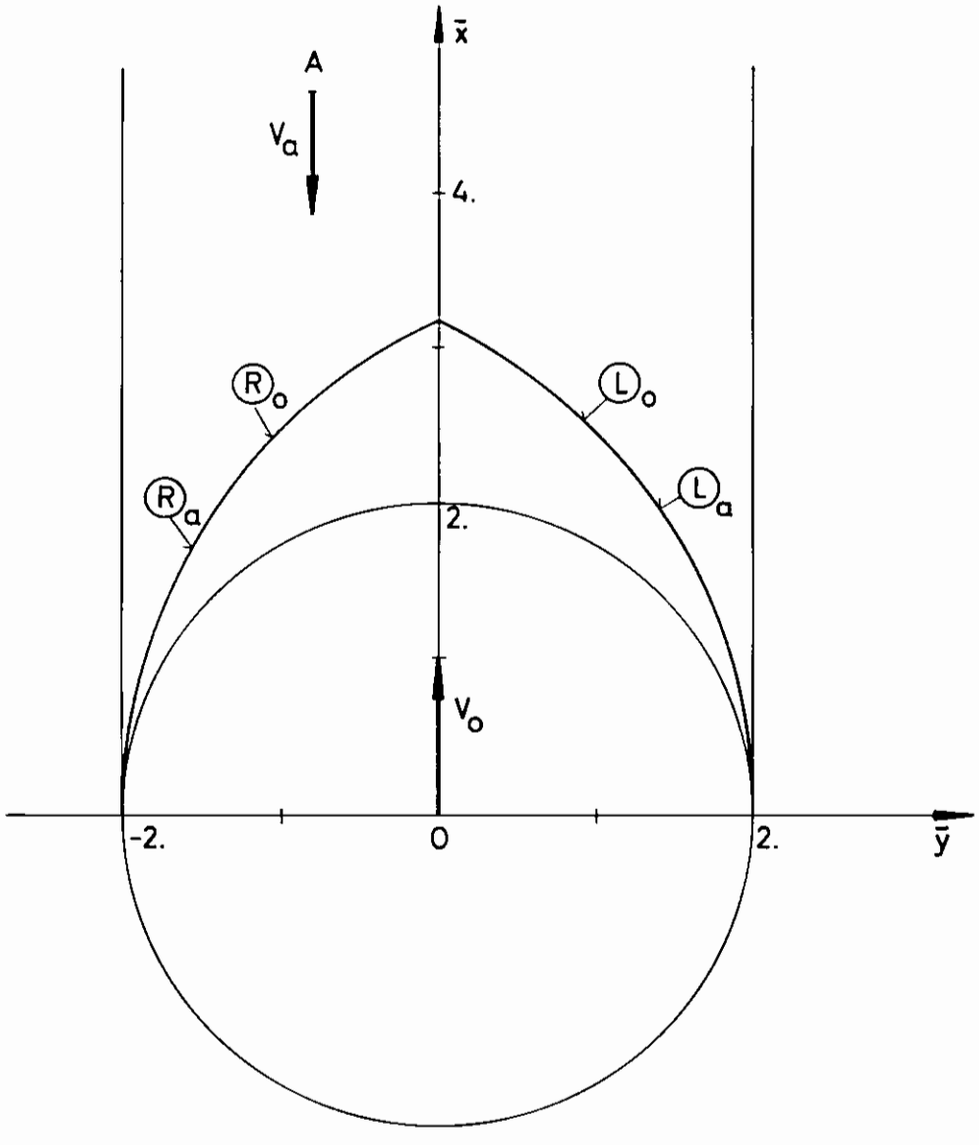

Fig. 25 Calculated barriers for collaborative two-ship maneuvers ($V_o > V_a$, $R_o > R_a$):
Case $\eta = 1/\sqrt{2}$, $l = 2$, $\lambda = 1/2$, $\theta = 180^o$

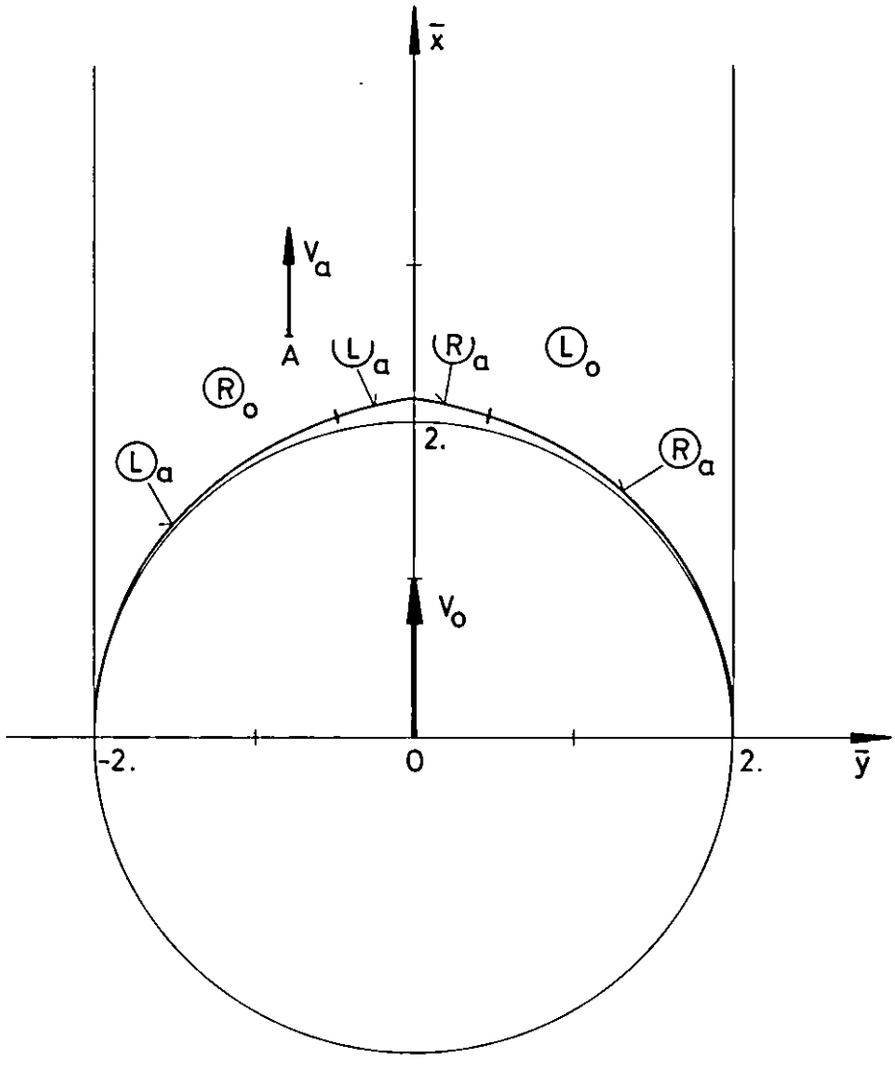

Fig. 26 Calculated barriers for collaborative two-ship maneuvers ($V_o > V_a$, $R_o = R_a$):
Case $\eta = 1/\sqrt{2}$, $l = 2$, $\lambda = 1$, $\theta = 0^o$

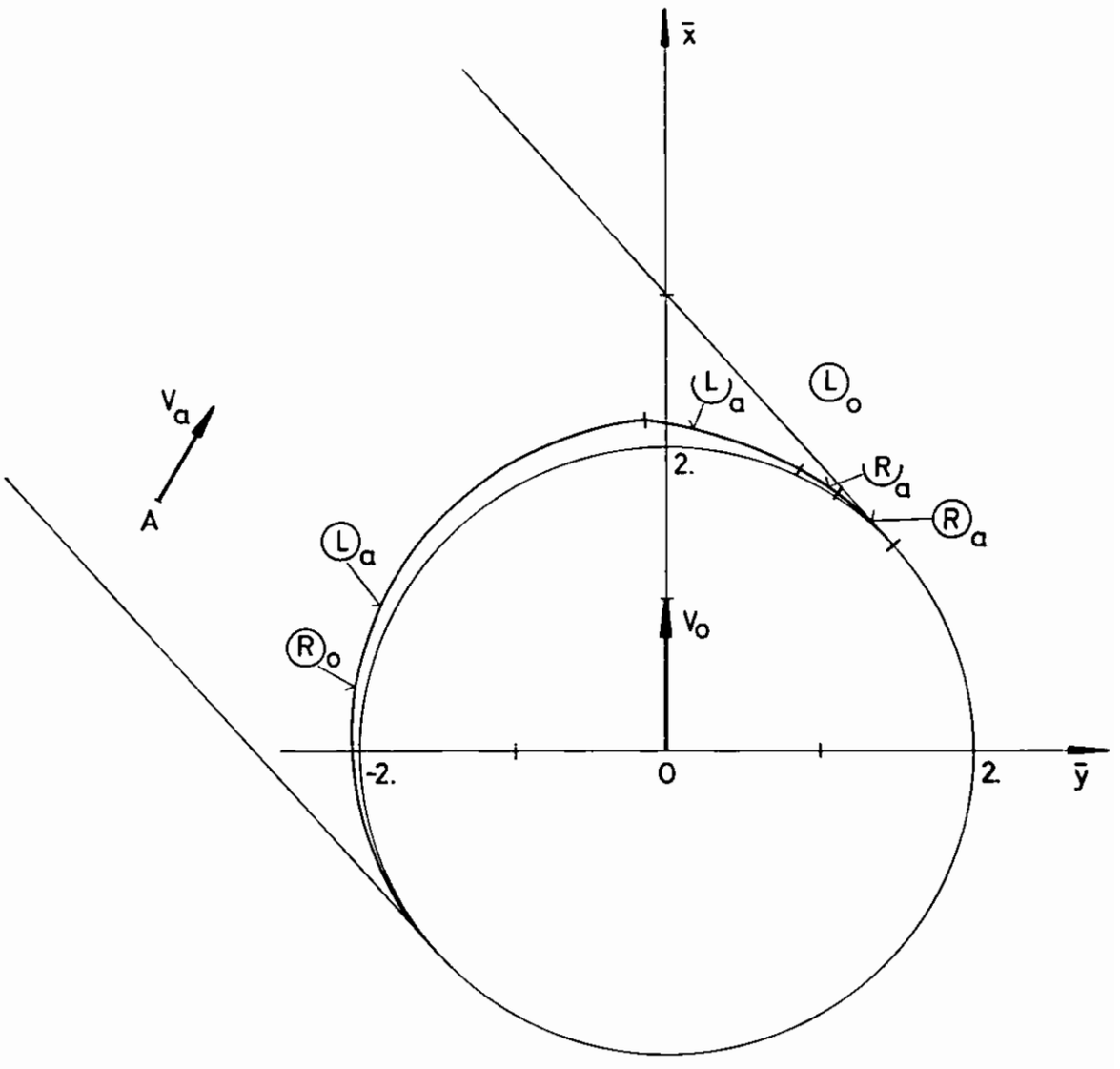

Fig. 27 Calculated barriers for collaborative two-ship maneuvers ($V_o > V_a$, $R_o = R_a$):
Case $\eta = 1/\sqrt{2}$, $l = 2$, $\lambda = 1$, $\theta = 30^o$

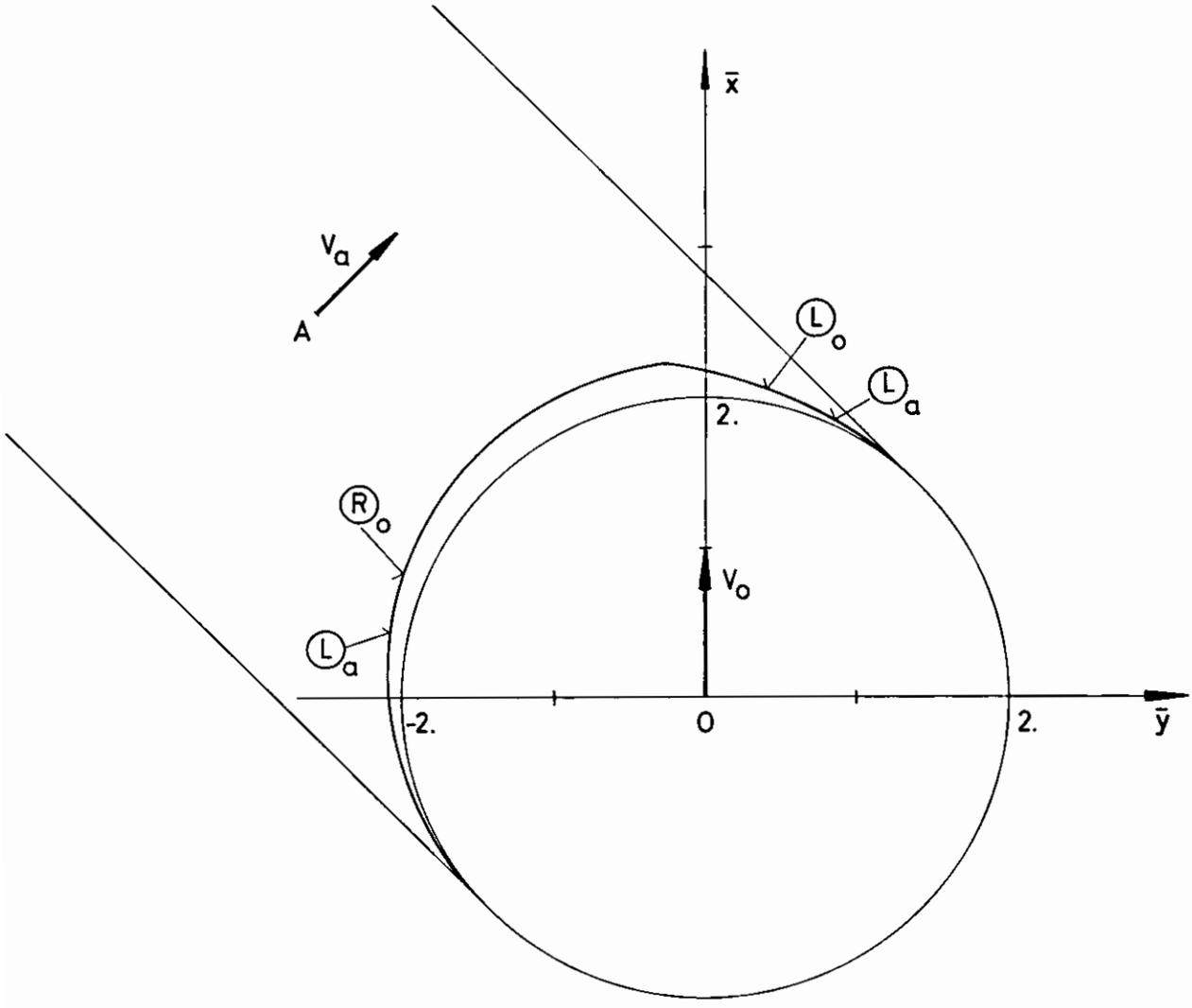

Fig. 28 Calculated barriers for collaborative two-ship maneuvers ($V_o > V_a$, $R_o = R_a$):
Case $\eta = 1/\sqrt{2}$, $l = 2$, $\lambda = 1$, $\theta = 45^o$

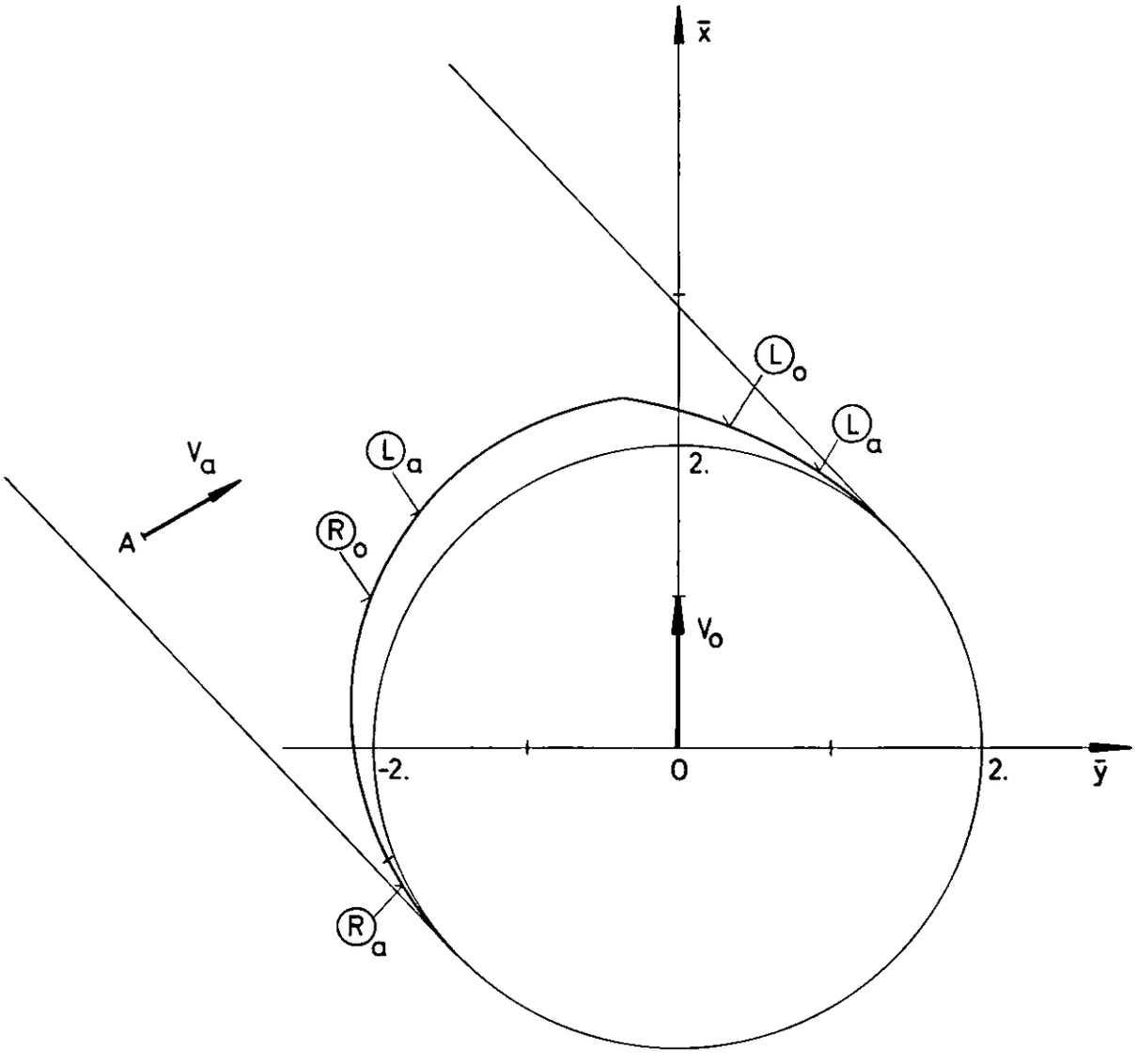

Fig. 29 Calculated barriers for collaborative two-ship maneuvers ($V_o > V_a$, $R_o = R_a$):
Case $\eta = 1/\sqrt{2}$, $l = 2$, $\lambda = 1$, $\theta = 60^o$

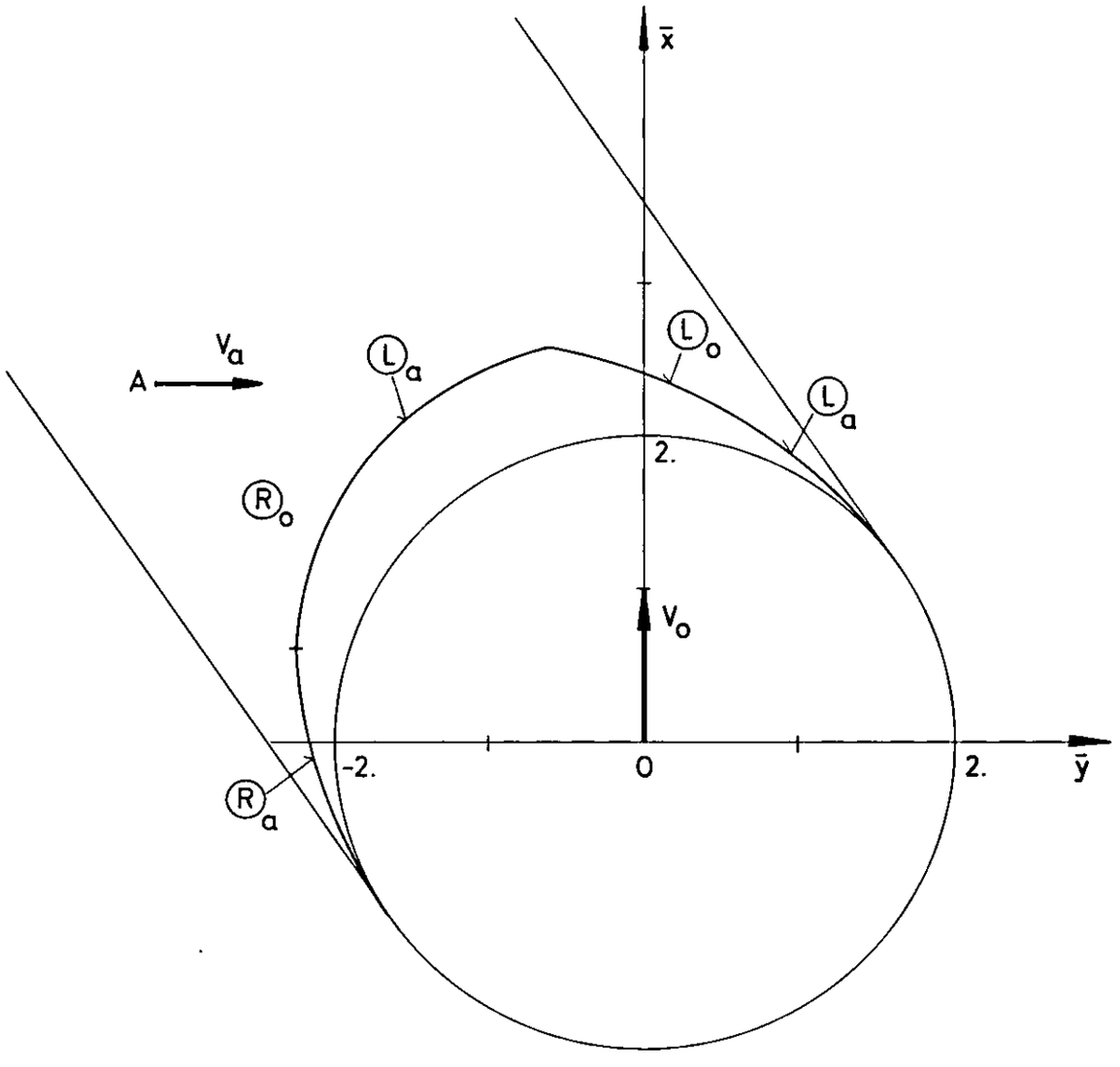

Fig. 30 Calculated barriers for collaborative two-ship maneuvers ($V_o > V_a$, $R_o = R_a$):
Case $\eta = 1/\sqrt{2}$, $\ell = 2$, $\lambda = 1$, $\theta = 90^o$

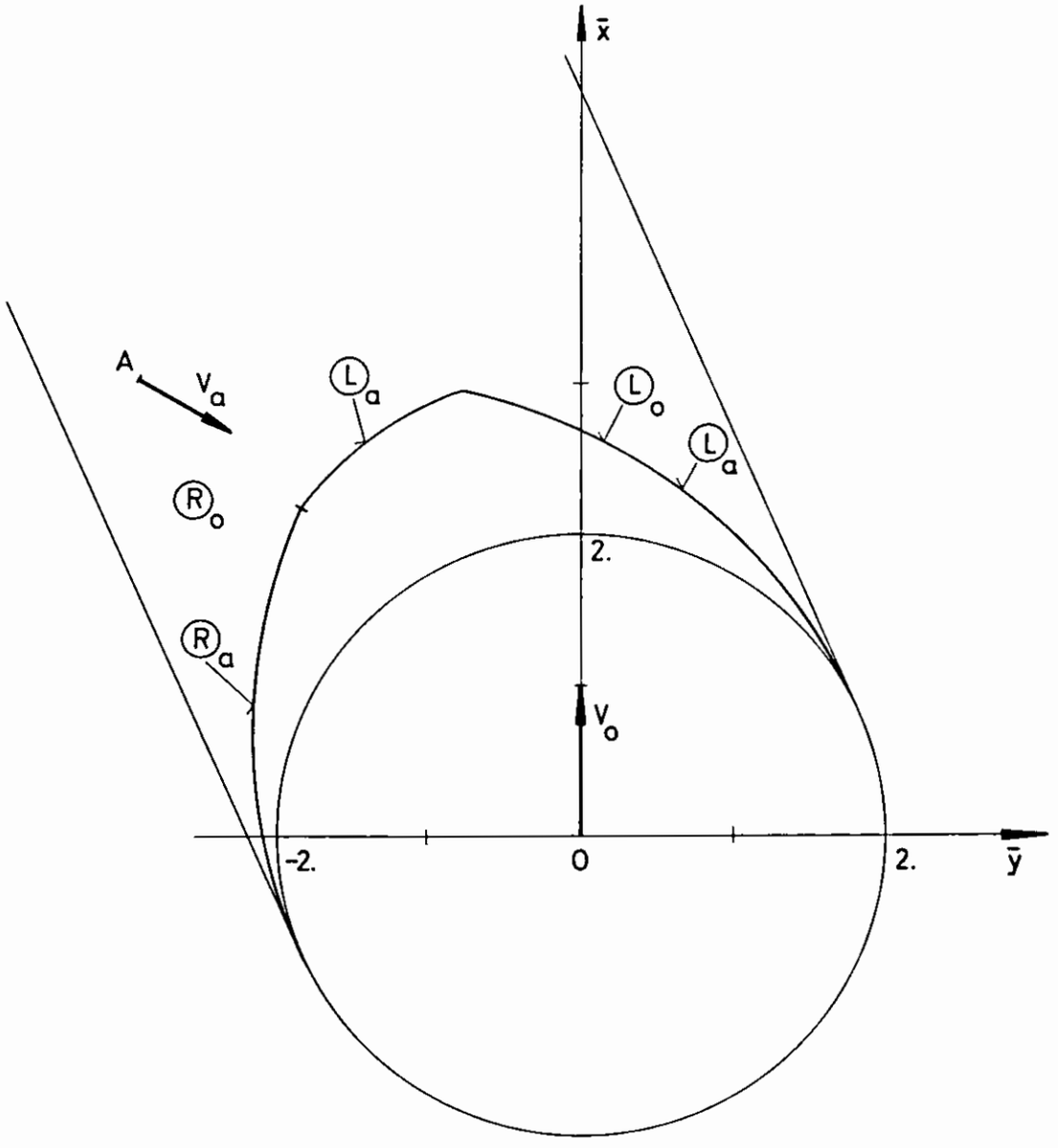

Fig. 31 Calculated barriers for collaborative two-ship maneuvers ($V_o > V_a$, $R_o = R_a$):
Case $\eta = 1/\sqrt{2}$, $l = 2$, $\lambda = 1$, $\theta = 120^\circ$

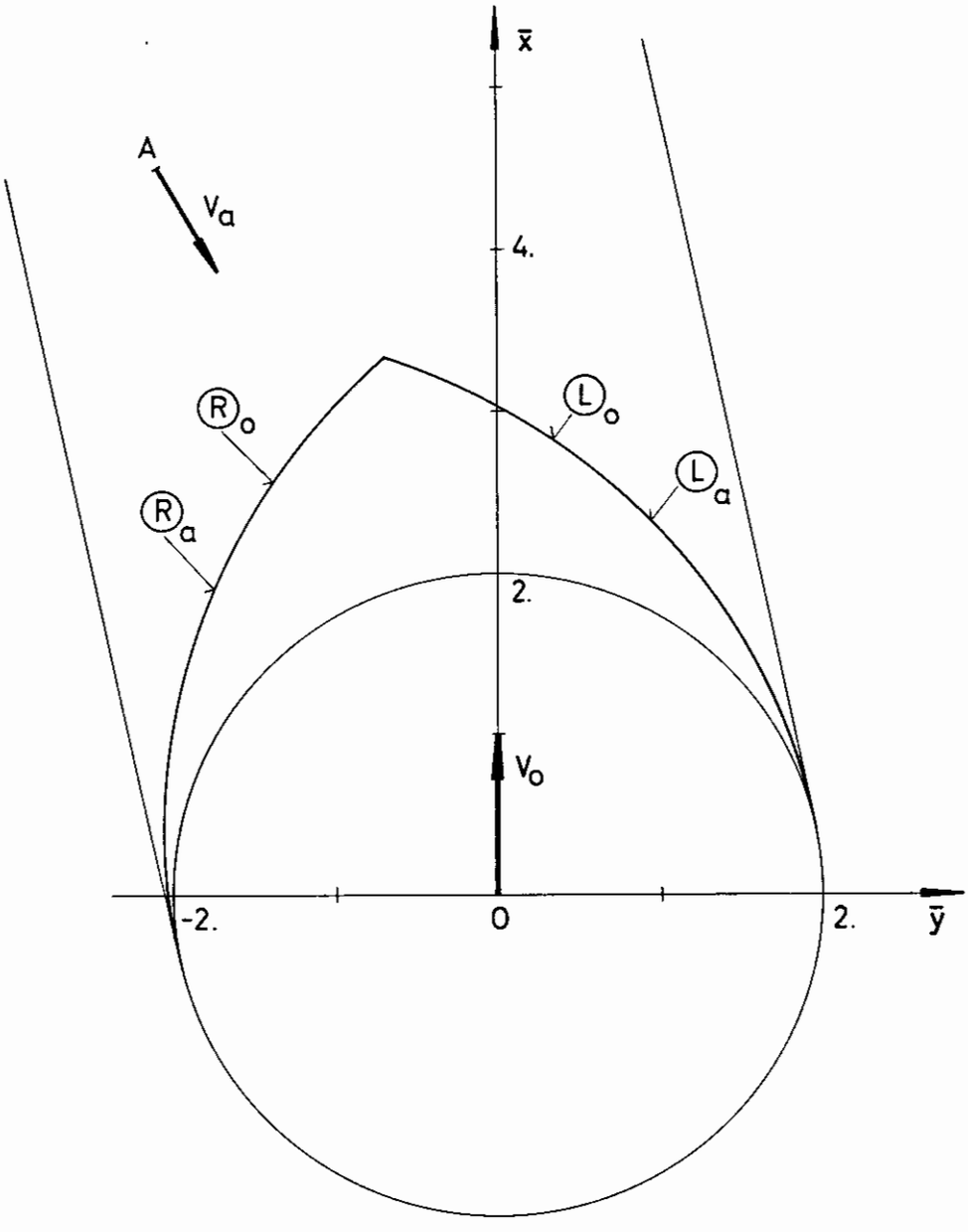

Fig. 32 Calculated barriers for collaborative two-ship maneuvers ($V_o > V_a$, $R_o = R_a$):
Case $\eta = 1/\sqrt{2}$, $l = 2$, $\lambda = 1$, $\theta = 150^o$

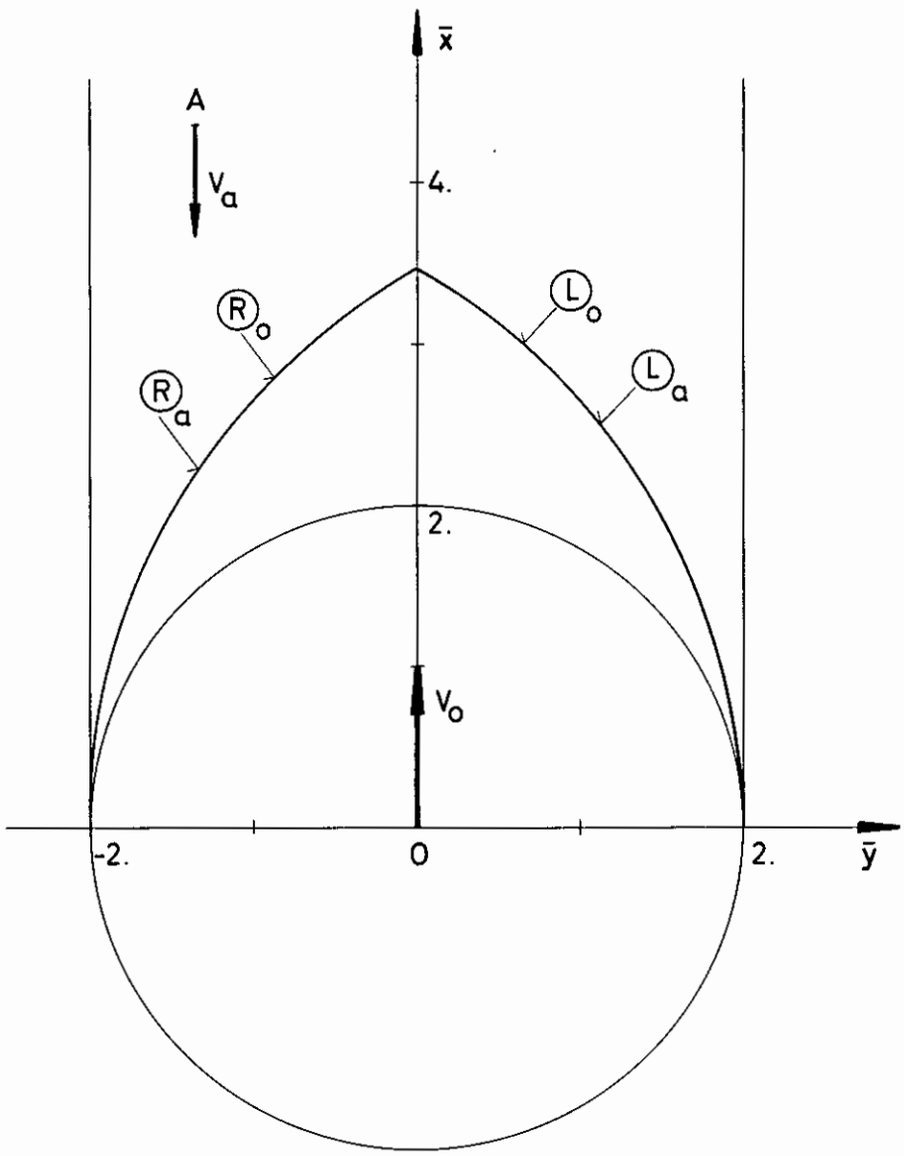

Fig. 33 Calculated barriers for collaborative two-ship maneuvers ($V_o > V_a$, $R_o = R_a$):
Case $\eta = 1/\sqrt{2}$, $l = 2$, $\lambda = 1$, $\theta = 180^\circ$

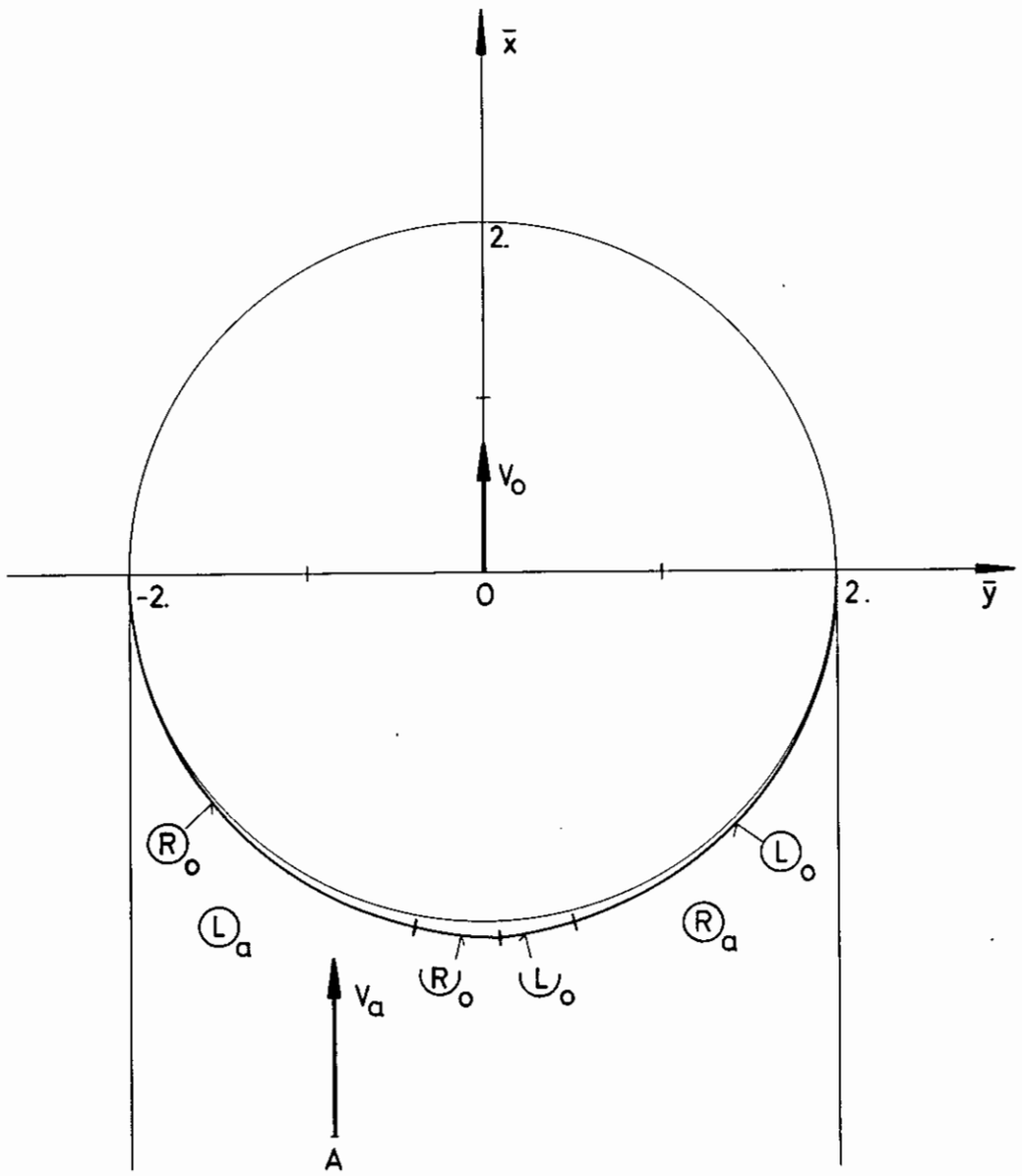

Fig. 34 Calculated barriers for collaborative two-ship maneuvers ($V_o < V_a$, $R_o > R_a$):
Case $\eta = \sqrt{2}$, $l = 2$, $\lambda = 1/2$, $\theta = 0^o$

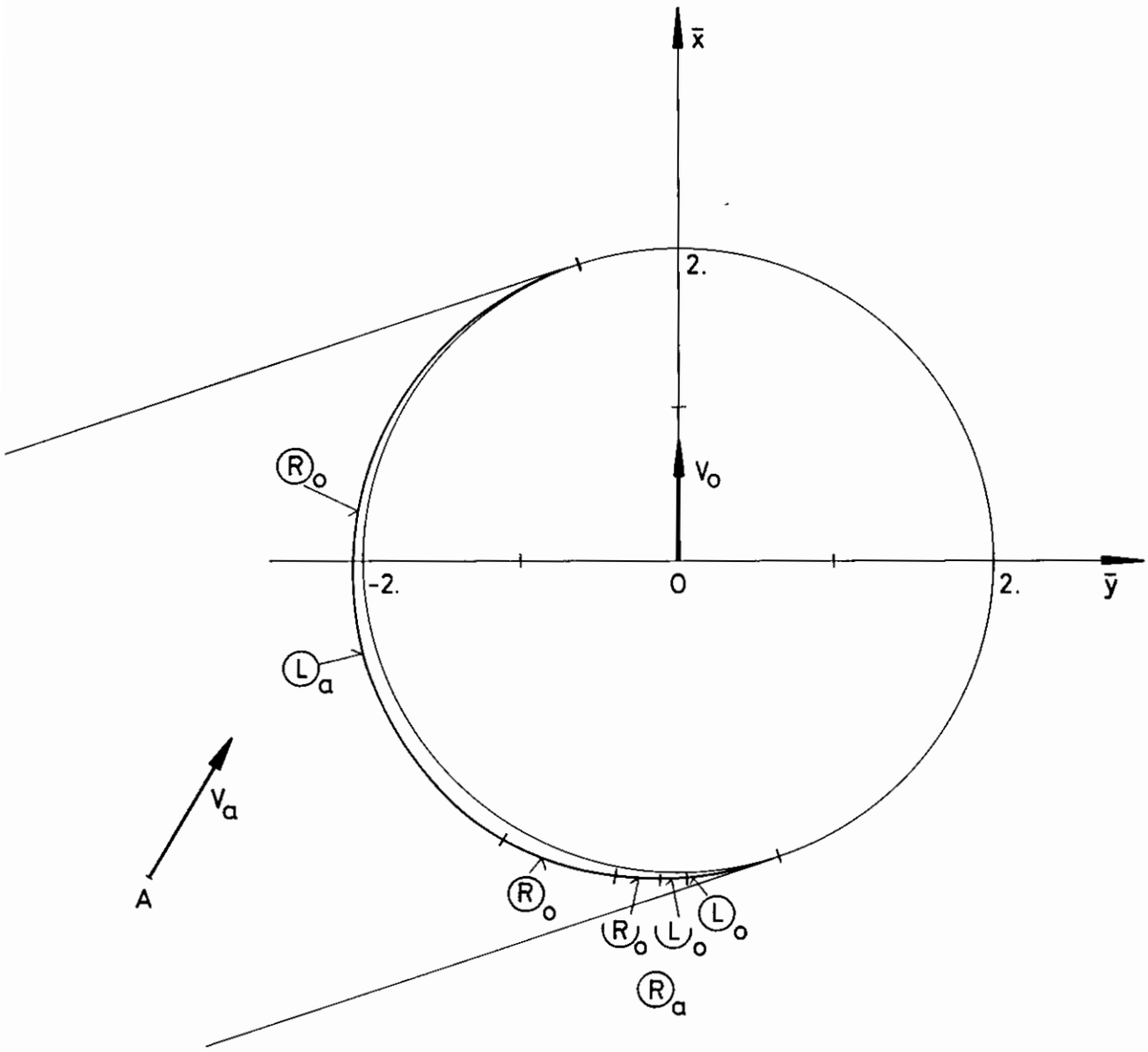

Fig. 35 Calculated barriers for collaborative two-ship maneuvers ($V_o < V_a$, $R_o > R_a$):
Case $\eta = \sqrt{2}$, $\ell = 2$, $\lambda = 1/2$, $\theta = 30^\circ$

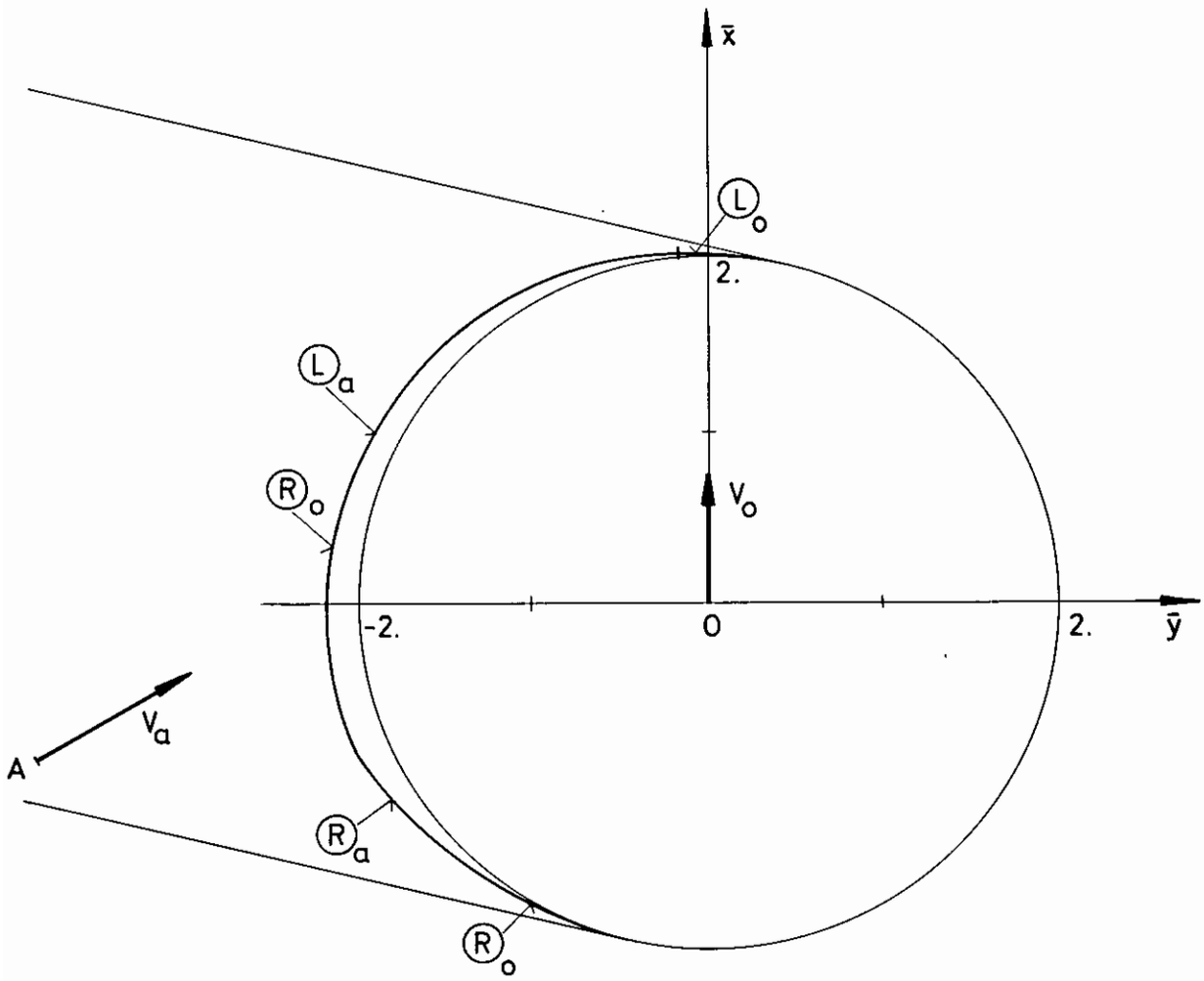

Fig. 36 Calculated barriers for collaborative two-ship maneuvers ($V_o < V_a$, $R_o > R_a$):
Case $\eta = \sqrt{2}$, $l = 2$, $\lambda = 1/2$, $\theta = 60^\circ$

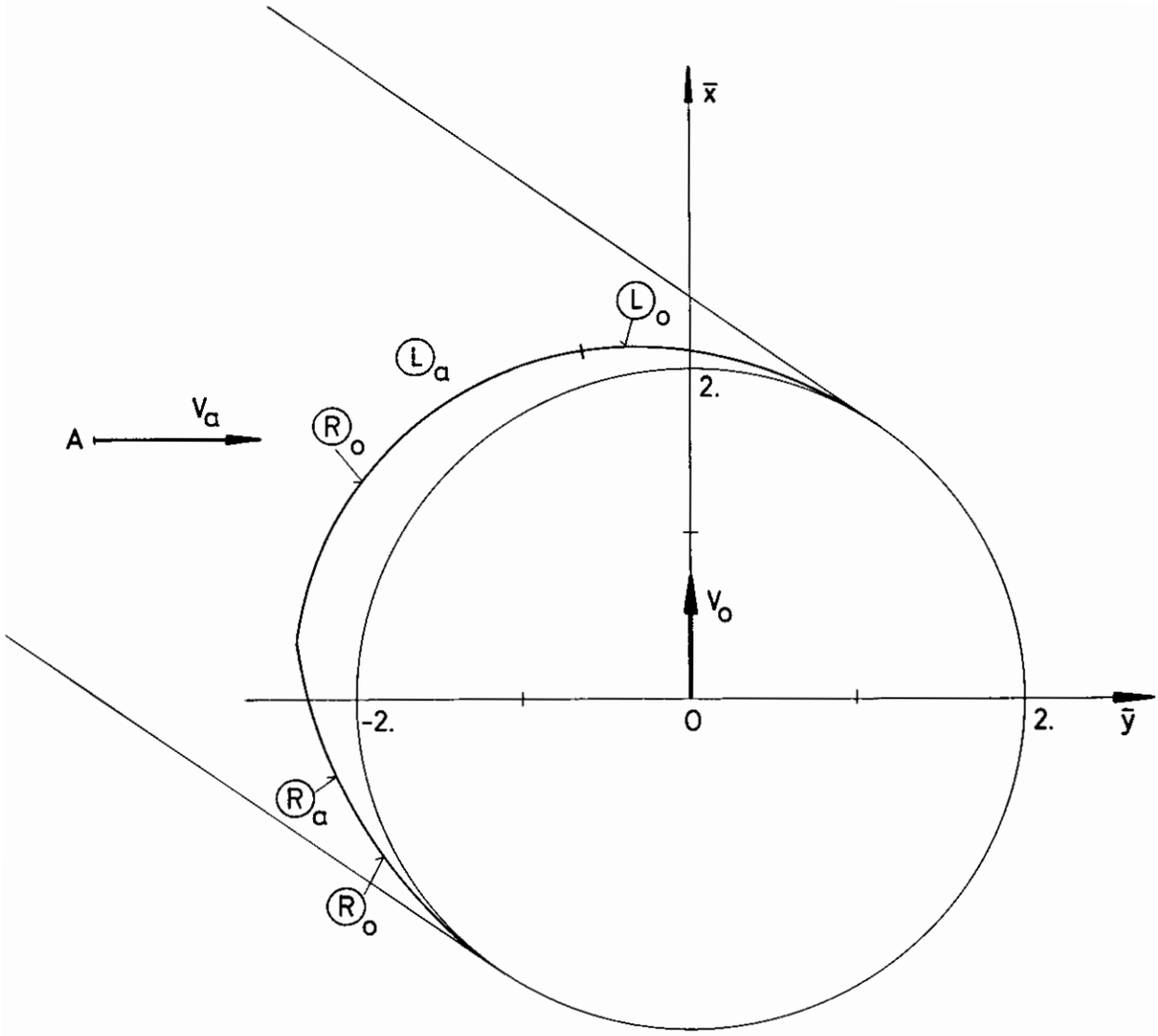

Fig. 37 Calculated barriers for collaborative two-ship maneuvers ($V_o < V_a$, $R_o > R_a$):
Case $\eta = \sqrt{2}$, $l = 2$, $\lambda = 1/2$, $\theta = 90^\circ$

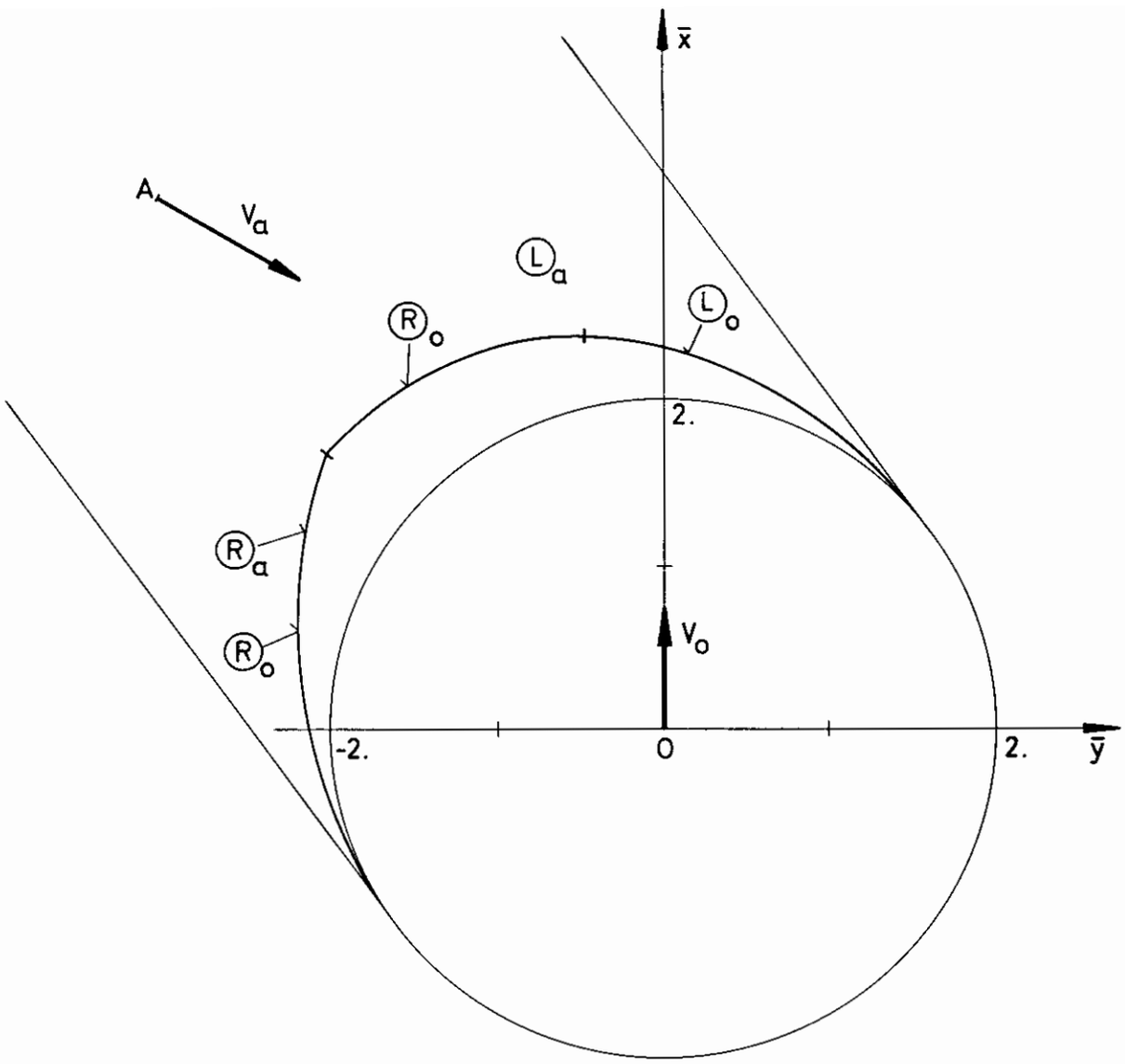

Fig. 38 Calculated barriers for collaborative two-ship maneuvers ($V_o < V_a$, $R_o > R_a$):
Case $\eta = \sqrt{2}$, $l = 2$, $\lambda = 1/2$, $\theta = 120^o$

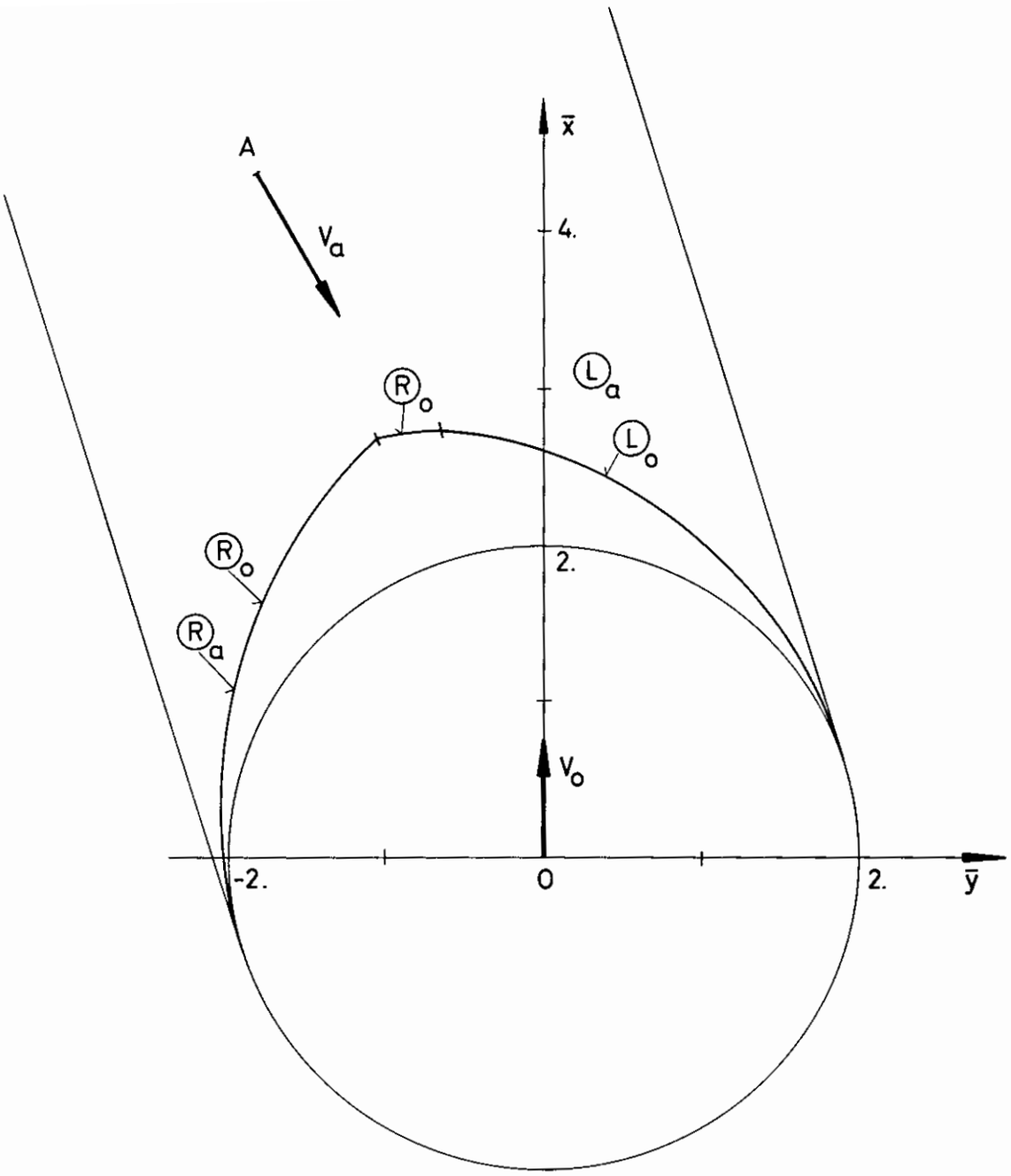

Fig. 39 Calculated barriers for collaborative two-ship maneuvers ($V_o < V_a$, $R_o > R_a$):
Case $\eta = \sqrt{2}$, $l = 2$, $\lambda = 1/2$, $\theta = 150^o$

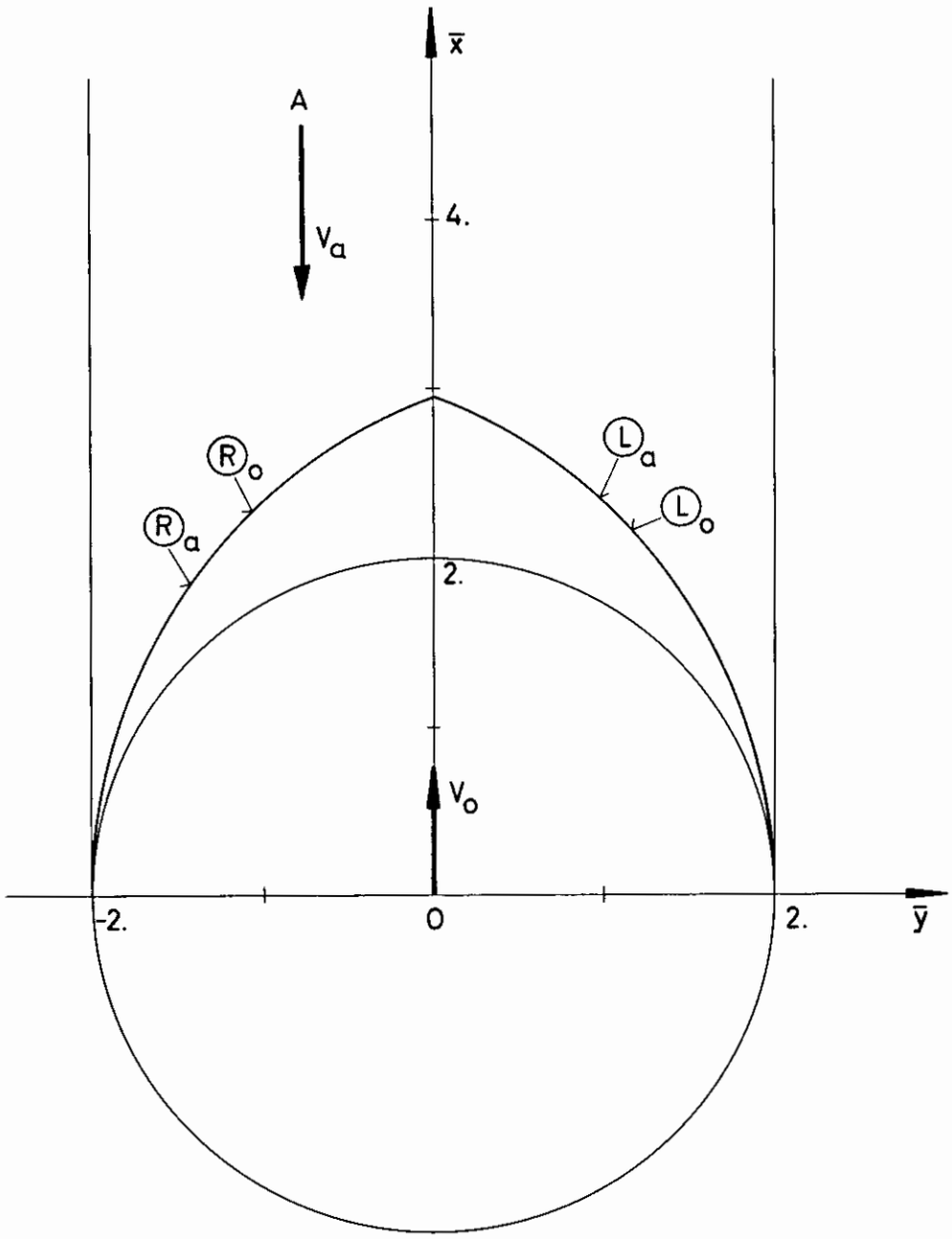

Fig. 40 Calculated barriers for collaborative two-ship maneuvers ($V_o < V_a$, $R_o > R_a$):
Case $\eta = \sqrt{2}$, $\ell = 2$, $\lambda = 1/2$, $\theta = 180^\circ$

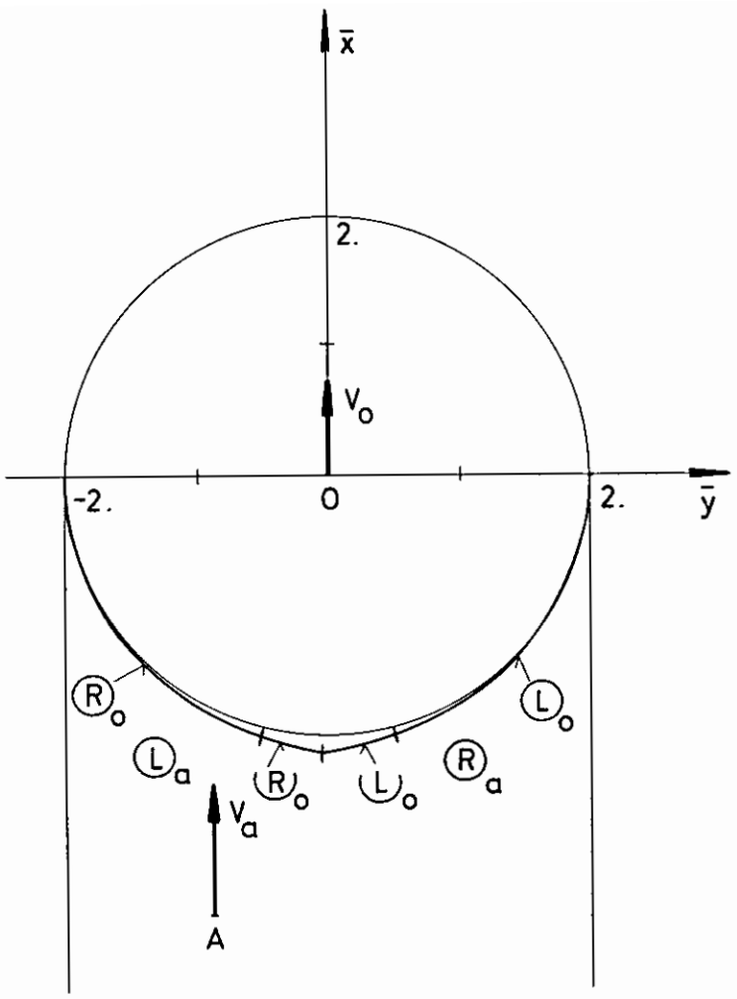

Fig. 41 Calculated barriers for collaborative two-ship maneuvers ($V_o < V_a$, $R_o = R_a$):
Case $\eta = \sqrt{2}$, $\ell = 2$, $\lambda = 1$, $\theta = 0^\circ$

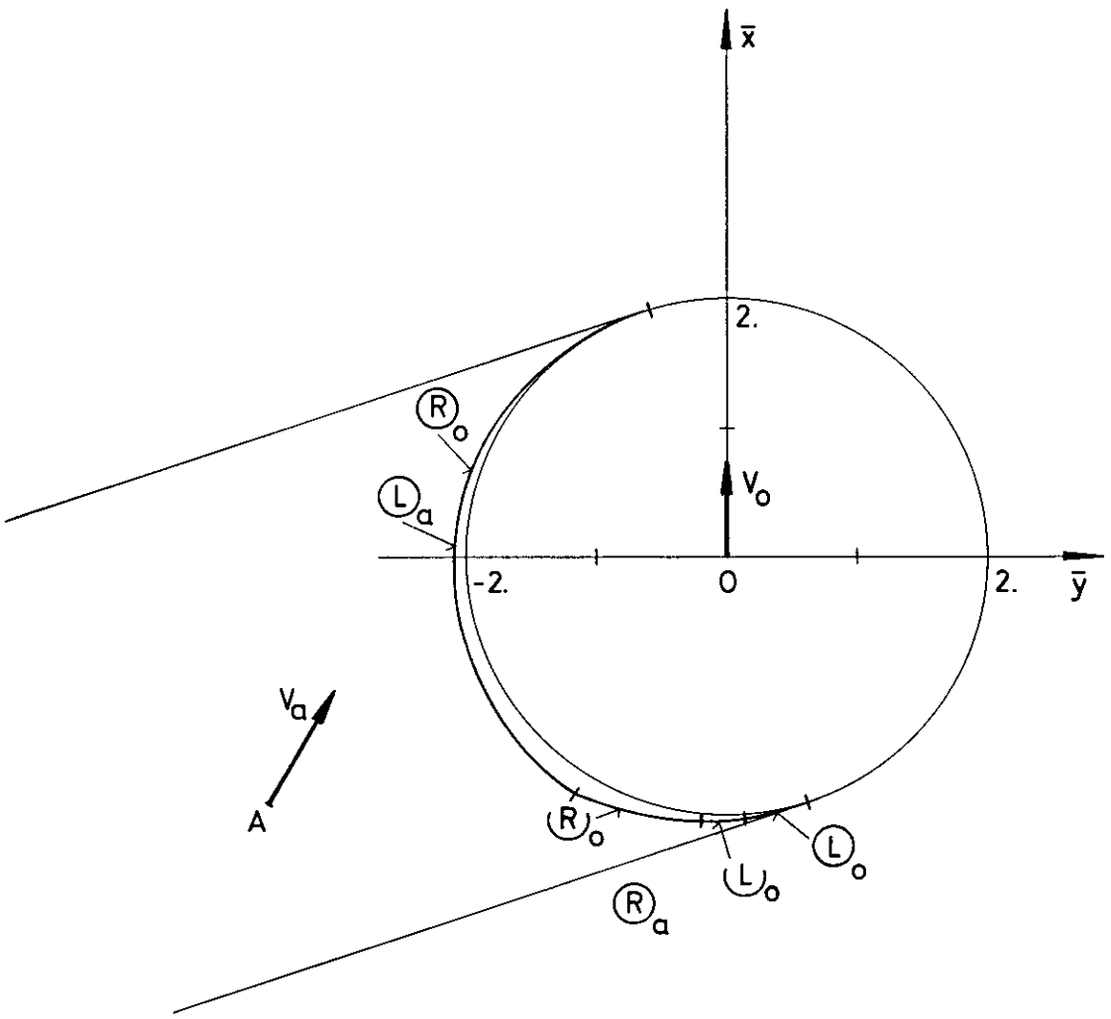

Fig. 42 Calculated barriers for collaborative two-ship maneuvers ($V_o < V_a$, $R_o = R_a$):
Case $\eta = \sqrt{2}$, $l = 2$, $\lambda = 1$, $\theta = 30^\circ$

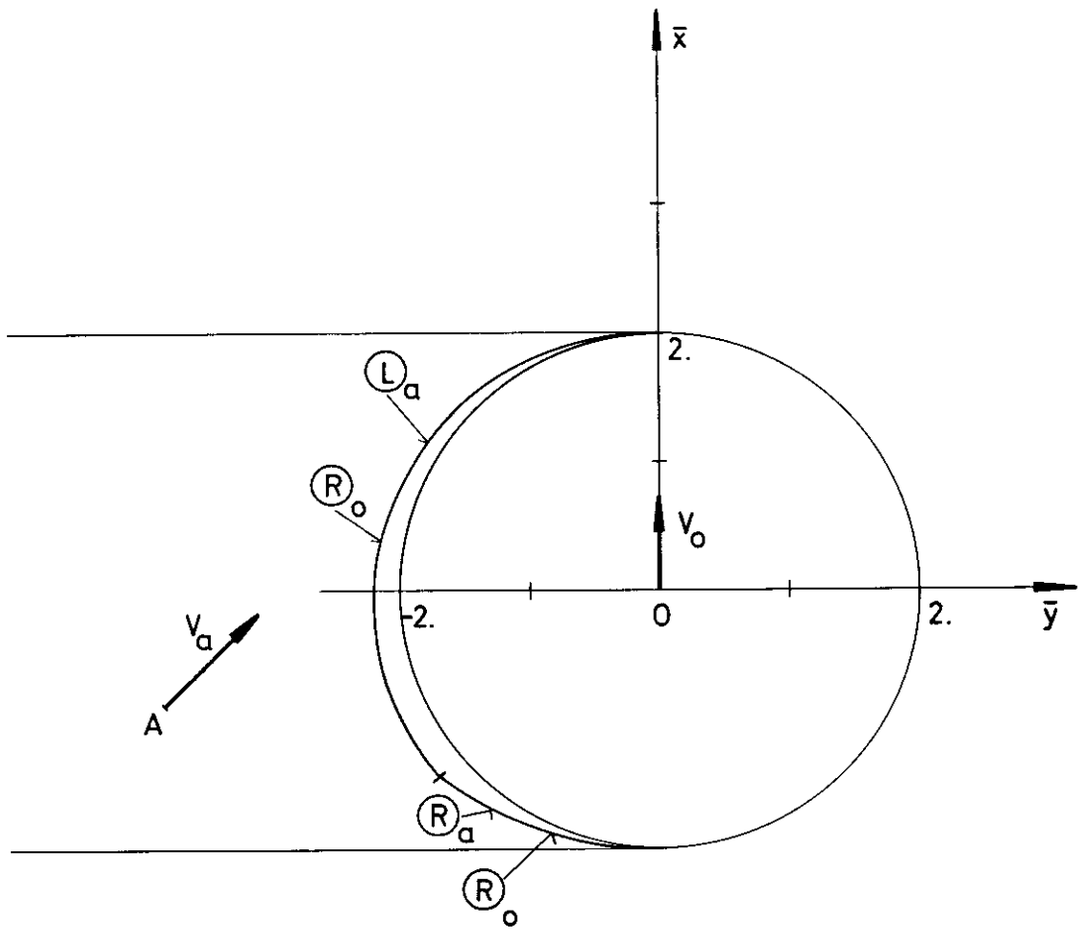

Fig. 43 Calculated barriers for collaborative two-ship maneuvers ($V_o < V_a$, $R_o = R_a$):
Case $\eta = \sqrt{2}$, $l = 2$, $\lambda = 1$, $\theta = 45^o$

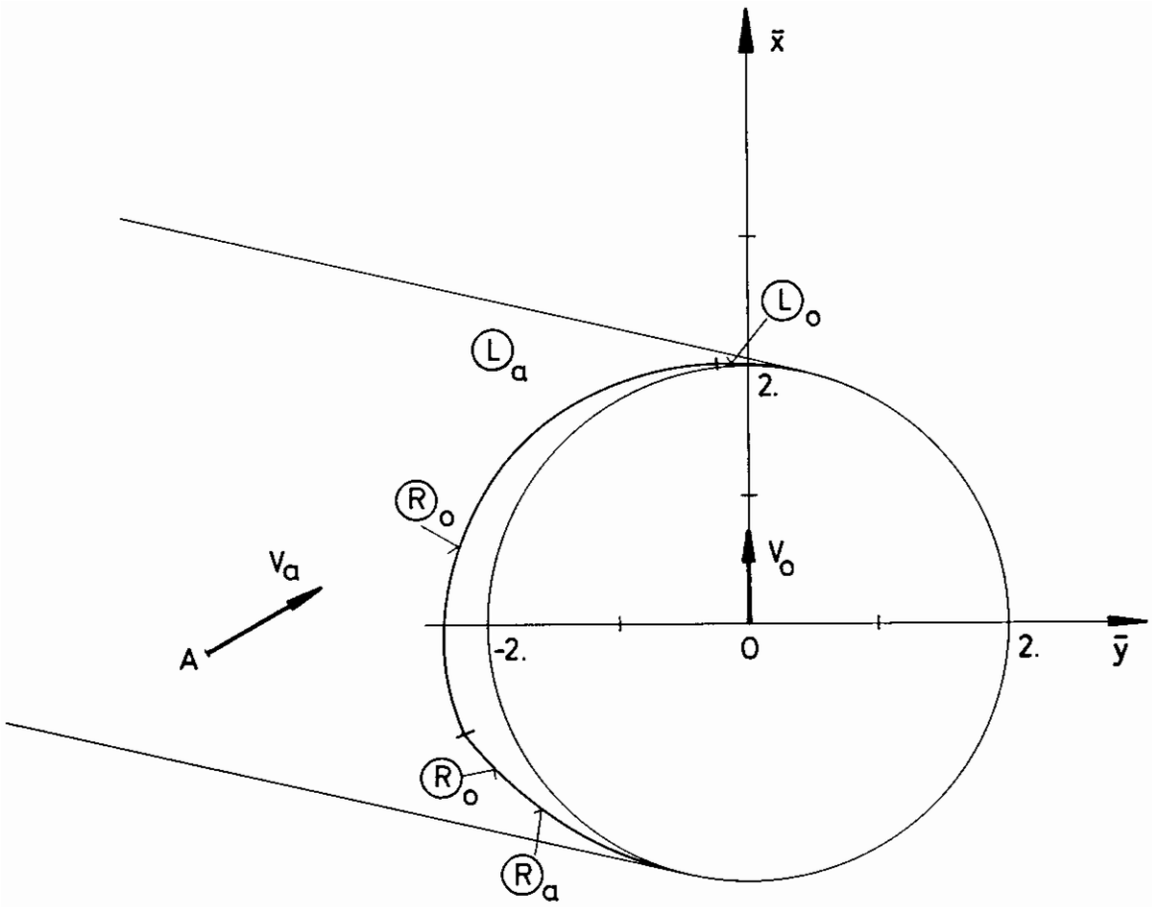

Fig. 44 Calculated barriers for collaborative two-ship maneuvers ($V_o < V_a$, $R_o = R_a$):
Case $\eta = \sqrt{2}$, $l = 2$, $\lambda = 1$, $\theta = 60^\circ$

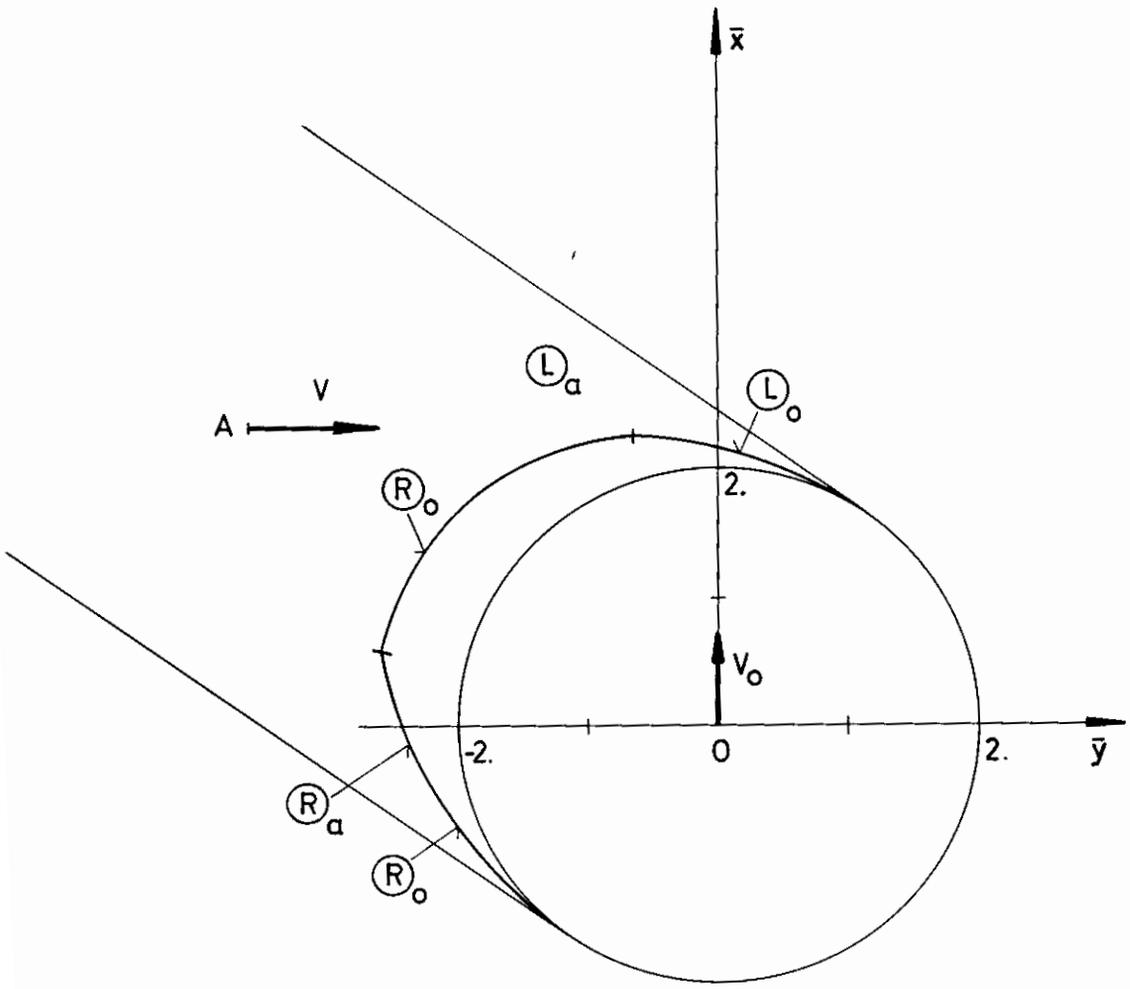

Fig. 45 Calculated barriers for collaborative two-ship maneuvers ($V_o < V_a$, $R_o = R_a$):
Case $\eta = \sqrt{2}$, $l = 2$, $\lambda = 1$, $\theta = 90^\circ$

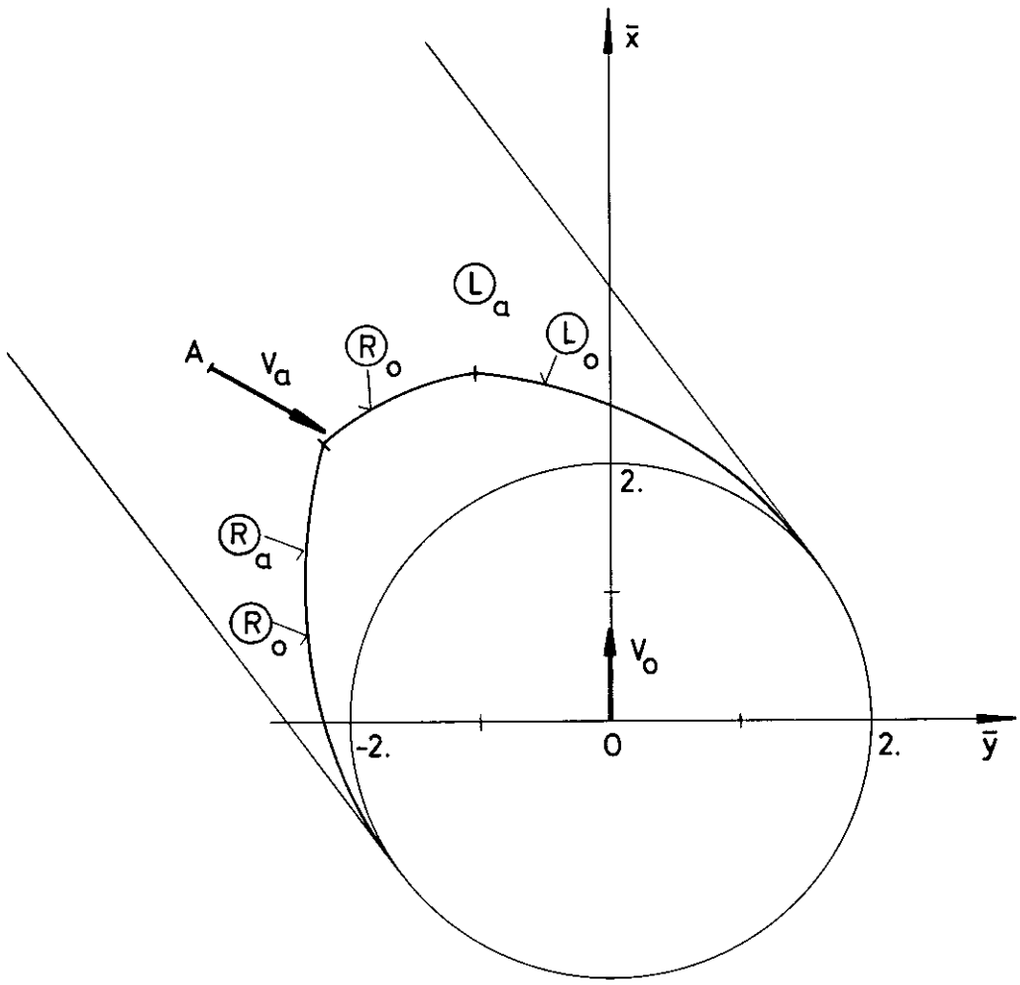

Fig. 46 Calculated barriers for collaborative two-ship maneuvers ($V_o < V_a$, $R_o = R_a$):
Case $\eta = \sqrt{2}$, $l = 2$, $\lambda = 1$, $\theta = 120^o$

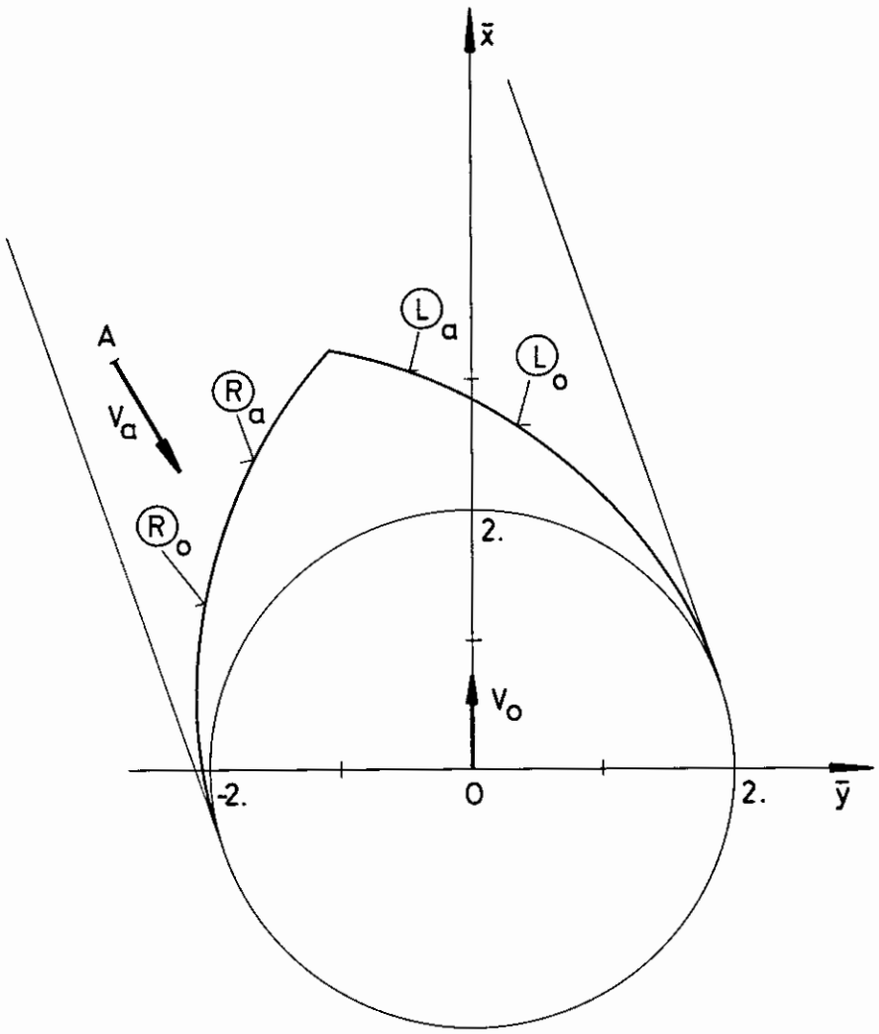

Fig. 47 Calculated barriers for collaborative two-ship maneuvers ($V_o < V_a$, $R_o = R_a$):
Case $\eta = \sqrt{2}$, $\ell = 2$, $\lambda = 1$, $\theta = 150^o$

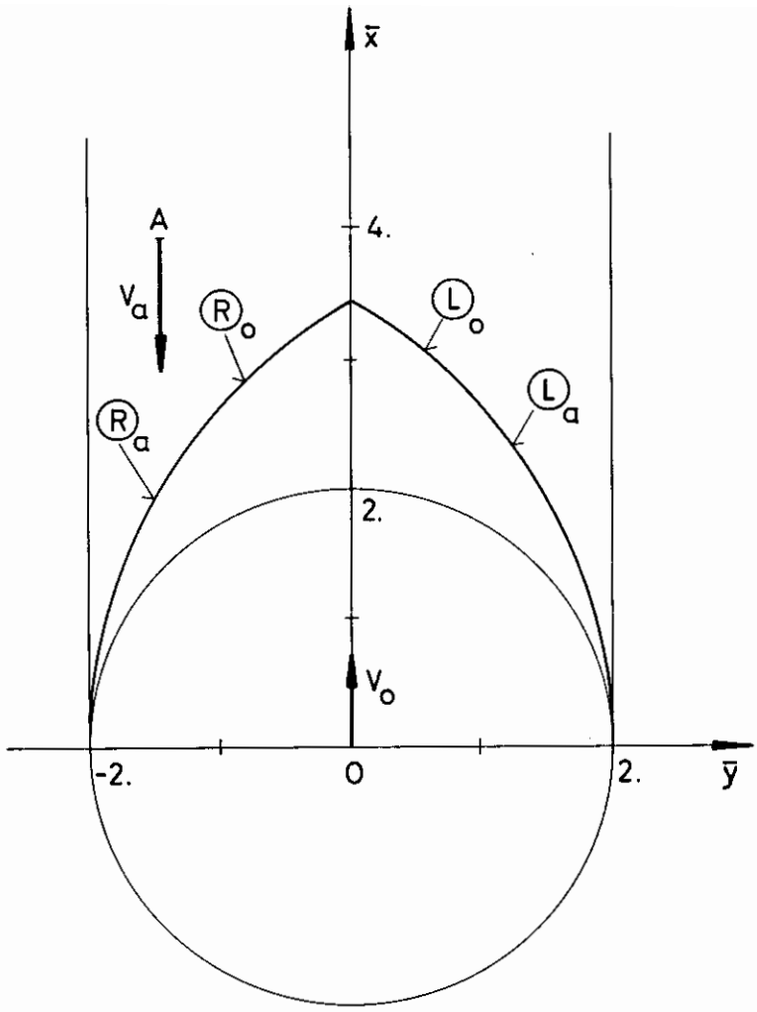

Fig. 48 Calculated barriers for collaborative two-ship maneuvers ($V_o < V_a$, $R_o = R_a$):
Case $\eta = \sqrt{2}$, $l = 2$, $\lambda = 1$, $\theta = 180^\circ$

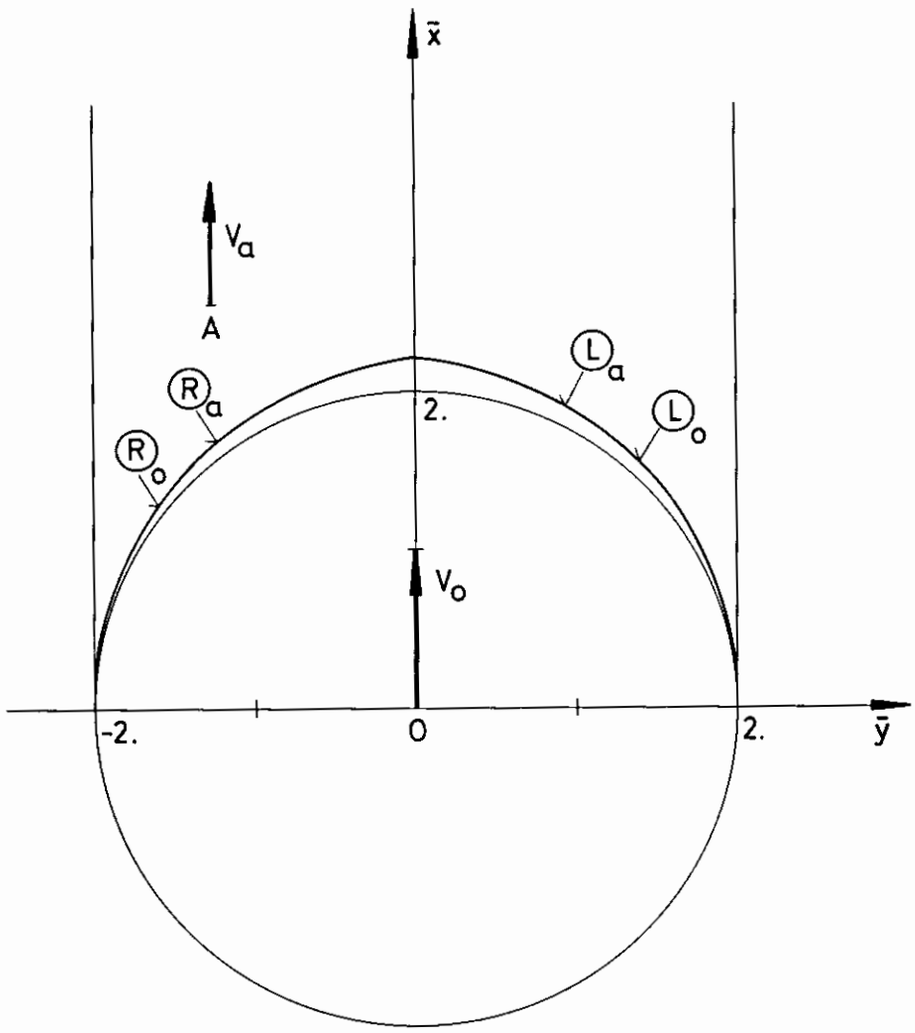

Fig. 49 Calculated barriers for conflicting two-ship maneuvers ($V_o > V_a$, $R_o = R_a$):
Case $\eta = 1/\sqrt{2}$, $l = 2$, $\lambda = 1$, $\theta = 0^o$

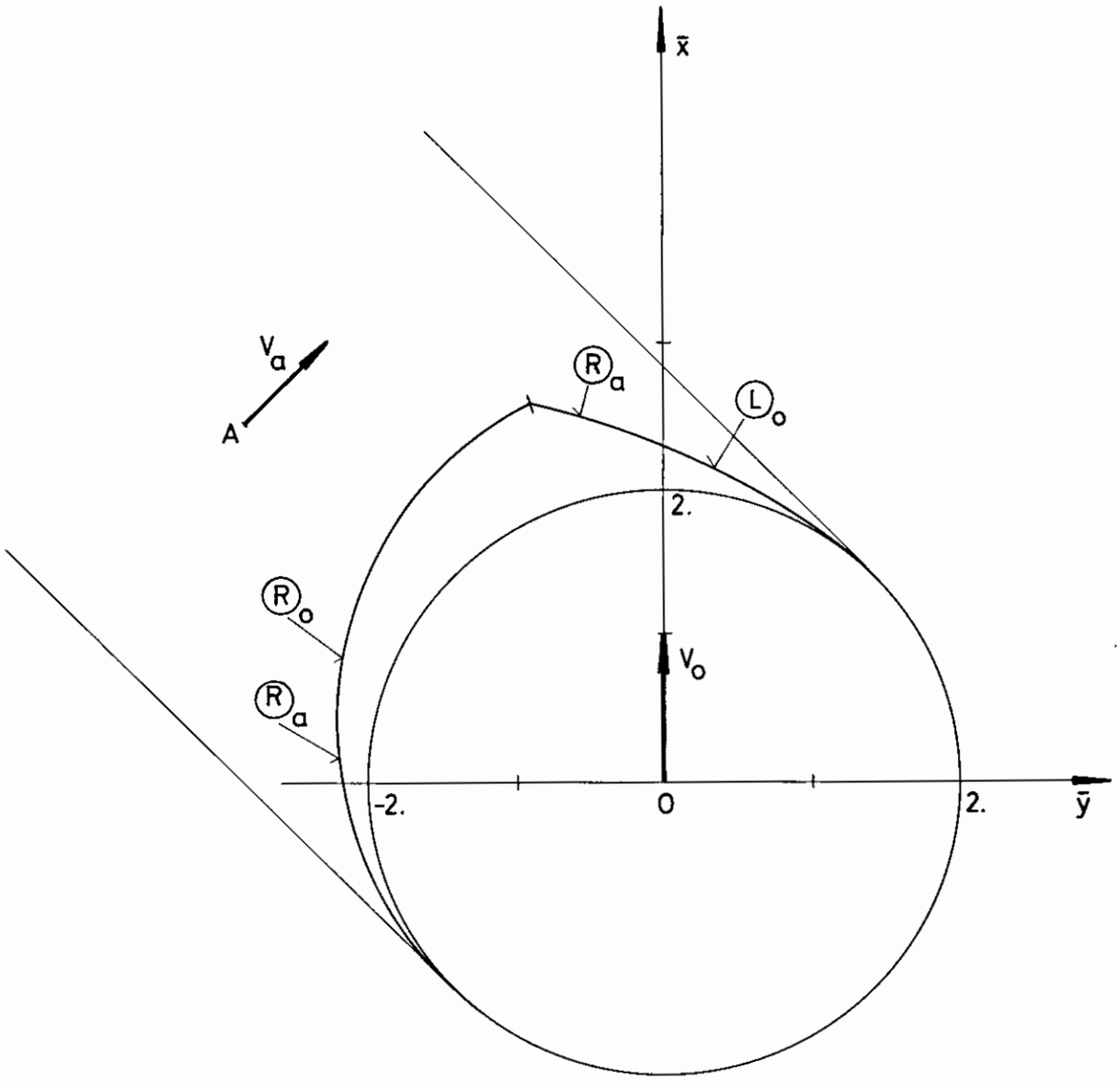

Fig. 51 Calculated barriers for conflicting two-ship maneuvers ($V_o > V_a$, $R_o = R_a$):
Case $\eta = 1/\sqrt{2}$, $l = 2$, $\lambda = 1$, $\theta = 45^\circ$

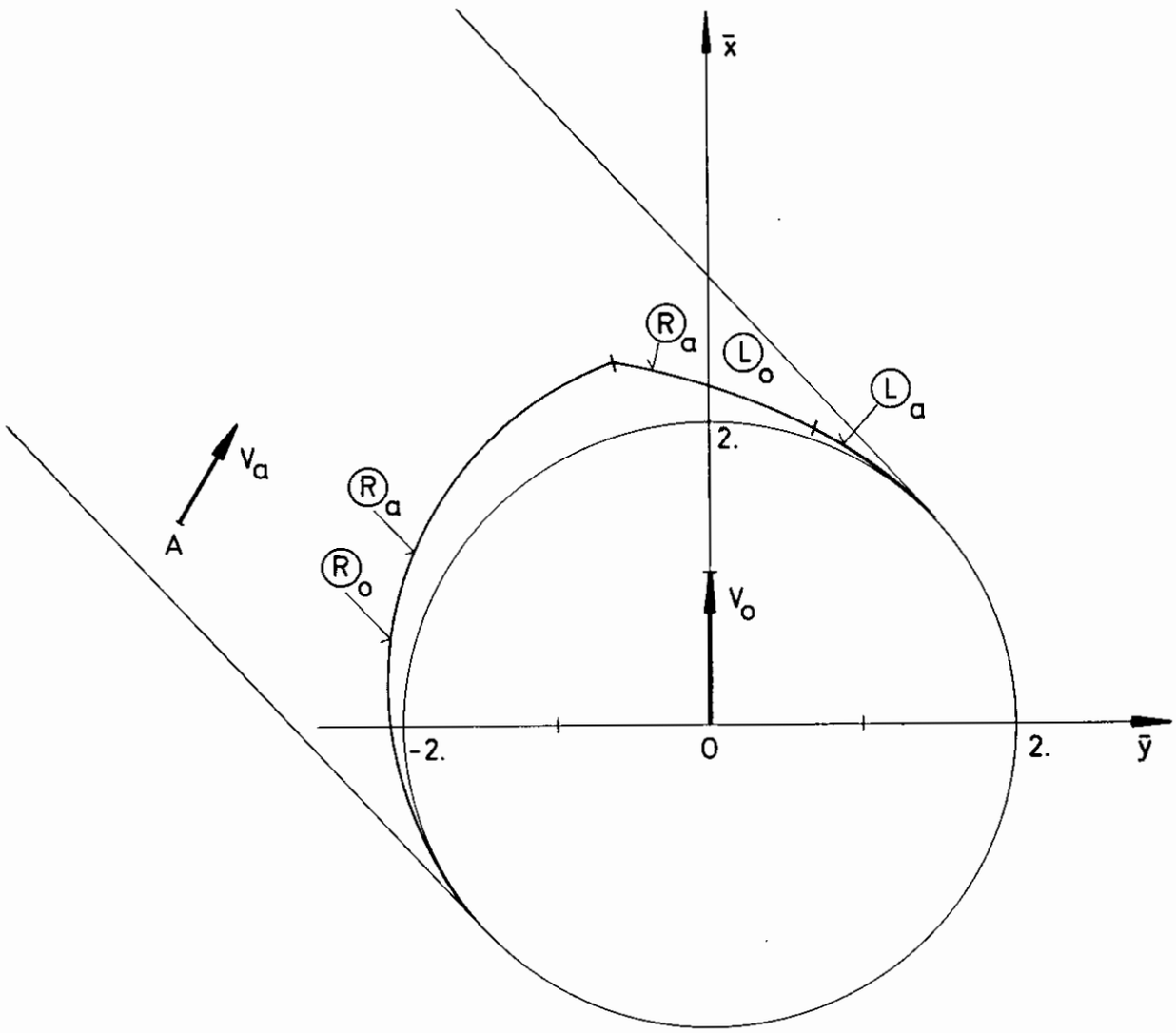

Fig. 50 Calculated barriers for conflicting two-ship maneuvers ($V_o > V_a$, $R_o = R_a$):
Case $\eta = 1/\sqrt{2}$, $l = 2$, $\lambda = 1$, $\theta = 30^o$

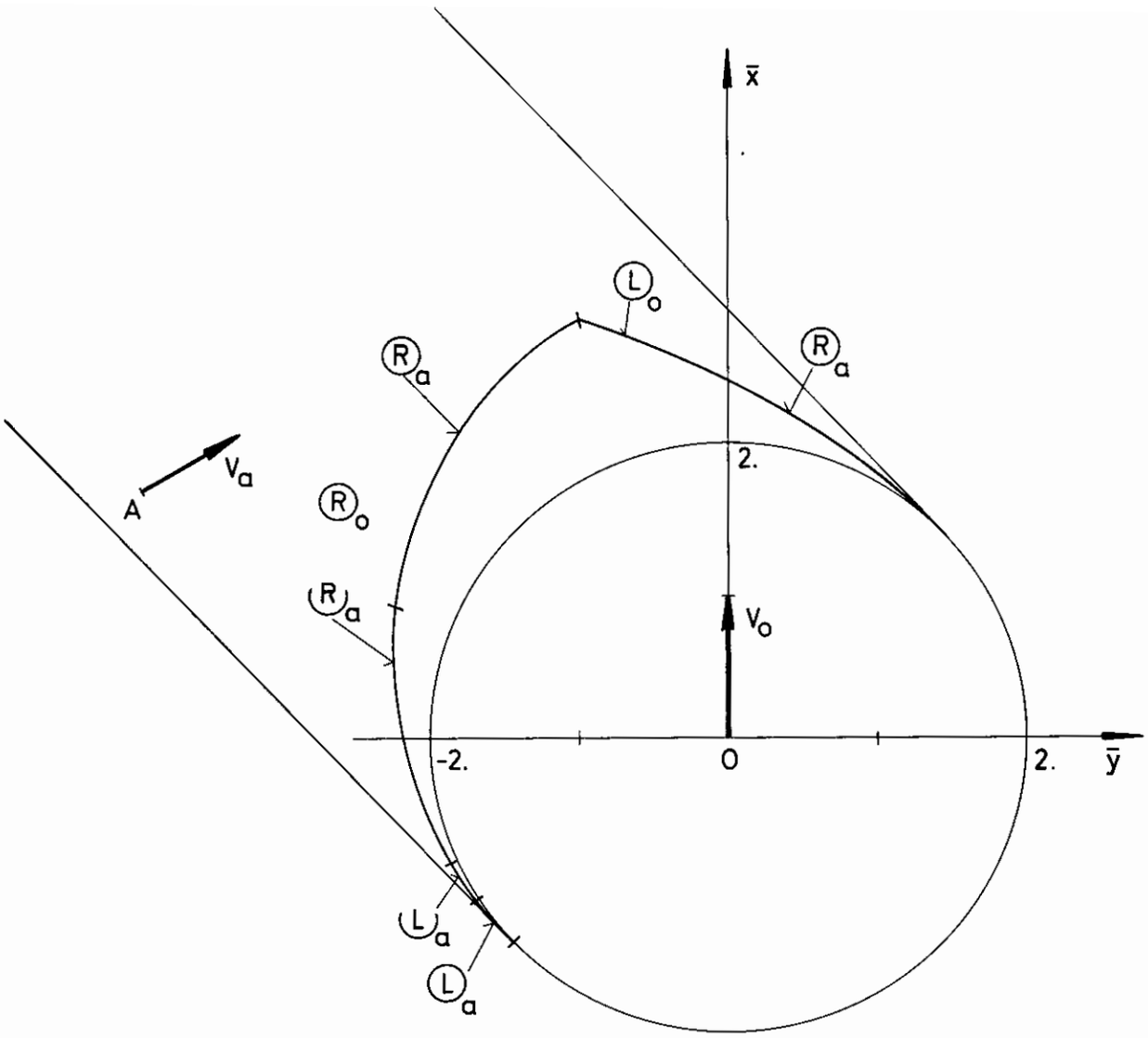

Fig. 52 Calculated barriers for conflicting two-ship maneuvers ($V_o > V_a$, $R_o = R_a$):
Case $\eta = 1/\sqrt{2}$, $l = 2$, $\lambda = 1$, $\theta = 60^\circ$

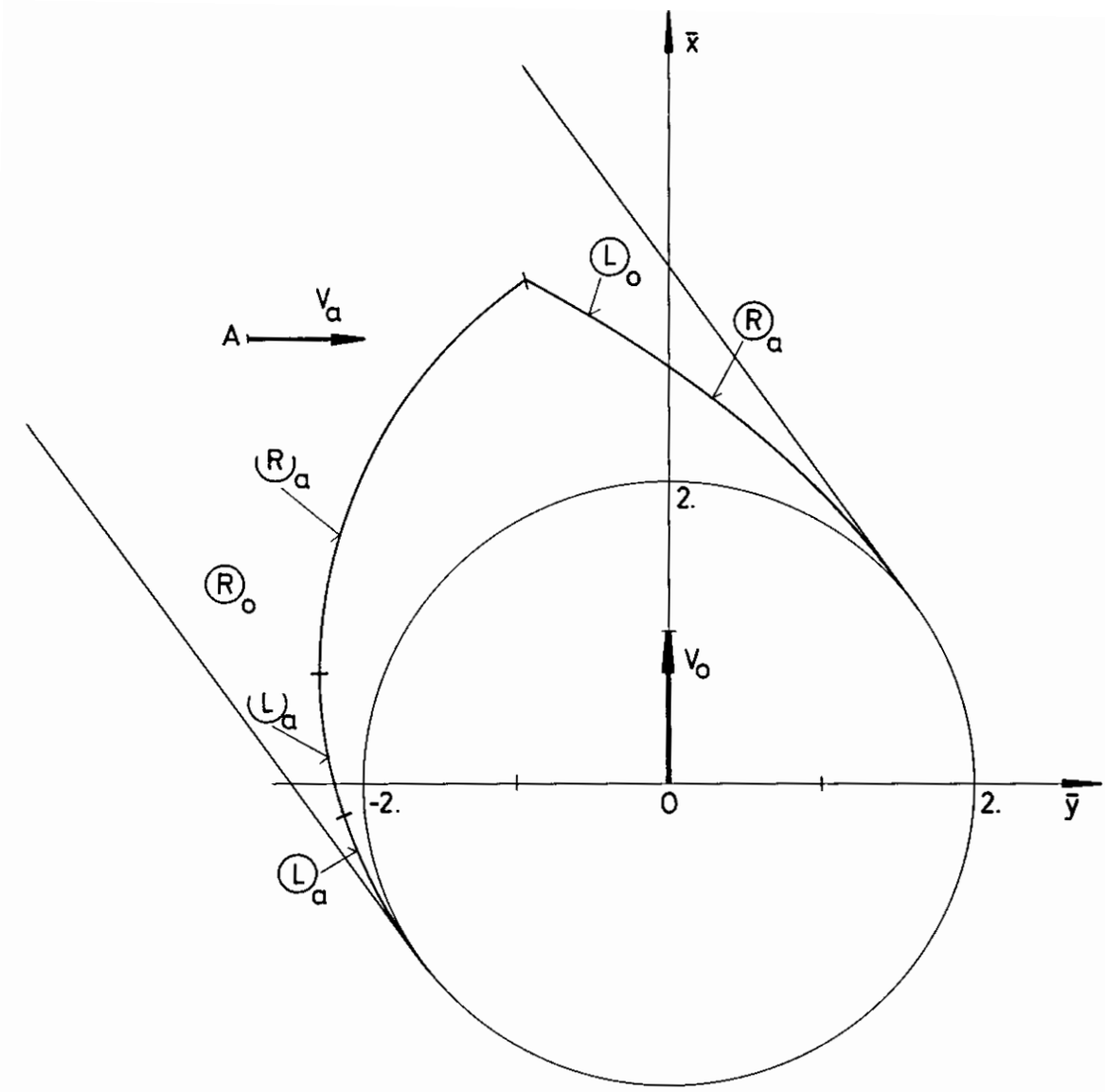

Fig. 53 Calculated barriers for conflicting two-ship maneuvers ($V_o > V_a$, $R_o = R_a$):
Case $\eta = 1/\sqrt{2}$, $l = 2$, $\lambda = 1$, $\theta = 90^o$

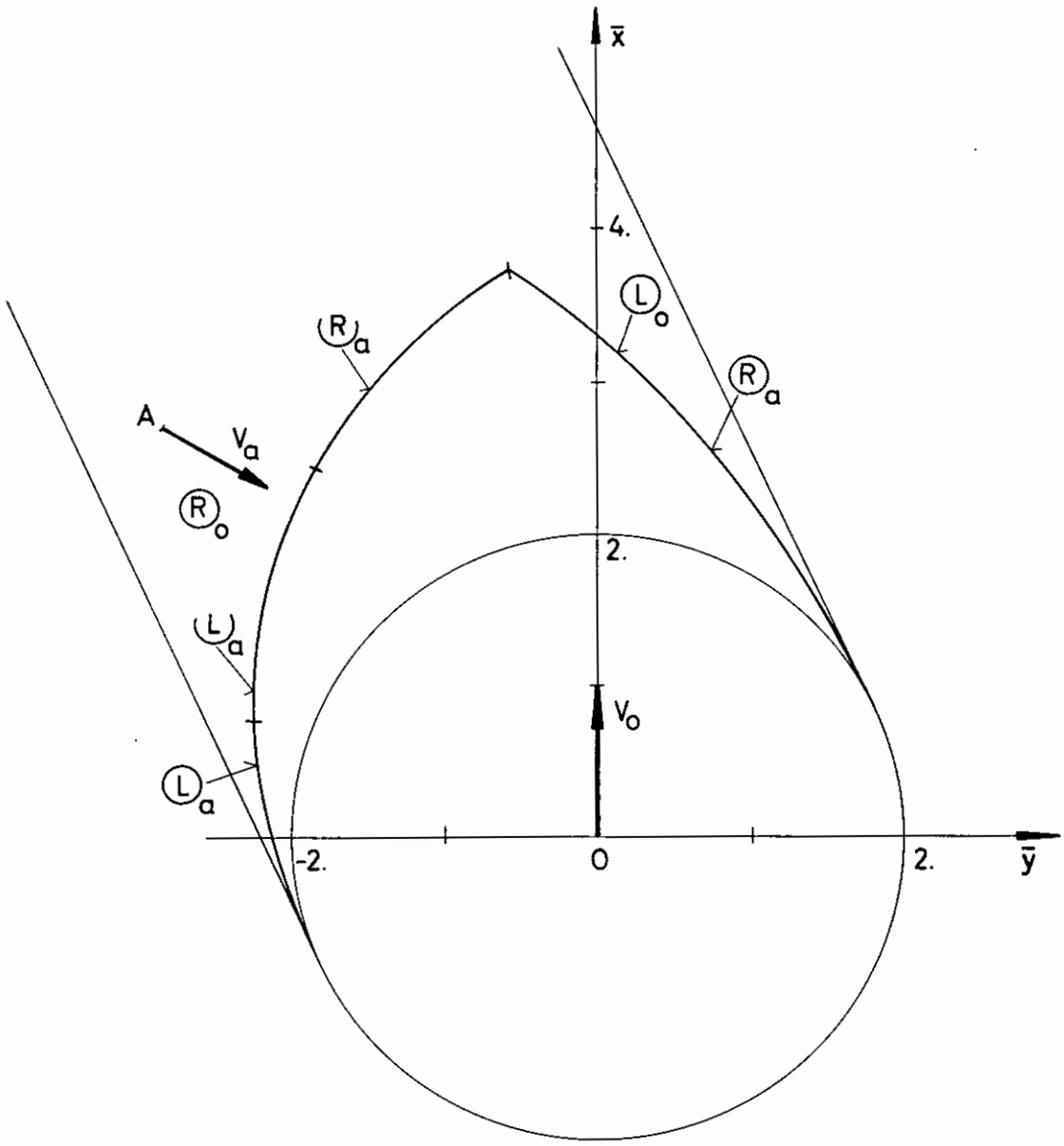

Fig. 54 Calculated barriers for conflicting two-ship maneuvers ($V_o > V_a$, $R_o = R_a$):
Case $\eta = 1/\sqrt{2}$, $l = 2$, $\lambda = 1$, $\theta = 120^\circ$

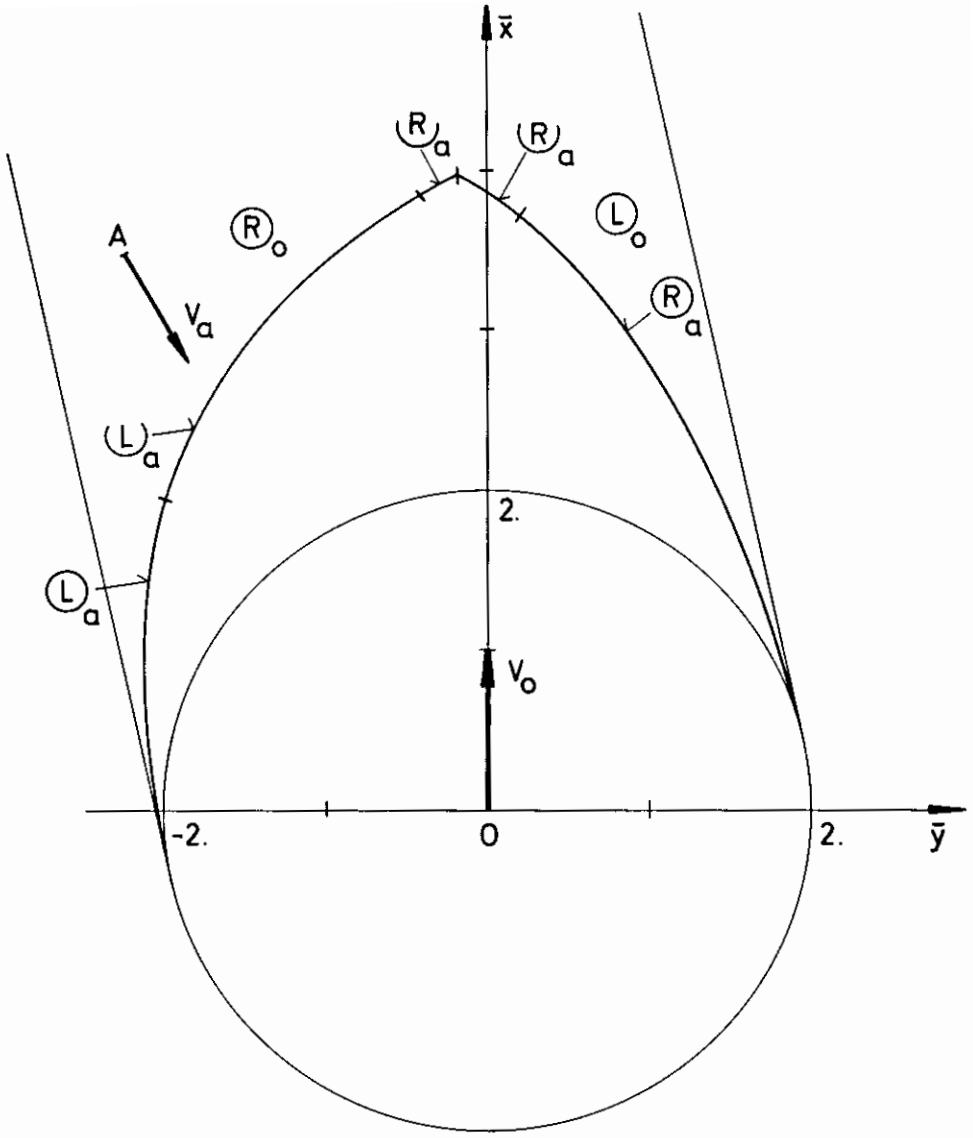

Fig. 55 Calculated barriers for conflicting two-ship maneuvers ($V_o > V_a$, $R_o = R_a$):
Case $\eta = 1/\sqrt{2}$, $l = 2$, $\lambda = 1$, $\theta = 150^\circ$

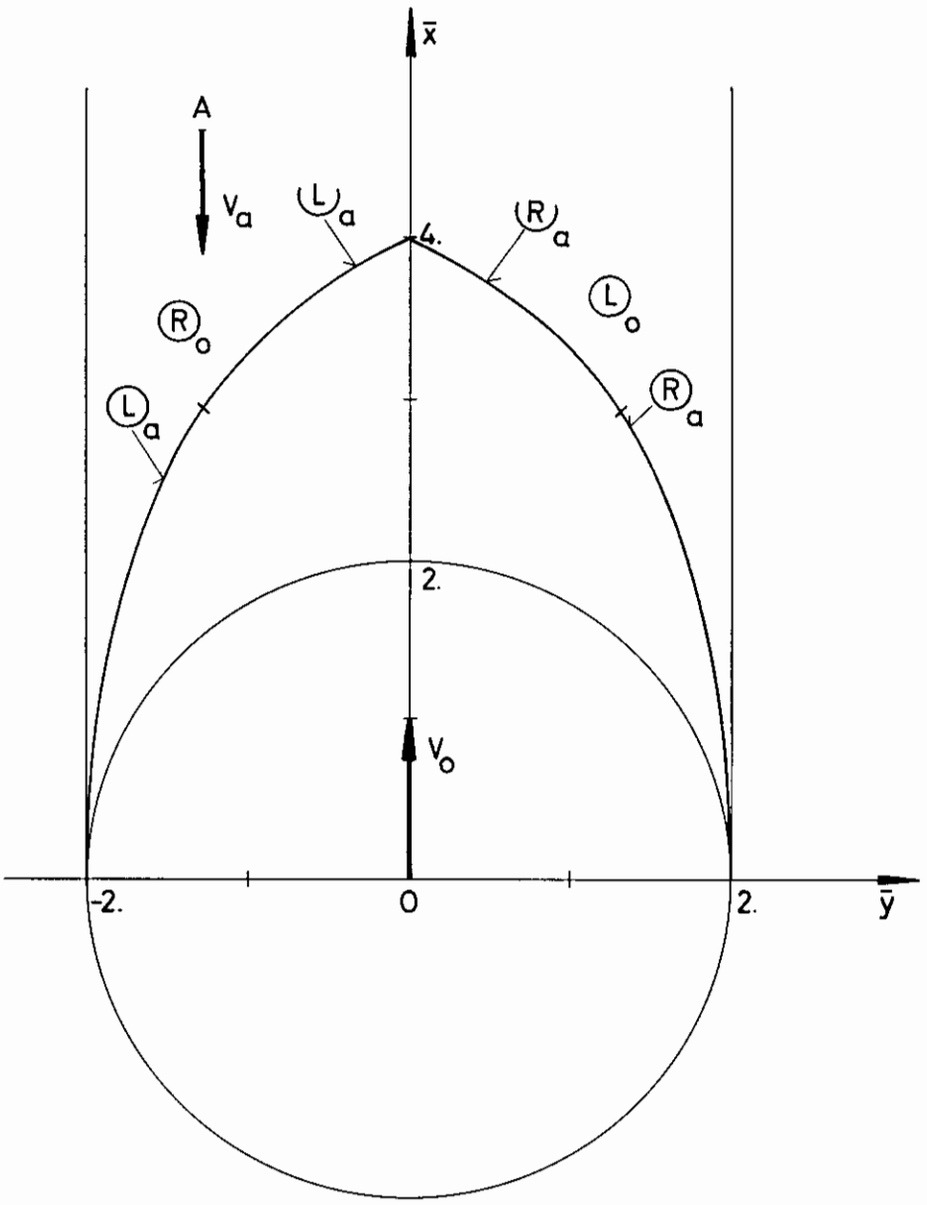

Fig. 56 Calculated barriers for conflicting two-ship maneuvers ($V_o > V_a$, $R_o = R_a$):
Case $\eta = 1/\sqrt{2}$, $l = 2$, $\lambda = 1$, $\theta = 180^o$

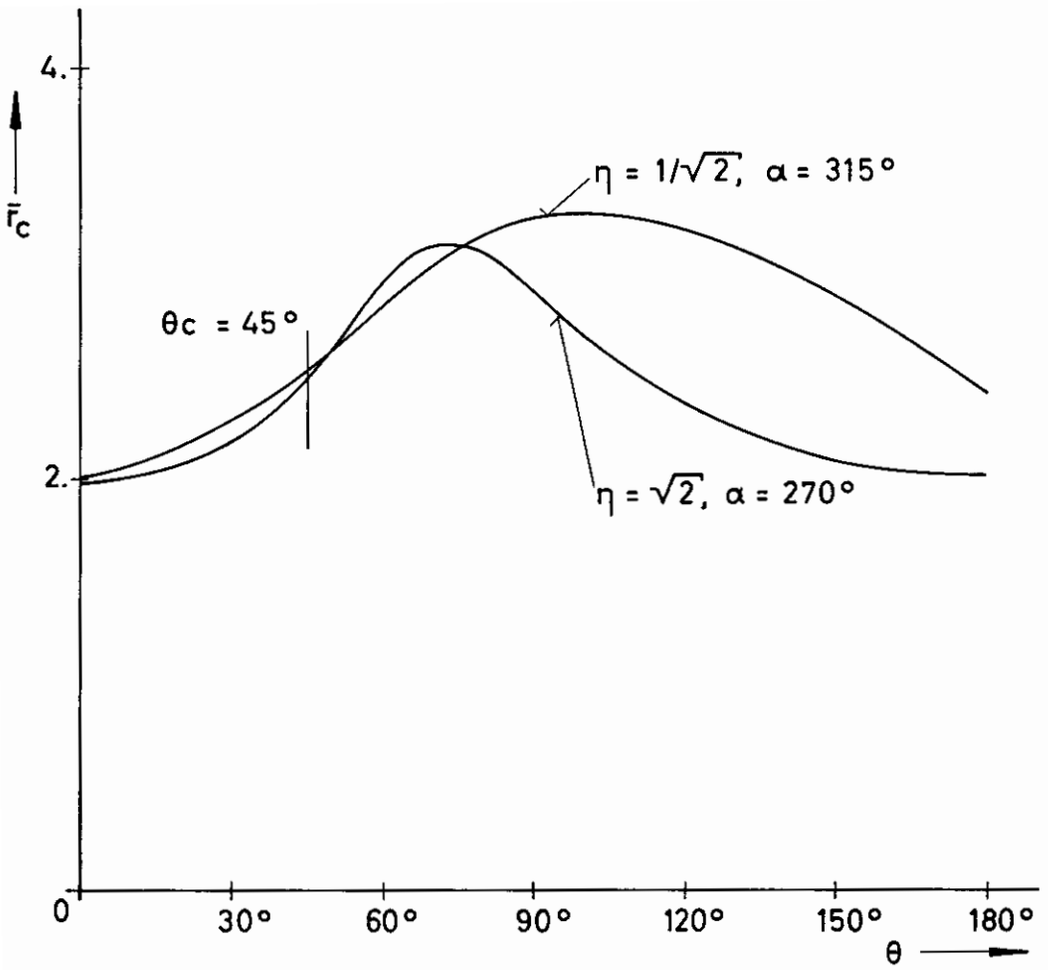

Fig. 57 Critical range versus relative course angle for $\eta = 1/\sqrt{2}$, $\alpha = 315^{\circ}$ and $\eta = \sqrt{2}$, $\alpha = 270^{\circ}$